APPLICATION OF LAKE AND SURFACE WATER HEAT EXCHANGER SIMULATIONS FOR ENERGY CALCULATIONS AND DETERMINATION OF DESIGN TEMPERATURES AND CONSTRAINTS

By

MANOJKUMAR SELVAKUMAR

Bachelor of Science in Mechanical Engineering

Anna University

Chennai, India

2009

Submitted to the Faculty of the
Graduate College of the
Oklahoma State University
in partial fulfillment of
the requirements for
the Degree of
MASTER OF SCIENCE
May, 2013

`

APPLICATION OF LAKE AND SURFACE WATER HEAT EXCHANGER SIMULATIONS FOR ENERGY CALCULATIONS AND DETERMINATION OF DESIGN TEMPERATURES AND CONSTRAINTS

Thesis Approved:

Dr. Jeffrey D. Spitler

Thesis Adviser

Dr. Daniel E. Fisher

Dr. David Lilley

`

Name: MANOJKUMAR SELVAKUMAR

Date of Degree: MAY 2013

Title of Study: APPLICATION OF LAKE AND SURFACE WATER HEAT EXCHANGER SIMULATIONS FOR ENERGY CALCULATIONS AND DETERMINATION OF DESIGN TEMPERATURES AND CONSTRAINTS

Major Field: MECHANICAL AND AEROSPACE ENGINEERING

Abstract:

Surface Water Heat Pump (SWHP) systems utilize a nearby surface water body e.g. lakes, ponds, or rivers as a heat source and/or heat sink for one or more heat pumps providing building heating and/or cooling. Despite growing interest in SWHP systems, there is a paucity of standard design data and procedures to aid engineers to efficiently design and analyze the system. This thesis work aims to develop the robust stand-alone FORTRAN lake model coupled with surface water heat exchanger model and implement that in the EnergyPlus program that can serve as a basis for energy calculations. In addition, the meteorological-data-and-model-driven approach is investigated to develop an easy-to-use database of design temperatures for surface water bodies across United States. This approach uses the developed stand-alone FORTRAN lake model to predict the design temperatures from typical meteorological weather data. Furthermore, the design guidelines are developed which recommends the maximum capacity of the lakes for acceptable SWHP system performance. The detailed study tell us how much of heat can be rejected or extracted from a lake without affecting the lake design temperatures.

`

TABLE OF CONTENTS

Chapter Page

`

`

LIST OF TABLES

Table Page

`

`

LIST OF FIGURES

Figure Page

`

`

`

`

NOMENCLATURE

A = lake horizontal area, [m^2]

C_d = drag coefficient [-]

C_p = specific heat capacity, [J/kg·°C]

d = heat exchanger tube diameter, [m]

d_{c_o} = heat exchanger outside coil diameter, [m]

De = Dean number [-]

EFT = heat exchanger entering fluid temperature, [°C]

$ExFT$ = heat exchanger exit fluid temperature, [°C]

f = dimensionless number

g = acceleration due to gravity, [m/s^2]

H_{ice} = ice thickness,[m]

$H_{ice,\ new}$ = New ice thickness due to congelation ice growth, [m]

H_{snow} = Snow thickness, [m]

$H_{snow\text{-}ice}$ = Thickness of slush layer formed when water mixes with the snow, [m]

h_c = surface convective heat transfer coefficient, [$W/m^2 \cdot K$]

h_{fg} = Latent heat of vaporization, [J/kg]

`

h_{lw} = long wave radiative heat transfer coefficient, [W/m^{2}·K]

K = thermal conductivity, [W/m·K]

k_z = vertical eddy diffusion coefficient, [m^2/day]

k_{zmax} = the maximum hypolimnion eddy diffusion coefficient, [m^2/day]

L_{freeze} = latent heat of freezing of ice, [J/kg]

$\dot{m}$ = mass flow rate, [kg/s]

m_{ice} = mass of ice surrounding the heat exchanger tube, [kg]

m_{water} = mass of water melted from ice surrounding the heat exchanger tube, [kg]

N = stability frequency or the Brunt Vaisala frequency, [s^{-1}]

$N_{circuit}$ = the number of heat exchanger circuits placed in the lake [-]

Nu = Nusselt number [-]

PE = Potential energy, [J]

$Pitch_{ratio}$ = Coil pitch ratio [-]

Pr = Prandtl number [-]

Q = Internal distribution of heat to each water layer due to the absorption of solar radiation, sediments and heat transfer from heat exchangers in the water column, [W/m^3]

q_{coil} = Heat transfer between the heat exchanger fluid and ice/water interface, [W]

$q_{deficit}$ = sensible heat deficit in the sub-cooled water layer converted into latent heat of ice, [W]

q_{lat} = latent heat to freeze the water or melt the ice formed at each segment, [W]

q_{sc} = sensible heat to sub-cool the ice during freezing at each segment, [W]

`

q_{sh} = sensible heat to superheat the water during the melting period at each segment, [W]

q_{wat} = heat transfer between the surrounding lake water and the ice/water interface, [W]

q''_{c} = convective heat flux from the lake surface to the atmosphere, [W/m^2]

q''_{e} = evaporative heat flux from the lake surface, [W/m^2]

q_{hx} = heat transfer from the heat exchanger to the surface water body, [W]

q''_{lw} = net long wave radiation incident on the lake surface, [W/m^2]

q = net heat flux on the lake surface, [W/m^2]

$q''_{net(z)}$ = net heat flux at the depth *z* inside the water column, [W/m^2]

$q''_{sediment}$ = heat flux from sediment to water, [W/m^2]

$q''_{sw(z)}$ = incoming short wave radiative heat flux absorbed at the depth z, [W/m2]

$q''_{sw\text{-}surface}$ = heat flux due to short wave radiation incident on the lake surface, [W/m^2]

r = radius of the heat exchanger tube, [m]

ρ' = surface reflectivity coefficient [-]

R, Res = Thermal resistances, [1/K]

Ra^* = modified Rayleigh number [-]

t = time, [s]

T = temperature, [°C]

TKE = Total kinetic energy, [J]

UA = global heat transfer coefficient, [W/K]

`

V_{epi} = Volume of the epilimnion, [m^3]

V_z = Volume of the layer below the epilimnion, [m^3]

W = Wind speed, [m/s]

W_{str} = Wind sheltering coefficient [-]

w_{air} = humidity ratio of air, [kg water/kg dry air]

$w_{surface}$ = humidity ratio of saturated air at the lake surface, [kg water/kg dry air]

z = lake depth, [m]

z_{epi} = Thickness of the epilimnion layer, [m]

$z_{M,\ epi}$ = Depth of the center of mass of the epilimnion, [m]

$\Delta z_{M,\ z}$ = Distance from the layers center of mass to the bottom of the epilimnion, [m]

Δx = horizontal center to center distance between adjacent heat exchanger tubes, [mm]

Δy = vertical center to center distance between adjacent heat exchanger tubes, [mm]

α_{sed} = sediment thermal diffusivity, [m^2/day]

β = thermal expansion coefficient, [K^{-1}]

β_w = water surface absorption coefficient = 0.4 [-]

ε = effectiveness of the heat exchanger [-]

ε_{water} = emissivity coefficient of water = 0.97 [-]

σ = Stefan Boltzmann constant, [$5.67 * 10^{-8}$ $W/m^2 \cdot K^4$]

μ = extinction coefficient of water, [m^{-1}]

ρ = density, [Kg/m^3]

`

θ = ice/water overlapping angle, [radians]

τ = Wind shear stress, [N/m^2]

Subscripts

fluid = Heat exchanger fluid

freeze = Freezing point

hx = Heat exchanger

i = Inside

o = Outside

sed = Sediment

water = Lake water

weq = Water equivalent

ws = Water-sediment layer

`

1.

INTRODUCTION

1.1. Overview of Surface Water Heat Pump Systems

Surface water heat pump (SWHP) systems are essentially a combination of heat pump and a system for exchanging heat with a surface water body such as a lake, pond, or river. A surface water body is used as a heat source and/or sink for one or more heat pumps providing building heating and/or cooling. These systems can be either open or closed loop systems.

Open-loop surface water heat pump (SWHP) have been in use since 1940s (Mitchell and Spitler 2013). These systems utilize surface water bodies like ponds, lakes and rivers as a heat source or sink for heating/cooling applications. Open loop systems have water intake structure from which the water is withdrawn from the depth of a water body, exchanges heat through a heat exchanger on dry land and discharges the water back to the water body. The point of withdrawn and the point of discharge will be located in a surface water body at a considerable distance.

Closed loop SWHP systems have been installed for commercial purposes since the 1970s (Johansson 1983). Closed loop systems utilize ponds, lakes and reservoirs with no or very low inflows and outflows. Closed loop systems consist of surface water heat exchangers (SWHE) submerged in a water body and a loop connecting the heat exchanger and the heat pump, through which heat transfer takes place to or from the water body. Most commonly used SWHEs are coiled high-density polyethylene (HDPE) pipe and metal flat plate heat exchangers (e.g. SlimJim ®). This thesis work is focused only on close loop SHWP systems in which a SWHE is

`

submerged in a pond, lake or reservoir. Unless otherwise specified, all three types of surface water bodies will be referred as ‘lakes’ in rest of this thesis document.

Air source heat pumps that reject or extract heat from ambient air are conventionally used heat pump systems worldwide. Most of the times it is difficult for an air source system to operate at an optimal design temperature, because of the fluctuation of air temperature over a day. The high outdoor dry bulb temperature during cooling mode and low outdoor dry bulb temperature during heating mode makes the system less effective. On the other hand, the surface water bodies maintain a relatively stable source/sink temperature at significant depths that makes SWHP systems to perform with higher efficiency than air source systems during much of the year. Unlike air temperatures, temperatures in the bottom region of deep lakes are warmer in winter and colder in summer. The bottom temperatures do not have direct impact of ambient air temperatures. This makes the heat transfer more effective because of relatively low difference between source/sink temperature and temperature of a conditioned space.

The heat transfer between a SWHE and a lake is driven by the lake temperatures at the depth where the heat exchanger is located. A crucial point for an accurate design and energy analysis of a surface water heat pump system is proper knowledge of the lake temperatures at the heat exchanger depth. Climate conditions, weather and bathymetry of a lake have prominent influence on the temperature characteristics of surface water bodies. The data and procedures to design and analyze air source heat pump systems have been studied extensively over many years. ASHRAE (2009) contains a huge set of statistical temperature and humidity data for 5564 locations around the world including 1085 locations in the United States. The data is available for both annual and monthly peak conditions. The monthly values are useful when the time of occurrence of annual peak load does not correspond to the occurrence of peak design temperature. Despite growing interest in SWHP systems, there is a paucity of standard design data and procedures to aid engineers to efficiently design and analyze the system. Only few

`

limited water temperature data sets are available (Hattemer and Kavanaugh 2005) and year-to-year variations further complicate and limit the use of such historical data for design purposes.

The sufficient length of a SWHE to sustain acceptable water temperatures for the heat pump is determined by knowing the overall heat transfer coefficient of the heat exchanger. The inside convective resistance, the conductive resistance of the pipe material and the outside convective resistance are the components which contributes for the overall heat transfer coefficient. The water temperatures surrounding a heat exchanger have profound influence on outside convective resistance and thus heat transfer between heat exchanger and lake water. Furthermore, the ice formation at the outside surface of the heat exchanger also affects the heat transfer. The ice formation may occur under low temperature conditions during winter and high heat extraction rates.

From the description provided so far, we can understand that it is critical to know the lake water temperatures at the heat exchanger depths to design SWHP systems. One of the possible ways is to acquire experimental water temperature measurements for the lakes. However, having the water temperature measurements seems to be successful to some point and limit the systems to only for the sites for which we have experimental data. Moreover, it leaves us with the question of what if a system is to be built on any other lakes that is not in the existing experimental database. For example, there are 11,378 lakes in the size range of 25 acres to 247 acres in the United States as estimated by Lehner and Döll (2004). The measured data sets are likely to cover only certain lake sizes, locations and limited to certain period. Since each lake is unique, the measured data alone are rarely sufficient and it makes difficult for an engineer to design and analyze the system. Therefore, a possible alternative is a lake model that can predict water temperatures with reasonable accuracy across depth and time for various lake sizes and locations. This thesis aims to develop robust lake model in order to predict the lake temperatures and to couple this with a surface water heat exchanger model, which can serve as a basis for a

`

design engineer to design and evaluate the SWHP systems. Next is a brief basic overview of the subsequent chapters.

1.2. Thesis Objectives and Scope

Chapter 2, 3 and 4 discusses about the literature review and development of lake model and SWHE model. The works described here in these chapters have been developed and written in collaboration with my colleague Krishna C. Bashyam. Hence, these chapters will be in identical to the literature review, lake model and SWHE model development chapters in Bashyam (2013).

Chapter 2 presents the literature review that discusses about what attempts have previously been made in the field of lake modeling and surface water heat exchanger modeling. To develop a robust model, a comprehensive grasp of previously developed lake models in the literatures are necessary to ensure model quality while maintaining its simplicity. The extensive literatures available in the field of lake modeling have been narrowed down to 1-D numerical modeling techniques in this chapter. Also, considerable literatures are presented in this chapter related to surface water heat exchanger modeling.

Chapter 3 presents the major portion of this thesis work. The chapter starts with the discussion of underlying physics in the heat transfer mechanisms of a lake. The following sections discuss about the assumptions, equations, model solution techniques developed in the 1-D numerical lake modeling. In addition, it discusses about modeling of different surface water heat exchanger types such as spiral-helical, flat spiral, vertical-horizontal slinky coil and flat plate. The algorithm developed to predict exiting fluid temperatures (ExFT), entering fluid temperatures (EFT) and heat transfer rate during ice-free and ice formation conditions are explained. Finally, the comprehensive validation of the lake model and SWHE model are presented. The lake model has been comprehensively validated with 13 different lakes across

`

United States. However, validation of only one lake is presented here. Furthermore, the validation of heat exchanger model with the experimental results obtained from OSU research pond located in Oklahoma is also presented.

Chapter 4 presents the complete structure of the stand-alone FORTRAN lake model coupled with the heat exchanger model. It explains the inputs/outputs and a brief description of each subroutines developed in the FORTRAN model. Furthermore, it presents a detailed flow chart to explain the algorithm of lake model coupled with SWHE model.

Chapter 5 describes about how the lake model and SWHE model is implemented in EnergyPlus environment as a separate module. The lake model and SHWE inputs needed to run the simulation of surface water heat pump system in EnergyPlus are discussed. Since the developed lake model is a daily time step model, special attention is paid to explain how the daily time step lake model is handled in an hourly time step EnergyPlus environment.

In Chapter 6, stand-alone FORTRAN model is used to investigate the lake temperature variation in a lake when it is loaded with heat rejection or extraction. The purpose of this study is to provide guidelines to a design engineer to assist them in selecting the maximum capacity of a lake that produces acceptable SWHP system performance. The case study has been performed separately for heat rejection and extraction cases using strip mall and apartment building loads. The analysis includes different lake sizes and placing it in different locations. The allowable rate of heat rejection and extraction are obtained from the study that causes the temperature variation of 1°C and 2 °C. Furthermore, the maximum heat rejection rate that partially destroys the temperature stratification of a lake is also analyzed.

Chapter 7 proposes the meteorological-data-and-model-driven procedure to predict design temperatures for different lakes sizes and heat exchanger depths for the locations across United States. The uncertainties in the design temperature prediction contributed by the model

`

and using TMY-type weather file are discussed. The design temperatures generated are presented through a series of isotherm plots that represents annual maximum and minimum temperatures of a lake at certain heat exchanger depths.

Final chapter of thesis summarizes the results and conclusions of every other chapter. Additionally, suggestions are recommended for future research in order to improve the model accuracy.

`

2.

LITERATURE REVIEW

The literature review of lake model and SWHE model has been performed in collaboration with my colleague Krishna Conjeevaram Bashyam. Hence, the sections of this chapter will be similar to the literature review sections in Bashyam (2013) thesis documentation.

2.1. Existing Lake Models

In recent years, several studies have been carried out in the field of lake modeling and number of lake models has been developed aimed for the purpose of ecological study. These models are mostly one-dimensional and can predict vertical temperature profiles that evolve with time. Some examples of one dimensional model are Imberger et al. (1978), Ford and Stefan (1980), Saloranta and Andersen (2007). There are also sophisticated models which may have large number of inputs and dimensionality greater than one such as Dargahi and Setegn (2011), Hayter et al. (1998) , Ji et al. (2001), Blumberg and Mellor (1987) and Hamrick (1992).

The 2D or 3D lake models may predict the lake temperatures more accurately than a 1D model. Nevertheless, these models are not necessarily useful for simulating SWHP systems because that they require large number of inputs and high computational time. Sometimes a design engineer may not easily access the required inputs to simulate a lake. From a design engineer perspective a model should take feasible number of inputs and less computational time. In such a way, the literature search has been narrowed down to the studies pertinent to 1D lake modeling.

`

In addition to the one-dimensional models listed above, work has been carried out by a number of other authors like Tucker and Green (1977), McCormick and Scavia (1981) and Sengupta et al. (1981). Saloranta and Andersen (2004) and Saloranta and Andersen (2007) have provided a detailed documentation of one such comprehensive 1D lake model. A lengthy research program directed by Professor H.G. Stefan at the University of Minnesota perhaps best illustrates the incremental developments in the field of lake modeling which is described further below. The work of Professor H.G Stefan and the work of Saloranta and Andersen (2004) were heavily utilized for developing the lake model described in this paper. All 1-D lake models in the literatures introduced before discretizes the lake into several depth layers to numerically calculate the temperature profile and assumes the vertical temperature transport by eddy diffusion except for Ford and Stefan (1980) which assumes temperature transport by molecular diffusion. Eddy diffusion approach requires calculation of eddy diffusion coefficients as a function of depth and time. The eddy diffusion coefficients represent the rate of heat and mass transfer through turbulent diffusion vertically within a lake.

Ford and Stefan (1980) initially developed a model to simulate temperatures and stratification in small lakes using an integral energy approach. This approach finds the depth in a lake where the wind balances the potential energy available from the natural stratification. This depth represents the upper mixed or epilimnion region and below this depth are the stratified metalimnion and hypolimnion regions. The model allowed only molecular diffusion in the thermocline and hypolimnion regions, but was able to predict the temperatures reasonably when validated against three lakes whose surface areas vary from (72- 447 acres) and depths from (9.1 – 27.4 m).

Riley and Stefan (1988) developed the MINLAKE program which utilizes a one-dimensional lake model based on the integral energy approach by Ford and Stefan (1980) to simulate temperatures and water quality to predict eutrophication in lakes. The model considers

`

the effect of eddy diffusion for temperature transport and calculates separate eddy diffusion coefficients for the epilimnion and hypolimnion layers. The MINLAKE program was developed with an intention to be applicable in predicting both water temperatures and water quality for temperate lakes with different bathymetries. The model considers the effect of mixing, stratification, inflow and outflow in lakes but does not consider the formation of ice/snow cover on the lake surface.

Gu and Stefan (1990) enhanced the existing MINLAKE program to predict the lake temperature characteristics under ice and snow conditions. They considered the importance of sediment heat transfer, which was not considered in the earlier version of the MINLAKE models. They also calculated the new heat transfer rates between the lake surface and the atmosphere when the surface of the lake is frozen, thus extending the MINLAKE program to simulate year round lake temperatures. Gu and Stefan (1990) validated the enhanced MINLAKE model with the experimental temperatures from Lake Calhoun in Minnesota (surface area 403 acres; maximum depth 27 m) with a good level of accuracy. Ellis et al. (1991) calculated the eddy diffusion coefficients for lakes under ice/snow cover based on their measurements from a small lake in Minnesota. Fang and Stefan (1996) developed a correlation to predict the eddy diffusion coefficients for lakes under ice/snow cover based on the results from Ellis et al. (1991).

The lake models discussed to this point do not consider the effects of surface water heat exchangers (SWHE) on lake temperatures. However, there are some less comprehensive lake models that can account for the effects of SWHE submerged in a lake. Pezent and Kavanaugh (1990) developed a model to simulate lakes as heat sources/sinks for heat exchangers with water source heat pump systems based on the solar pond model by Srinivasan and Guha (1987) and river/reservoir model by Raphael (1962). The model was developed to predict lake temperatures in the southern warm climatic regions and does not consider the formation of surface ice on the water body. The lake is initially divided into three stratification regions (epilimnion, metalimnion

`

and hypolimnion) with pre-defined region thicknesses. The model does not consider the effects of wind stress on stratification and the mechanism of temperature transport by turbulent diffusion. The seasonal variation in the stratification is calculated based on experimental observations of certain lakes in Alabama. With all these assumptions, the model could only match the temperature profile for a lake in Alabama in the epilimnion and hypolimnion regions. It could not follow the experimental temperature profile in the thermocline region reasonably and had a maximum temperature difference of around 7 °C in the thermocline region.

Chiasson et al. (2000) developed a one dimensional shallow pond model with an SWHE to serve as a supplemental heat rejecter for ground source heat pump systems. The model includes the heat transfer effects by the heat exchanger in calculating the pond temperatures. The model was developed for shallow ponds that were assumed to be well mixed, thus there was no need to determine stratification. The pond heat exchangers were "slinky" configurations of HDPE pipe placed either horizontally or vertically in the pond.

2.2. Existing Surface Water Heat Exchanger Models

Modeling surface water heat exchanger is the most critical part of SWHP system. The heat transfer between a lake and heat exchanger depends on the geometry of the surface water heat exchanger. Surface water heat exchangers (SWHE) may take a number of forms. Many SWHE have been formed from HDPE or other piping. These include piping laid flat on the bottom of the lake or embedded in the lake bottom (Svensson and Sorman 1983), slinky coils (Chiasson et al. 2000), spiral-helical coils and flat spiral coils (Hansen 2011). Another common SWHE is the vertical flat plate (Slim Jim®).

In current practice, the most commonly used SWHE seem to be spaced bundles and vertical flat plates, and these are the only configurations treated in the current model. The spaced bundles might be called "stacked spiral" or "spiral-helical" heat exchangers as each horizontal

`

layer is a spiral connected either at the outside or inside to the layer above. Other than the work by them, there have been no published studies on such configurations, though Prabhanjan et al. (2004) and Ali (2006) presented measurements and correlations for submersed helical coils.

Hansen (2011) conducted experimental tests in a 1.2-hectare (3 acre) pond, measuring overall thermal resistance and then deriving correlations to calculate outside heat transfer coefficients for heat exchanger types which include spiral-helical coils, flat spiral coils, vertical and horizontal slinky coils, loose coils and metal flat plate heat exchangers. In order to estimate the outside convective resistance, the inside convective resistance for the coils was estimated with convection correlations (Rogers and Mayhew 1964; Salimpour 2009) that considered the effect of tubing curvature. Flat plate heat exchangers are commonly constructed from spot-welding two panels together, welding the edges and expanding the gap between the plates. The resulting gap between the panels forms one or more flow paths or non-circular and irregular cross-section. For the flat plate heat exchangers, inside Nusselt number is calculated based on the Dittus-Boelter (Incropera and DeWitt 1996) correlation for straight pipes.

During high heat extraction, the outer surface of the heat exchanger can get low near freezing temperatures and forms ice on the heat exchanger. There are no specific literatures to focus on SWHE coil freezing. However, there are freezing models developed for thermal storage systems. (Silver et al. 1989; Jekel et al. 1993 and Neto and Krarti 1997). The techniques used in these thermal storage models can be used in our ice-on-coil model.

`

3.

LAKE SIMULATION MODEL

The development of the one-dimensional lake model has been performed in collaboration with my colleague Krishna Conjeevaram Bashyam. Hence, several sections of this chapter will be similar to the lake model development chapter in Bashyam (2013) thesis documentation

3.1. Lake Physics

Water density is a non-linear function of temperature; it increases with decrease in temperature until 4°C (39°F) and decreases below 4°C (39°F). In other words, when the water cools below 4°C (39°F), instead of getting denser, the water gets less dense. The variation of water density with respect to temperature is shown in Figure 3-1. This unique temperature/density relationship of water is the main reason for temperature stratification in the lakes. When the surface water is cooled and reaches the temperature of 4^0C (39°F), it sinks down to the depth of a lake and reaches the bottom because of its high density at 4^0C (39°F). On the other hand, if bottom water is heated, it has the tendency to rise due to less density at temperatures higher than 4^0C (39°F).

`

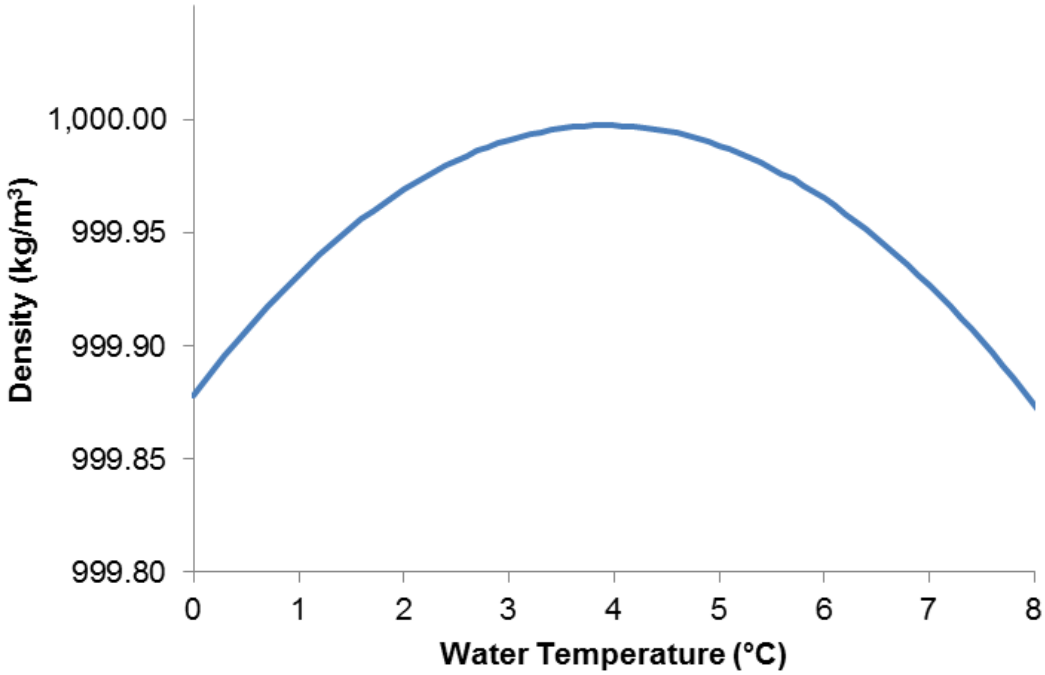

Figure 3-1 Density of water as a function of temperature

Thermal characteristics of the lakes vary along the depth and with time due to continuous process of heating and cooling the lake water. Shortwave solar radiation and conduction from sediment to the lake are different sources of lake heating. The mechanisms that remove the heat from the lake include the longwave radiation emitted from the surface to the atmosphere and convection of heat from the lake surface to the cold air above it. Most portion of solar radiation is absorbed by the lake surface and remaining penetrates towards the water column. In summer, the less dense and warm water floats on the surface of the lake while the cold and denser water remain below the surface of the lake. After summer, the surface water gets cool in fall due to radiation and evaporation losses. They become denser than the water below and sink through the water column that mixes the lake. Eventually in winter, the surface water cools further but become less dense and forms an inverse stratification because of different density behavior of

`

water below 4 ^{0}C. Figure 3-2 shows the experimentally measured temperature profiles of Ice Lake located in Minnesota.(WOW 2011)

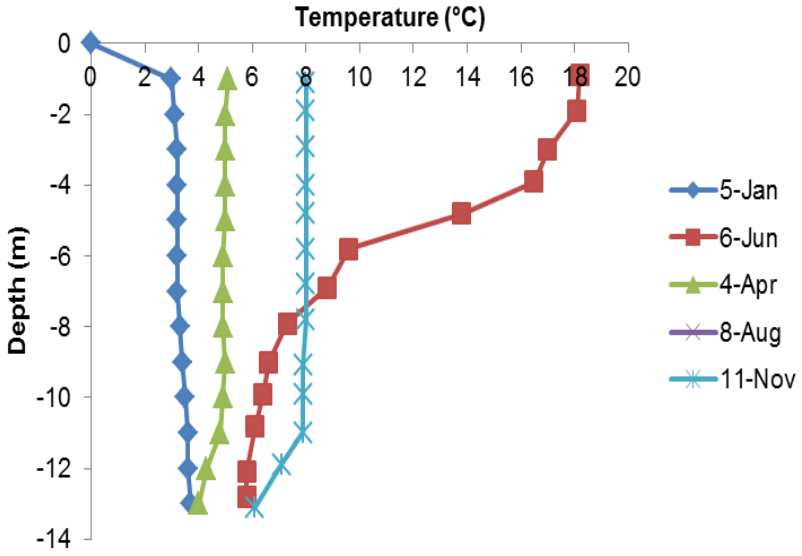

Figure 3-2 Lake temperature profiles of Ice Lake, MN

Thus, the seasonal temperature variation across the depth stratifies the lake into three distinct regions epilimnion, metalimnion (thermocline) and hypolimnion. The epilimnion is the upper well-mixed surface layers which have constant temperature profile (Imberger and Hamblin 1982).In the temperature profile on June 6(Figure 3-2) epilimnion depth is observed from surface till 2 m depth. In stagnant water bodies without inflows and outflows, the most important action causing lake motion and mixing is wind. The influence of wind on the surface exerts momentum and turbulent kinetic energy which mixes some portion of the water column and forms the epilimnion layer. The epilimnion depth depends on the strength of the dissipation of the kinetic energy. The water layers below the epilimnion layer resist wind mixing forces in deep lakes whereas the combined action of solar penetration till the bottom of the lake and wind mixing are strong enough to cause the de-stratified constant temperature profile in the shallow lakes.

`

The metalimnion and the hypolimnion are the layers below epilimnion which resist wind mixing forces in deep lakes. The metalimnion layer starts from the point where the temperature and density changes sharply and the temperature gradient in this region are typically greater than 1°C m^{-1}. The temperature in the thermocline region changes rapidly with depth. In the temperature profile on June 6 (Figure 3-2) thermocline depth is observed approximately from 2 m to 10 m depth. The hypolimnion is the bottom cold region, which has high-density water. For example it can be observed on June 6 at the depth below 10 m. The mixing in the hypolimnion region is through the diffusion of turbulent kinetic energy through the depth called eddy diffusion. In the case of deep lakes, the influence of wind to mix the entire water column is less because the temperature and density changes rapidly in the thermocline region of large lakes and separates the epilimnion and hypolimnion regions (Imberger et al. 1978)

3.2. Lake Model Development

It appears from the discussion of literatures in the preceding section that several options are available in developing a lake model. These different lake simulations are developed for ecological modeling, which may require detailed inputs and high computational time. Aside from practical feasibility, if we build similar kind of lake model, then many of the features may turn out to be a wasted effort and may not be necessarily useful for design and energy analysis. From the practical standpoint, a design engineer must need a tool that requires less computational time and less number of inputs. Therefore, the crucial work of this study would be to render the model, which requires less number of feasible inputs and less computational time by balancing the accuracy.

The underlying model assumptions required to build such a model are explained initially before the lake model development to ensure that the model is still valid for the intended use and

`

it is not oversimplified. This lake model is developed as a stand-alone FORTRAN model. It is a 1-D daily time-step model that can predict the lake temperatures as a function of depth and time.

Lake Model assumptions

1. The first assumption is that the lake model predicts daily lake water temperatures using daily meteorological input data.
2. The lake model is a one-dimensional model, which implies that the temperature and density varies only in the vertical direction and no horizontal variations. The model can predict the lake temperatures across the depth of a lake. For most of the lakes, the horizontal temperature gradients are weak; communicated over several kilometers and get damped by horizontal advection and convection quickly within few hours in a day (Hamilton and Schladow 1997). Thus, 1-D model is valid for daily time step simulation.
3. The surface water body is assumed to contain no inflows (from streams or rivers) and outflows.
4. The effect of wind shielding and lake shading due to presence of tall structures or vegetation around the water body are neglected.
5. The volume of the surface water body is assumed to be constant throughout and change in water levels due to evaporation and precipitation is neglected.
6. Variation of lake turbidity with time is neglected and an average value of lake turbidity is assumed throughout the simulation.

The above set of assumptions are made in the model development is to accommodate the input data that most design engineers can access.

3.2.1. Governing equations

Equation (1) is a 1-D differential governing equation adopted from Hondzo and Stefan (1993) solved in an iterative scheme for the simulation of heat transfer process in the lake model

`

to calculate the lake temperatures across the depth. Most of the theoretical framework and the assumptions for the lake model are adopted from Saloranta and Andersen (2004).

$$A(z)\frac{\partial T}{\partial t} = \frac{\partial}{\partial z}\left(K_z A(z)\frac{\partial T}{\partial z}\right) + \frac{Q^*}{\rho_w c_{p,w}} \quad (1)$$

Where,

A is the horizontal area of the lake in [m^2], T is the water temperature as a function of both depth and time in [°C], k_z is the vertical eddy diffusion coefficient in [m^2/day], Q^* is the heating rate of a surface water body at a depth z by solar radiation, sediments and heat exchangers in [W/m^3], ρ_w is the density of water in [kg/m^3] and $c_{p,w}$ is the specific heat capacity of water [J/kg·°C]

The governing equation was developed to its final form by considering constant values for water density and specific heat (Dake and Harleman 1969). Although, this assumption resulted in a simplified form of the governing equation; the flow of energy in this equation is not completely balanced. However, this small energy imbalance has little impact on the calculated water temperatures.

3.2.2. Heat transfer mechanisms at the surface

The net heat energy input to a surface water body includes the heat exchange with the atmosphere and within the water column. Hence, the heating rate (Q) for the surface water body has to be calculated separately at the water body surface and within the water column. The net heat added at the surface of the water body is,

$$Q = \frac{q''_{net-surface} A_{surface}}{V_{surface}} \quad (2)$$

Where,

`

$q''_{net\text{-}surface}$ is the net heat flux available at the surface of the water body in [W/m^2] , $A_{surface}$ is the surface area of the water body in [m^2] and $V_{surface}$ is the volume of the surface layer of the water body in [m^3].

Description on lake surface, surface layer and volume of the surface layer are described under the "spatial discretization" section. The heat transfer due to convection, evaporation and radiation are the major mechanisms which decide the surface temperatures of the lake (Edinger et al. 1968). The effects of convection, evaporation and longwave radiation occurs only at the surface and it is highly important factors, which decide the temperature stratification. The flux incoming to the surface is taken as positive. The governing equation describing the heat transfer mechanisms at the surface is

$$q''_{net-surface} = q''_{sw-surface} + q''_{lw} - q''_{conv} - q''_{e} \quad (3)$$

$q''_{net\text{-}surface}$ the net heat flux on the lake surface in [W/m^2], $q''_{sw\text{-}surface}$ is the heat flux due to short wave radiation incident on the pond surface in [W/m^2], q''_{lw} is the heat flux due to net long wave radiation incident on the pond surface in [W/m^2], q''_{conv} is the convective heat flux from the pond surface to the atmosphere in [W/m^2], q''_{e} is the evaporative heat flux from the pond surface to the atmosphere in [W/m^2]

It is important to note that, this energy balance is applied only during ice-free conditions at the surface. The mechanism of heat exchange with the atmosphere at the lake surface differs when it is frozen. The surface heat fluxes acting on the ice-cover surface is discussed later in the ice formation section.

3.2.2.1. Shortwave radiation

Dake and Harleman (1969) explains that lake receives maximum amount of heat energy by the fraction of solar radiation absorbed at the surface. A portion of shortwave radiation gets

`

absorbed at the surface and remaining amount has the ability to penetrate into the water column. Shortwave radiation penetrated into the water column is discussed later in Section 3.2.3.1.

The heat flux due to incident shortwave radiation absorbed by the lake surface is calculated as

$$q''_{sw-surface} = q''_{solar}(1-\rho'_w)\alpha_w \qquad (4)$$

Where, q''_{solar} is the incident solar radiation on the lake in [W/m^2], ρ'_w is the water surface reflectivity coefficient [-] and α_w is the water surface absorption coefficient [-]. Albedo or coefficient of reflectance or reflectivity (ρ') determines the fraction of radiation reflected from the surface. The reflectivity of water usually changes with time of a year and it depends on solar altitude angle, cloud cover, latitude and surface conditions. However, we implemented the approach from Hamilton and Schladow (1997) which calculates daily average reflectivity based on day of a year that is more suitable for the daily time step lake model.

$$\rho'_w = 0.08 + 0.02\left[\frac{2\pi n}{365} \pm \frac{\pi}{2}\right] \qquad (5)$$

Where, n is the day of the year $1 \leq n \leq 365$, and the term $\pi/2$ added for the northern hemisphere and subtracted for southern hemisphere. The ratio of absorbed to the transmitted radiation at the surface of the water body is surface absorption coefficient for water (α_w). The surface absorption coefficient is assumed to be equal for all lakes and is taken as 0.4 (Dake and Harleman 1969; Hondzo and Stefan 1993)

3.2.2.2. Longwave radiation

The incoming long-wave radiation from the atmosphere to the lake heats the lake surface, while the radiation reflected back from the surface cools the lake surface. The later one is the significant mechanism of heat loss from the lake. In accordance with the Stefan-Boltzmann law,

`

the amount of radiation from any surface depends on the emissivity of that surface and the fourth power of its absolute temperature. The heat flux due to net long-wave radiation determined in the model from the difference between incoming and reflected radiation similar to Chiasson et al. (2000).

$$q''_{lw} = h_{lw}\left(T_{sky} - T_{surface}\right) \tag{6}$$

Where, q''_{lw} is the net long wave radiative heat flux on the lake surface [W/m^2], h_{lw} is the linearized radiation coefficient [W/m^2·K], T_{sky} and $T_{surface}$ are the sky temperature and lake surface temperature in [K] respectively.

$$h_{lw} = 4\varepsilon_w \sigma \left[\frac{T_{surface} + T_{sky}}{2}\right]^3 \tag{7}$$

T_{sky} is calculated from Swinbank (1963) equation

$$T_{sky} = 0.552 \bullet T_{surface}^{1.5} \tag{8}$$

Where, ε_w is the emissivity coefficient of water taken as 0.97 (Omstedt 1990) and σ is the Stefan-Boltzmann constant [5.67 * 10^{-8} W/m^2·K^4].

3.2.2.3. Convection and evaporation

Heat is added or lost from the lake surface by convection, which is driven by air-water temperature difference (free convection) and wind force acting on the surface (forced convection). Evaporation in a lake involves the contribution of both free and forced convection process in which heat is removed from the lake (Adams et al. 1990). Like the long-wave radiation, evaporation is another significant process that contributes for heat loss. Evaporation is driven by a vapor pressure gradient between the lake surface and the dry air above the water

`

surface. The phase change of water from liquid to water results in the latent heat loss from the lake surface.

There are profusion of correlations on evaporation and convection available in literature. These correlations are developed for various applications and for different surfaces including swimming pools, heated plate and small ponds. Several such equations have been found and implemented in the lake model. The accuracy of each model is tested with 14 different lake sizes, based on the accuracy of water temperature prediction. A detailed uncertainty analysis of all these models is presented in Bashyam (2013). From this study, the best suitable and generally applicable sub-models are identified depending on lake size.

Based on our validation and sensitivity studies on 14 different lakes, the surface convection correlation by Molineaux et al. (1994) has been identified to predict lake temperatures with a good level of accuracy. The study and the validation details of the different surface convection and evaporation correlations are presented in detail in Bashyam et al. (2013b). The correlation by Molineaux et al. (1994) to calculate the convective heat transfer coefficient is given below,

$$h_c = 3.1 + 2.1W \tag{9}$$

Where, h_c is the convective heat transfer coefficient in [W/m^2·K] and W is the wind speed over the lake surface in [m/s]. Finally, the heat flux due to convection at the lake surface can be computed by

$$q''_{conv} = h_c (T_{air} - T_{surface}) \tag{10}$$

Where, $A_{surface}$ is the surface area of the lake in [m^2] and T_{air} is the ambient air temperature in [°C].

`

The equation to calculate the evaporative heat flux (q''_e) based on the convective heat transfer coefficient from Molineaux et al. (1994) can be written as,

$$q''_e = \frac{h_{fg} h_c}{c_{p,air}} (w_{surface} - w_{air}) \quad (11)$$

Where, h_{fg} is the latent heat of vaporization [J/kg], w_{air} is the humidity ratio of the ambient air in [kg water/kg dry air], and $w_{surface}$ is the humidity ratio of the saturated air at the lake surface in [kg water/kg dry air].

3.2.3. Heat transfer mechanisms in the sub-surface

The heating rate at a particular depth z_1 inside the water body is calculated as,

$$Q = \frac{q''_{sw-abs}(z_1) A(z_1) + q''_{sediment}(z_1) A(z_1) + q_{hx}}{V(z_1)} \quad (12)$$

The heat transfer regimen in the sub-surface layers differs from the lake surface due to the process of heat advection and diffusion in the sub-surface waters. Heat can be transported through the water column by the following processes

- Penetration of short-wave radiation
- Turbulent diffusion process
- Sediment heat transfer
- Heat transferred from heat exchanger

3.2.3.1. Shortwave penetration

As we already discussed a small portion of shortwave solar radiation is absorbed at the surface while remaining penetrates to an appreciable depth in the water column. The penetration of solar radiation is influenced by the amount of suspended solids in a lake. The changes in transparency of water alter the attenuation of solar radiation and thus the amount of heat added to

`

the sub-surface layers. . The amount of penetration is increased with the transparency of a lake which is characterized by light extinction coefficient is a function of Secchi depth. The lake model requires a single average extinction coefficient that is calculated from average annual Secchi depth value given as the input

$$\mu = \frac{1.86}{d_{\sec chi}} \tag{13}$$

Secchi depth (d_{secchi}) is a depth at which a Secchi disk gets disappeared into a water column.(Hondzo and Stefan 1993). Secchi disk is used to measure the transparency of water column in a lake. In the lake model, the penetration is calculated based on Lambert – Beer law that is a function of lake turbidity. The expression is adopted from Stefan et al. (1983), which calculates the exponential decay of short wave radiation down the water column.

The radiative heat flux incident at a depth z inside the water column is calculated as,

$$q''_{sw}(z) = q''_{solar}(1-\rho'_w)(1-\alpha_w)\exp(-\mu z) \tag{14}$$

Where, μ is the extinction coefficient of water in [m^{-1}], which is a function of lake turbidity. The amount of radiative heat flux absorbed at a particular depth is calculated by the difference in the incident radiative heat flux at consecutive depths.

3.2.3.2. Sediment heat flux

Heat transfer from the ground (sediment) is a significant source of heat gain to a surface water body during ice cover period (Gu and Stefan 1990). Lake simulation model incorporates the theory of sediment heat transfer from Fang and Stefan (1996) and the solution methodology from Saloranta and Andersen (2004). A one-dimensional, unsteady heat conduction equation is solved to calculate the sediment temperatures as given in Equation 15. The sediment and the water column are discretized into a number of layers and the partial differential equation is solved

`

by implicit finite difference method using Tri-diagonal matrix algorithm (TDMA). The procedure for solving the one-dimensional sediment heat conduction equation is similar to the solution methodology of the one-dimensional temperature transport equation discussed in section 3.2.4

$$\frac{\partial T_{sed}}{\partial t} = \alpha_{sed} \frac{\partial^2 T_{sed}}{\partial z_{sed}^2} \tag{15}$$

Where, T_{sed} is the sediment temperature in [°C], z_{sed} is the depth of the sediment column in [m] and α_{sed} is the thermal diffusivity of the sediments [m^2/day]. The ground temperature is assumed to remain constant at 10 m below the lake bottom and hence the sediment temperature profiles are solved in 10 m thick sediment columns. The temperature of the sediment surface in contact with water (topmost sediment layer) is assumed to be equal to the water temperature at that depth. The heat flux at the water-sediment (*ws*) interface depends on the temperature gradient $\left(\frac{\partial T_{sed}}{\partial z_{sed}}\right)_{ws}$ and the interface area.

$$q''_{sediment}(z_1) = -k_{sed}\left(\frac{\partial T_{sed}}{\partial z_{sed}}\right)_{ws}\left(\frac{A_{sed}(z_1)}{A(z_1)}\right) \tag{16}$$

Where, k_{sed} is the thermal conductivity of the sediments = 1.01 [W/m·K] (Fang and Stefan 1996), $A(z_1)$ is the horizontal area of the surface water body at a particular depth in [m^2], $A_{sed}(z_1)$ is the water-sediment interface area in [m^2]. The water-sediment interface area at a particular depth is approximately calculated from the difference in the horizontal area of the surface water body at consecutive depths.

3.2.3.3. Eddy diffusion

Mixing dynamics by eddy diffusion for a surface water body varies with the surface area and other lake physiological factors. Correlations to predict the eddy diffusion coefficient are calculated on the experimental observation either on a single surface water body or on water

`

bodies of similar characteristics. The lake model contains eleven different correlations to calculate the eddy diffusion coefficients for surface water bodies of varying sizes (shallow ponds, small, medium and large lakes). Based on validation and sensitivity studies the eddy diffusion correlation by Gu and Stefan (1995) is found to predict the temperatures of shallow ponds with good level of accuracy. The study of different eddy diffusion models, their validation results and the criteria used in selecting the best models are discussed in Bashyam et al. (2013b). The eddy diffusion coefficient (k_z) determined by Gu and Stefan (1995) for shallow wastewater ponds is,

$$k_z = \min\left[k_{z\max}, k_{z\max} CN^{-1}\right] \tag{17}$$

Where, k_{zmax} is the maximum hypolimnion eddy diffusion coefficient [m^2/day], N is the stability or the Brunt Vaisala frequency[$1/s^2$] , C is a constant taken as $8.66*10^{-3}$ [s^{-1}] (Jassby and Powell 1975). The stability frequency is estimated by Hondzo and Stefan (1993) as,

$$N = \sqrt{\left(\frac{g}{\rho_w}\right)\left(\frac{\partial \rho_w}{\partial z}\right)} \tag{18}$$

Where, g is the acceleration due to gravity in [m/s^2] and ρ_w is the density of the water [kg/m^3]. The maximum hypolimnion eddy diffusion coefficient (k_{zmax}) represents the diffusion coefficient that in a lake observed during weakly stratified or un-stratified conditions. This occurs due to extensive turbulent mixing of water layers. Hondzo and Stefan (1993) derived the relationship between k_{zmax} and the surface area of the lake as,

$$k_{z\max} = 0.048\left(A_{surface}\right)^{0.56} \tag{19}$$

The expression for k_{zmax} holds good for large ponds and lakes. In case of shallow ponds, which tend to stratify and un-stratify many times in a day, there does not appear to be a standard procedure to estimate the value of k_{zmax}. Gu and Stefan (1995) estimated the k_{zmax} value of

`

0.1m^2/day for their 1.8 acre rectangular wastewater pond in Minnesota with a maximum depth of 1.8 m. In the case of the 3 acre research pond maintained by the Oklahoma State University in Oklahoma, which has a maximum depth of 3.8 m the values of k_{zmax} was estimated as 5 m^2/day.

3.2.3.4. Heat transferred from heat exchanger

The SWHE placed in the lake results in heat being added to the lake during heat rejection and removed from the lake during heat extraction, which in turn depends on building loads. The distribution of heat rejection/extraction from the lake to the water layers in the lake depends on the depth at which the heat exchanger is placed. The calculations pertinent to heat exchanger heat transfer are discussed in the SWHE implementation section.

3.2.4. Model solution

3.2.4.1. Spatial discretization

The lake model solves the governing equations by using a series of discretized horizontal layers characterized by depth from the surface. The model uses a constant and a fixed layer thickness for the entire depth of the lake. The area and volume of each layer is calculated based on the morphometry of the lake basin from the equations given by Johansson et al. (2007). Temperature and heat flux calculations are performed separately for each water layer. The layer thickness, horizontal area and eddy diffusion coefficient are evaluated at the layer interfaces, while the layer temperature and volume represent the mean value of the layer and hence can be assumed to be in the middle of a layer. The illustration of the spatial discretization is shown in Figure 3-3

`

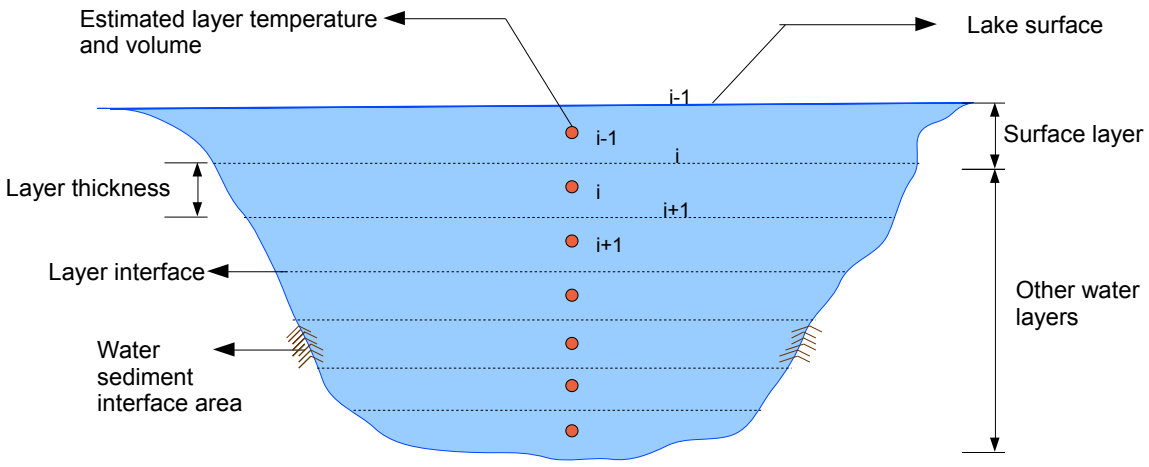

Figure 3-3 Illustration of the model spatial discretization

3.2.4.2. Formulation of TDMA coefficients

The discretization of a lake into set of one-dimensional layers results in a set of linear equations, one for each layer. Since the concentration of a variable in a layer is dependent on its concentration in the adjacent layers, the set of equations are arranged in tri-diagonal matrix form and solved simultaneously. Integrating the one dimensional advection diffusion equation (Equation 1) between z_i and z_{i+1}, where i is the layer number, gives

$$\int_{z_i}^{z_{i+1}} A\frac{\partial T}{\partial t}dz = \int_{z_i}^{z_{i+1}} \frac{\partial}{\partial z}\left[k_z A\frac{\partial T}{\partial t}\right]dz + \int_{z_i}^{z_{i+1}} A\frac{Q}{\rho_w C_p}dz \tag{20}$$

$$V_i\frac{dT_i^*}{dt} = \left[k_z A\frac{\partial T}{\partial t}\right]_{z_{i+1}} - \left[k_z A\frac{\partial T}{\partial t}\right]_{z_i} + V_i\frac{Q_i^*}{\rho_w C_p} \tag{21}$$

Where, V_i is the volume of the layer i, $T_i^* = V_i^{-1}\int ATdz$ is the volume averaged temperature for /;the layer i, and $Q_i^* = V_i^{-1}\int AQdz$ is the layer averaged heating rate. The heat balance terms in Equation 3 are transformed to a set of linear derivatives over the time and depth increments Δt

`

and Δz. Since, the lake model operates on a daily time step the time increment Δt is taken to be 24 hours.

$$\frac{V_i}{\Delta t}[T_i^*(t) - T_i^*(t-\Delta t)] = k_{z(i+1)}A_{i+1}\frac{1}{\Delta z}[T_{i+1}^*(t) - T_i^*(t)] - k_{z(i)}A_i\frac{1}{\Delta z}[T_i^*(t) - T_{i-1}^*(t)] + V_i\frac{Q_i^*}{\rho_w C_p} \quad (22)$$

Simplifying the equation by dividing with $V_i/\Delta t$ and introducing the notations

$$\alpha_i = \frac{\Delta t}{\Delta z}\frac{A_i}{V_i}k_{z(i)}$$

$$\beta_i = \frac{\Delta t}{\Delta z}\frac{A_{i+1}}{V_i}k_{z(i+1)}$$

$$\gamma_i = 1 + \alpha_i + \beta_i$$

Equation 22 can be rearranged to get a generalized TDMA equation for a layer *i*.

$$-\alpha_i T_i^*(t) + \gamma_i T_i^*(t) - \beta_i T_{i+1}^*(t) = T_i^*(t-\Delta t) + \frac{Q_i^*}{\rho_w C_p}\Delta t \quad (23)$$

Assuming zero diffusion between the air-water interface and zero bottom area of the lowermost layer we get $\alpha_1=\beta_n=0$. Therefore, for the surface the TDMA equation transforms into

$$(1+\beta_1)T_1^*(t) - \beta_i T_2^*(t) = T_1^*(t-\Delta t) + \frac{Q_{surface}^*}{\rho_w C_p}\Delta t \quad (24)$$

Where, $Q^*_{surface}$ is the heat added at the surface layer from the surface heat flux terms. The lake model uses the temperature of the previous time step and the local heating of the layers of the current time step to calculate the current time step temperature values.

`

Since, many of the terms in the heat flux equations require the water temperature term for the current time step to be known, an iterative method is employed to calculate the water layer temperatures. At the start of every time step the lake model assumes the previous day temperature profile and surface ice thickness value (if ice is predicted on the lake surface) to calculate the current day heat flux terms. From the heat flux terms, the current day temperature profiles and surface ice thickness are calculated. Once again, the heat flux terms for the current time step are computed from the calculated temperature profiles and ice thickness values. This procedure is repeated until both the temperature and ice thickness values of the current time step converges. Separate convergence criteria are set up for water layer temperature and surface ice thickness terms.

3.2.5. Lake mixing

The major reason for lake stratification and de-stratification is lake mixing. It is the process by which the cold water from the bottom region of the lake is scooped up and mix with the epilimnion region. Two distinct mixing mechanisms are implemented in the lake model one is the wind induced mixing and the other one is convective mixing due to buoyancy.

3.2.5.1. Wind mixing

Mixing usually takes place in lakes by wind acting on the surface of the lake and natural convective mixing due to buoyancy differences. Inflows and outflows can also mix the lake to certain extent in lakes which are connected to rivers or streams. But lake model does not account for this type of mixing. Wind mixing during open water season determines the depth of the epilimnion (upper-mixed layer); large exposure to wind causes deeper thermoclines in large lakes and complete de-stratification in small lakes. The kinetic energy imparted by the wind near the surface causes the water to move in the downward direction and in turn, the bottom waters move towards the surface.

`

The amount of mixing depends on the balance between kinetic energy input to the lake and stability of the lake. Stability of the lake is the potential energy required to overcome the buoyancy forces due to stratification and completely mixes the water column without addition or loss of heat i.e. to transform density stratified water layers into new uniform density water layers. (Lawson and Anderson 2007).

A sharp change in the density of water layer at the base of epilimnion identifies the mixed layer depth, calculated at the point where the turbulent kinetic energy and potential energy gets balanced. Ford and Stefan (1980) and Saloranta and Andersen (2004) explained the algorithm for this process based on turbulent kinetic energy (TKE) input to a lake, potential energy (PE) and a relative balance between them.

Total kinetic energy [J] available at the surface of the lake due to the wind shear stress,

$$TKE = W_{str} A_{surfce} \sqrt{\frac{\tau^3}{\rho_w}} \Delta t \qquad (25)$$

Where, τ is the wind stress [N/m^2] and W_{str} is the wind sheltering coefficient [-].

The wind stress is calculated as

$$\tau = \rho_{air} C_d W^2 \qquad (26)$$

Where, C_d is the drag coefficient [-], which is dependent of the surface wind speed.

Wind sheltering coefficient determines the fraction of TKE available at the lake surface. Wind sheltering effect on lakes is due to the proximity of trees and buildings, and the coefficient includes this effect by reducing the wind speed acting on the surface of the lake.Hondzo and Stefan (1993) defined it as a coefficient which defines the wind-affected portion of the lake surface area and it is calculated from an empirical relationship

`

$$W_{str} = 1.0 - \exp(-0.3 \bullet A_{surface}) \quad (27)$$

Potential energy, the lifting energy used to mix the layer below the epilimnion with the epilimnion, which increases the mixing depth, is calculated as,

$$PE = g\Delta\rho_w \frac{V_{epi}V_z}{V_{epi}+V_z}\left(z_{epi} + \Delta z_{M,z} - z_{M,epi}\right) \quad (28)$$

Where, $\Delta\rho_w$ is the density gradient between the epilimnion and the layer below that needs to be converted to uniform density [kg/m^3], g is the acceleration due to gravity in [m/s^2], z_{epi} is the thickness of the epilimnion layer in [m], $\Delta z_{M\text{-}z}$ is the distance from the layer's center of mass to the bottom of the epilimnion layer in [m], and $z_{M\text{-}epi}$ is the depth where the center of mass of the epilimnion layer is present in [m]. V_{epi} is the total volume of the epilimnion layers in [m^3]. V_z is the volume of the water layer at depth z in [m^3].

If TKE > PE then, the mixing depth is increased by mixing the first layer below the epilimnion and volume averaging the temperature of whole epilimnion water column. This is to form a new uniform density distribution in the mixed layer. The potential energy consumed by that layer is deducted from the TKE input available. The process is continued until the TKE is dissipated into the lake as internal energy and no more TKE is available to mix the water layers i.e. the mixing depth is calculated at the point when TKE < PE.

3.2.5.2. Convective mixing

In addition to wind mixing, there will be change in mixed layer depth and thermocline position due to buoyancy instabilities. During the period of lake cooling, the heat is lost from the surface water, becoming denser than the water at the bottom. Therefore, there will be complete inversion, where the incoming cool water from the surface replaces the warmer water at the bottom and start to mix vertically called convective mixing.

`

Once the water temperatures are calculated, the lake model checks for the presence of an unstable density condition (i.e.) the presence of higher density water layer(s) above the lower density layers. If such condition occurs, water layer(s) with unstable density profiles are mixed completely with the first stable layer below the unstable layers. This is handled in the simulation by numerically mixing the unstable adjacent water layers i.e. by calculating volume weighed average temperatures of unstable water layers which represents the uniform average density mixed water layers.

3.2.5.3. Turnover

Lake Turnover is the process in which the whole water column reaches a uniform temperature of maximum density near 4 °C. Physically, similar to convective mixing, during cold season the cooler surface water creeps into the water column causing warmer and less dense hypolimnion water to the surface. Eventually, the continuous surface cooling results in mixing of entire water column and forms a complete mixed layer by destroying the stratification. The description above holds for a process called 'fall turnover' while there may be another turnover called 'spring turnover' in few other climates. Spring turnover is when the ice formed on the surface melts and whole water column become warm to its maximum density near 4 °C. The process is numerically handled by fixing a constraint of 3.98 °C (T_{maxrho}) to a surface water temperature. If $T_{surface} > T_{maxrho}$, then all the layers below the surface whose temperature jumped over 3.98 °C including the surface layer are set to 3.98 °C. The energy gained by this process is distributed exponentially to the water column in a same way as shortwave radiation is attenuated.

3.2.6. Sub-model to calculate surface ice thickness

Ice cover on the surface of the lakes during winter is significant part of lake modeling because it alters the heat and momentum transfer at the air-water interface. The lake model includes a sub model for the calculation of ice formation, ice growth and melting of ice on the surface of the lake. The thermodynamic focuses in the sub model are

`

- Calculation of heat released during freezing in order to calculate the initial ice formation
- Calculation of ice temperature to calculate the amount of ice growth from the initial ice thickness
- Calculation of surface heat fluxes acted which induces melting of ice from the top surface
- Calculation of conduction heat fluxes at the bottom ice-water interface which induces the bottom melting of ice.

The 1-D model concepts adopted from Saloranta (2000) are applied on ice, snow-ice and snow formation this sub-model.

3.2.6.1. Ice formation

Ice formation is dependent on water and air temperatures. During early winter, when air temperatures are adequately low (≤0˚ C), the surface water temperatures can cool below freezing point of water and initial ice is formed on the surface. The is handled in the lake model in such a way, if the surface water temperature goes below freezing temperature then the ice formation is triggered. The water which is below 0˚ C gives up the 'heat of crystallization' when it is transformed to initial ice layer on the surface and it is calculated in the model as

The thickness of ice formed at the very first time in a lake (start of the freeze-up period) is calculated from $Q_{deficit}$ (Saloranta and Andersen 2004).

$$Q_{deficit} = \frac{\rho_w V_z c_{p,w} \left(T_{freeze} - T_{w,z}\right)}{\Delta t} \qquad (29)$$

Where, $q_{deficit,i}$ is the sensible heat deficit in the i^{th} sub-cooled water layer converted to latent heat of ice in [W], $T_{water,i}$ and V_i are the temperature in [°C] and volume of the i^{th} water layer in [m^3] respectively, $c_{p,water}$ is the specific heat capacity of water [J/kg·°C] and Δt is the model time step in [s].

`

$Q_{deficit}$ is calculated for each super cooled water layers and initial ice thickness (H_{ice}) is calculated from the sum of $Q_{deficit}$ released by all super cooled layers. H_{ice} represents the volume of ice per unit area

$$m_{ice} = \frac{Q_{deficit,sum}\Delta t}{L_{freeze}} \tag{30}$$

$$H_{ice} = \frac{m_{ice}}{\rho_{ice} A_{surface}} \tag{31}$$

Where, m_{ice} is the mass of ice formed on the lake surface in [kg], $q_{deficit,sum}$ is the sum of heat deficit in all the sub-cooled water layers in [W], and L_{freeze} is the latent heat of freezing of ice in [J/kg] and ρ_{ice} is the density of ice in [kg/m^3].

3.2.6.2. Ice growth

The duration and the maximum ice thickness formed for the entire winter depend on the trend of air temperatures. Due to congelation of ice, ice thickness gets increased if there is a continuous ice formation on the surface. The effective ice thickness evolved from the previous day ice thickness is calculated as

$$H_{ice,new} = \sqrt{H_{ice}^2 + \frac{2k_{ice}}{\rho_{ice} L_{freeze}} \left(T_{freeze} - T_{ice}\right)\Delta t} \tag{32}$$

Where k_{ice} is the thermal conductivity of ice [W/m.K]. The temperature of ice (T_{ice}) is used in the equation to include the ice-atmosphere coupling and snow insulation effects thereby preventing the overestimation of the speed of ice growth as explained in Lepparanta (1991).

T_{ice} is calculated as

`

$$T_{ice} = \frac{pT_{freeze} + T_{air}}{1+p} \tag{33}$$

Where, p is a parameter calculated for snow-free in Equation 33 or snow-cover conditions in Equation 34.

$$p = \frac{1}{10H_{ice}} \tag{34}$$

$$p = \frac{\kappa_{ice} H_{snow}}{\kappa_{snow} H_{ice}} \tag{35}$$

Where, k_{snow} is the thermal conductivity of snow [W/m·K] and H_{snow} is the snow thickness [m]. The continuity condition is assumed such that the heat flux at the ice/air interface is equal to the heat fluxes through the ice and through the air and heat flux at the ice/snow interface is equal to the heat fluxes through the ice and through the snow. Snow on the ice surface form superimposed ice and increases the ice thickness which is due to the low conductivity of snow.

Large snowfall potentially increases the weight of the snow and if its crosses the weight of ice cover then lower part of snow is submerged into water. This eventually causes the formation of slush layer at ice-snow interface as water flooding occurs on top of the ice. Then snow-ice is formed from the freezing of slush. Thus snow ice formed is superimposed on ice growth and it is subtracted from the snow thickness (Lepparanta 1991). The amount of new snow-ice thickness which favored additional ice growth is calculated from the equation

$$H_{snow-ice} = \max\left[0, \left\{ H_{ice}\left(\frac{\rho_{ice}}{\rho_{water}} - 1\right) + H_{snow,weq} \right\}\right] \tag{36}$$

`

Where, $H_{snow\text{-}ice}$ is the thickness of snow-ice (slush layer) formed when water mixes with the snow in [m] and $H_{snow,weq}$ is the water equivalents of snow thickness in [m] and it is calculated as,

$$H_{snow\text{-}weq} = H_{snow}\left(\frac{\rho_{snow}}{\rho_{water}}\right) \tag{37}$$

Where, ρ_{snow} is the simulated bulk density of the snow cover in [kg/m^3].

Thermal conductivity of snow is calculated from Saloranta (2000)

$$k_{snow} = 2.2232(\rho_{snow})^{1.885} \tag{38}$$

The bulk density of snow has an initial value of 250 kg/m^3. If the air temperature is below the freezing temperature, snow density increases due to compaction of snow and the increased snow density is calculated using the equation given by Yen (1981).

$$\rho_{snow} = C_1\rho_{snow}\frac{H_{snow,weq}}{2}\exp(-C_2\rho_{snow})\exp\left\{-0.08\left(T_{freeze} - \frac{T_{ice}+T_{air}}{2}\right)\right\}.\Delta t \tag{39}$$

Where, C_1 and C_2 are empirical coefficients taken as 7.0 m^{-1}h^{-1} and 0.021 m^3/kg respectively (Yen 1981;Saloranta 2000). If air temperature is above the freezing temperature then the bulk density of snow is set to a maximum value of 450 kg/m^3.

The water layer beneath the ice tends to reduce the ice thickness by melting the ice from the bottom. The heat flux between the ice-water interfaces, which tends to reduce the ice growth, is calculated from the temperature difference between ice and water layer temperatures just beneath the ice. The net ice growth for the time step is calculated from the difference between the total ice thickness formed at the surface and the amount of ice melted from the bottom.

`

3.2.6.3. Ice melting

Ice layer formed on the surface partially absorbs the solar radiation similar to open surface water; the heat added through this absorption is the major reason for ice melting. Other factor that accelerates ice melting is the conductive heat flux from the lake water below ice. The net heat flux determines the rate of surface melting which is calculated from surface heat fluxes like convection, evaporation, net shortwave radiation and net long wave radiation. The fluxes towards the air-ice interface are taken as positive.

If the air temperature increases above the freezing point of water, surface melting is triggered in the model. Snow if present on the water body surface will melt completely before the melting of surface ice could begin. Since the reflectivity (albedo) of snow is high, the incident shortwave radiation penetrated into the ice layer is assumed to negligible (Launiainen and Cheng 1998). So snow layer is melted first and the remaining energy is used to melt the ice layer beneath the snow. In the same way, if the net surface heat flux is sufficient enough to melt the ice formed in a time step, the remaining flux is exponentially distributed to the warm the water layers below.

Shortwave radiation

A portion of shortwave radiation penetrated into the ice (only when no snow on the ice) plays a major role in melting of ice. It dominates the net surface heat flux, because the convective and evaporative heat fluxes are lower due to low air-water temperature difference. The net shortwave radiation at the surface during surface snow-ice conditions is calculated as,

$$q''_{sw-surface} = q''_{solar}(1-\rho'_{ice/snow})(1-\alpha_{ice}) \qquad (40)$$

Where, $\rho'_{ice,snow}$ is the surface reflectivity coefficient for a water body when it is covered by snow or ice. The bulk fraction of solar radiation penetrated into the ice is represented by α_{ice}. It is represented as 0.18 for clear sky conditions and linearly varies according to the cloudiness factor (N) calculated from equation below

`

$$\alpha_{ice} = 0.18\left(1 - \left[\frac{N}{10}\right]\right) + 0.35N \qquad (41)$$

Where, N is the cloudiness for a particular day [-]. The surface reflectivity and the solar absorptivity of snow are relatively high and therefore the value of α_{ice} is assumed to be zero during snow-cover period. Ice and snow surface have high reflectivity values compared with open water lake surface. $\rho'_{ice,snow}$ is primarily depends on ice/snow properties on the surface and it changes with incident angle of solar radiation. But then again, since it is a daily time step model, these values are assumed to be constant and taken as 0.77 for snow and 0.3 for ice respectively (Perovich 1996;Saloranta 2000)

Long-wave radiation

The effect of net long wave radiation is calculated from the difference of incoming long wave radiation from atmosphere and the amount emitted back from the surface. We calculate this from the equation given in Saloranta (2000) adopted from Omstedt (1990)

$$q''_{lw} = \varepsilon_w \sigma \left(T_{air}^4 \left(0.68 + 0.0036\sqrt{v_p}\right)\left(1 + 0.18\left(\frac{N}{10}\right)^2\right) - T_{w,surface}^4 \right) \qquad (42)$$

Where, a, b, c are empirical constants whose values are 0.68, 0.0036 and 0.18 and 'e' is the air water vapor pressure in [N/m^2].

Convective heat flux

The sensible (convective) heat flux at the ice surface is determined from the temperature differences as in equation

$$q''_{conv} = \rho_{air} c_{p,air} C_h \left(T_{air} - T_{surface}\right) W \qquad (43)$$

`

Evaporative heat flux

Evaporative heat flux at the ice surface is determined from the humidity ratio differences as in equation

$$q''_e = h_{fg}\rho_{air}C_e\left(w_{surface} - w_{air}\right)W \quad (44)$$

Where, ρ_{air} is the air density in [kg/m^3], $c_{p,air}$ is the specific heat capacity of air [J/kg·K] and C_h and C_e are the convective and evaporative heat exchange coefficients between air and ice surface assumed to be 0.00175 (Crocker and Wadhams 1989)

Bottom ice-water flux

The temperature of water beneath the ice layer is above zero (relatively warmer than the surface), which generates heat flux from the water to ice bottom surface. The heat flux at the ice-water interface reduces the ice growth at the bottom of ice and thus counteracts ice growth. This conductive heat flux in the model is simplified as the temperature difference between ice and second water layer from the bottom of ice (Saloranta and Andersen 2004)

3.3. Surface Water Heat Exchanger Model Development

This section has been written in collaboration with my colleague Krishna Conjeevaram Bashyam Hence, several portions of this section will be identical with the SWHE model development chapter discussed in Bashyam (2013) thesis

The SWHE model predicts the exit fluid temperatures (ExFT), entering fluid temperatures (EFT), heat exchanger heat transfer and buoyancy force (during the conditions of heat exchanger ice formation) for four types of SWHE's namely spiral-helical, flat spiral, vertical-horizontal slinky coil and flat vertical plate heat exchangers. This paper provides a detailed discussion about the model and correlations used for a spiral-helical coil heat exchanger.

`

The SWHE model utilizes separate algorithms in calculating the ExFT, EFT and heat transfer during ice-free and ice formation conditions. They are explained in detail in sections 5.1 and 5.2 respectively. The SWHE model operates on a daily time step takes in the lake temperatures at the heat exchanger depth (predicted by the lake model), daily averaged building loads and heat pump performance as inputs in its calculation.

3.3.1. Outside Convective Heat Transfer

The model uses the outside Nusselt number correlation developed by Hansen (2011) for spiral-helical coils to calculate the outside heat transfer coefficient. This outside Nusselt number correlation is calculated at the film temperature surrounding the heat exchanger and is dependent on the outside tube diameter and the vertical and horizontal spacing between the adjacent tubes.

$$Nu_o = 0.16\left(Ra_o^*\right)^{0.264}\left(\frac{\Delta y}{d_0}\right)^{0.078}\left(\frac{\Delta x}{d_0}\right)^{0.223} \tag{45}$$

Where, Nu_o is the outside Nusselt number and Ra_o^* is the modified Rayleigh number calculated at the outside film temperature ($T_{film\text{-}o}$). $T_{film\text{-}o}$ is the average temperature value between the heat exchanger tube and the surrounding water in [°C]. Δy and Δx are the vertical center-to-center distance and horizontal center-to-center distance between the adjacent heat exchanger tubes in [mm] and d_o is the heat exchanger outside tube diameter in [mm].

The modified Rayleigh number is calculated as,

$$Ra_o^* = \frac{g\beta q''_c L^4 \,\mathrm{Pr}}{k_{f,o}\vartheta_{f,o}^2} \tag{46}$$

`

Where, g is the acceleration due to gravity in [m/s^2], β is the thermal expansion coefficient in [1/K], $k_{f,o}$ is the thermal conductivity of the surface water in [W/m·K] and $\upsilon_{f,o}$ is the water kinematic viscosity in [m^2/s], all calculated at the outside film temperature ($T_{film\text{-}o}$). q''_c is the coil heat flux in [W/m^2], L is the characteristic length of the heat exchanger coil in [m] and Pr is the Prandtl number.

The outside convective heat transfer coefficient is calculated based on the outside Nusselt number as shown in equation below.

$$h_0 = \frac{Nu_o k_{f,o}}{d_0} \tag{47}$$

3.3.2. Inside Convective Heat Transfer

The inside Nusselt number correlation for spiral-helical is obtained from Salimpour (2009). The thermal parameters are calculated based on the inside fluid temperature (T_{fluid}) which is the average temperature value between the heat exchanger EFT and ExFT for the time step.

$$Nu_i = 0.152 De^{0.431} \mathrm{Pr}^{1.06} p^{-0.277} \tag{48}$$

$$De = \mathrm{Re}\sqrt{\frac{d_i}{d_{c_o}}} \tag{49}$$

$$p = \frac{\Delta y}{\pi d_{C_o}} \tag{50}$$

`

Where, Nu_i is the inside Nusselt number, De is the Dean number, p is the dimensionless pitch ratio, d_i is the inside tube diameter in [mm], d_{c_o} is the heat exchanger outside coil diameter in [mm] and Re is the Reynolds number. The inside convection coefficient is calculated from the inside Nusselt number.

$$h_i = \frac{Nu_i k_{f,i}}{d_i} \tag{51}$$

Where, $k_{f,i}$ is the thermal conductivity of the heat exchanger fluid in [W/m·K].

3.3.3. Heat Transfer between HX Fluid and the Lake

The thermal resistances of the pipe material and inside/outside interfaces are calculated first. Then, the global heat transfer coefficient is calculated from the total resistance.

The global heat transfer coefficient (UA_{hx}) for the heat exchanger is then calculated.

$$UA_{hx} = \frac{1}{R_i + R_{tube} + R_o} \tag{52}$$

Where, R_i, R_{tube} and R_o are the inside, heat exchanger tube and outside convection resistances in [°C/W] respectively.

At any given time step the heat transfer behavior is modeled as a steady state. The heat transfer between the heat exchangers and the surrounding water body is calculated as,

$$q_{hx} = \varepsilon\, \dot{m}_{hx}\, c_{p,hx}(EFT_i - T_{lake})(N_{circuits}) \tag{53}$$

Where, q_{hx} is the heat exchanger heat transfer in [W], ε is the effectiveness of the heat exchanger calculated based on the NTU formulation, $\dot{m}_{hx}$ is the mass flow rate of the heat exchanger fluid [kg/s] and $c_{p,hx}$ is the specific heat capacity of the heat exchanger fluid [J/kg·°C], EFT_i is the heat exchanger entering fluid temperature for the i^{th} time step, T_{lake} is the daily average lake

`

temperature for the depth range where the heat exchangers are placed in [°C] and $N_{circuits}$ is the number of SWHE circuits placed in the lake.

Finally, the heat exchanger entering and exiting fluid temperatures for the i^{th} time step are calculated by the following equations

$$EFT_i = T_{lake} - \frac{q_{hx}}{\varepsilon C_{\min}} \tag{54}$$

Since we assume the temperature of the fluid is uniform across the length of the heat exchanger, the exiting fluid temperature is a simple equation of fluid properties, lake temperature and entering fluid temperature.

$$ExFT_i = EFT_i - \frac{q_{hx}}{C_{\min}} \tag{55}$$

3.4. Ice-on-coil Model Development

Conditions such as high heat extraction rates along with low lake water temperatures might cause the formation of ice around the SWHE's. The formation of ice reduces the heat transfer, and as this condition prevails, the ice around the heat exchangers gradually builds up, creating a buoyant force, which tends to lift the heat exchangers to the surface of the lake. Excessive formation of ice around the heat exchanger coils could cause the overlapping of ice between adjacent coils. This phenomenon completely limits the exterior convection by the heat exchanger, which further reduces the heat transfer. A numerical model to simulate the development, growth and melting of ice around the SWHE's and thereby to calculate the resultant heat transfer during freezing and melting conditions has been developed. The model also simulates ice-overlapping phenomenon for spiral-helical coil heat exchangers. This model

`

follows the approach similar to the ice-on-coil model for a thermal storage tank by Neto and Krarti (1997).

The rate of formation, growth and melting of ice varies along the length of a SWHE. For coil type SWHE configurations (spiral-helical, flat spiral and slinky coil), the model divides the coil into a number of segments along the length and the ice thickness is calculated for each segment at every time step. In the case of vertical flat plate heat exchangers, the model considers it as a single entity.

This section discusses the model developed for a coil type SWHE. Energy balance is performed at every coil segment to calculate the ice thickness. Figure 3-4 shows a cross sectional view of a coil segment and a thermal network diagram during ice formation period.

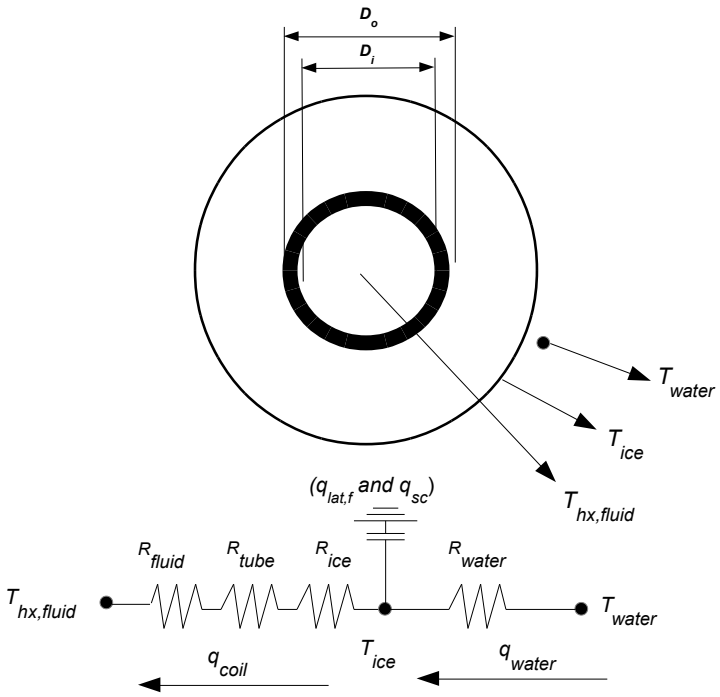

Figure 3-4 Cross-sectional view of a heat exchanger coil segment and thermal network for ice formation period

`

The coil heat transfer is dependent on the ice thickness and vice-versa. Hence, the ice-on-coil model iteratively calculates the segment ice thickness until an energy balance is achieved. The following energy balance equation is applied to each coil segment '*j*'.

$$q_{coil,j} = q_{water,j} + q_{lat,f,j} + q_{sc,j} \tag{56}$$

Where,

$q_{coil,j}$ is the heat transfer between the heat exchanger fluid and the ice/water interface in [W]

$q_{water,j}$ is the heat transfer between water surrounding the heat exchanger segments and the ice/water interface on the heat exchanger in [W]

$q_{lat,f,j}$ is the latent heat to freeze the water or melt the ice formed at each segment in [W] and

$q_{sc,j}$ is the sensible heat to sub-cool the ice during freezing at each segment in [W]

The heat transfer between the ice/water interface and the heat exchanger fluid for every heat exchanger segment during the freezing period is calculated as,

$$q_{coil,j} = UA_{f,j}\left[T_{ice} - EFT_i\right] \tag{57}$$

T_{ice} is the temperature of ice at the ice-water interface (0°C (32°F)), *EFTj* is the heat exchanger entering fluid temperature for the j^{th} segment and UA_f is the overall heat transfer coefficient for the segment in [W/°C], which is calculated as,

$$UA_{f,j} = \frac{1}{R_{fluid} + R_{tube} + R_{ice}} \tag{58}$$

Where, R_{fluid}, R_{tube} and R_{ice} are the thermal resistances of the heat exchanger fluid, tube and the surrounding ice in [°C/W] respectively. The thermal resistances are given by the following equations.

`

$$R_{fluid} = \frac{1}{(2\pi - \theta_j) r_i L_{tube} h_{fluid}} \tag{59}$$

$$R_{tube} = \frac{\ln\left(\frac{r_o}{r_i}\right)}{(2\pi - \theta_j) L_{tube} k_{tube}} \tag{60}$$

$$R_{ice} = \frac{\ln\left(\frac{r_{ice}}{r_i}\right)}{(2\pi - \theta_j) L_{tube} k_{ice}} \tag{61}$$

Where, r_i, r_o and r_{ice} are the heat exchanger inside tube radius, outside tube radius and radius of the ice in [m] respectively. h_{fluid} is the fluid convective heat transfer coefficient in [W/m^2·K] and θ is the overlapping angle of ice in [radians] between the coil segments which are adjacent to each other. For a spiral helical coil, a coil segment could have a maximum of four adjacent segments depending on the location of the segment in the coil. The model includes a simple algorithm to calculate the overlapping angle for the spiral-helical coil configuration. It specifically assumes that every turn of the coil as one segment. Since the ice-overlapping angle is also dependent on the location of the coil segment, the model also assumes a pre-defined segment configuration. Though the definition and the assumption a typical coil segment is different between the overlapping angle algorithm and the rest of the model, the ice radius predicted in the ith segment by the ice-on-coil model is taken in as the ith segment value in the overlapping algorithm.The calculation of the overlapping angle is described in detail in (Neto and Krarti 1997). The model does not calculate the ice overlapping angle for the flat spiral and slinky coils due to their complicated geometry.

`

The heat transfer between the surrounding water around the ice to the ice/water interface ($q_{wat,i}$) can be calculated as,

$$q_{wat,j} = \left(2\pi - \theta_j\right) r_{ice} L_{tube} h_{wat-ice} \left(T_{water,j} - 0^{\circ} C\right) \tag{62}$$

Where, $h_{wat\text{-}ice}$ is the convective heat transfer coefficient at the ice/water interface in [W/m^{2}·K], $T_{water,j}$ is the water temperature surrounding each coil segment in [°C]. The latent heat to freeze the water around the coils $q_{lat,f,j}$ in [W] is given by,

$$q_{lat,f,j} = \frac{\Delta M_{ice,j}}{\Delta t} HF_{ice} \tag{63}$$

Where, $\Delta M_{ice,i}$ in [kg] is the mass of ice formed at the j^{th} segment during the daily time step Δt in [s] and HF_{ice} is the latent heat of freezing of ice in [J/kg].

The heat transfer to sub-cool the ice $q_{sc,j}$ in [W] is calculated as,

$$q_{sc,j} = \frac{\Delta M_{ice,j}}{\Delta t} c_{p,ice} \left(0^{o} C - T_{bulk}\right) \tag{64}$$

Where, $Total\Delta M_{ice,i}$ is the total mass of ice formed until the current time step, $c_{p,ice}$ is the specific heat capacity of ice in [J/kg·K], T_{bulk} is the bulk temperature for the ice formed in the current time step in [°C], and $T_{bulk,formed\ ice}$ is the bulk temperature for the ice formed till the previous time step in [°C].

Once, the ice thickness values of the heat exchanger segment is converged the heat exchanger ExFT for every segment is calculated as

$$ExFT_j = EFT_j + \frac{q_{coil,j}}{m_{fluid} c_{p,fluid}} \tag{65}$$

`

This procedure is repeated for all the coil segments. The calculated ExFT for a tube segment is taken as the EFT for the successive tube segment. The heat transfer from each tube segment $q_{coil,j}$ is summed up to calculate the overall heat transfer of the heat exchanger coil (q_{hx}).

During the ice melting period, heat transferred from the heat exchanger fluid is used to melt the ice surrounding the heat exchanger. The thermal network during the ice melt period is shown in Figure 3-5.

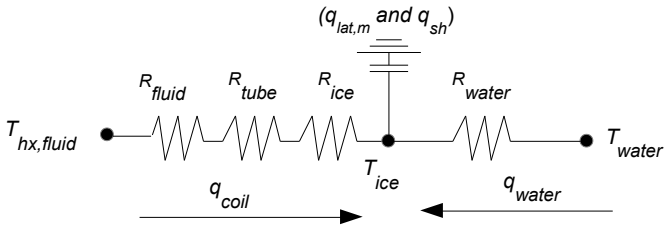

Figure 3-5 Thermal network for ice melt period

The model assumes the ice melting to take place in one direction, and the heat from the coil is applied to the outside surface of the ice. The heat balance equation during the ice melting period can be written as,

$$q_{coil,j} + q_{water,j} = q_{lat,m,j} + q_{sh,j} \tag{66}$$

Where, $q_{lat,m,j}$ is the latent heat to melt the ice around the tube segments in [W] and $q_{sh,j}$ is the sensible heat to increase the water bulk temperature above the freezing point in [W].

The heat transfer between the ice/water interface and the heat exchanger fluid for every heat exchanger segment during the melting period is calculated as,

$$q_{coil,j} = UA_{m,j}(EFT_j - T_{ice}) \tag{67}$$

`

$q_{lat,m,j}$ and $q_{sh,j}$ are calculated as.

$$q_{lat,m,j} = \frac{\Delta M_{water,j}}{\Delta t} HF_{ice} \tag{68}$$

$$q_{sh,j} = \frac{\Delta M_{water,j}}{\Delta t} c_{p,water}(T_{bulk} - 0^{o}C) \tag{69}$$

Where, $\Delta M_{water,j}$ is the mass of water in [kg] formed due to the melting of ice in the current time step Δt. The $ExFT_i$ can be calculated using Equation 65. This procedure is again repeated for all the coil segments.

In order to determine the separate and combined accuracies of the lake model and the surface water heat exchanger model three types of validations are performed.

- Validation of the lake model without the effects of the heat exchanger
- Validation of the surface water heat exchanger model
- Validation of the surface water heat exchanger model when coupled with the lake model

The lake model without the effects of the heat exchanger is validated with the experimental measurements from Ice Lake (validation of temperature and stratification) and a research pond maintained by the Oklahoma State University (OSU) (validation of surface ice thickness). Validation of the heat exchanger model is performed based on the experimental data obtained for a spiral-helical heat exchanger coil from the indoor heat extraction test performed in our test facility. Finally, the validation of the heat exchanger model when coupled with the lake model is performed based on the experimental data from a spiral-helical coil when tested in the research pond maintained by the OSU.

`

3.5. Results and Discussion

3.5.1. Lake water temperature validation

The lake model has been subjected to comprehensive lake temperature validation using the experimental temperatures of 13 different lakes across Unites States. The validation of Ice Lake one of the medium size lake is presented in this thesis. The discussion and the results of remaining validation are presented in Bashyam (2013). Ice Lake (45°18'55" N, 92°46'08" W) is located in the city of Grand Rapids in Minnesota which has a surface area of 17 Ha (41 acres) and depth of 16 m (52 ft). The experimental measurements of the lake is obtained from WOW (2012) and compared with the simulation temperatures. Since the meteorological parameters are significantly responsible for the water temperature profiles, the actual weather data of Grand Rapids is used in the lake model to simulate the water temperatures instead of typical meteorological weather data.

A comparison of model predicted temperatures with measurements have been made using daily water temperatures usually measured in mid-afternoon during summer season of Ice lake. Figure 3-6 shows the comparison of vertical temperature profiles for the months between June-September 2003.

The plot shows that the lake temperatures are highly stable so that the thermocline region is distinctive and shows strong stratified profiles through the summer season. The comparison shows that the results are promising because the differences between measured experimental and predicted results are within 1.5 °C. However, on a closer look, it can be seen that the thermocline region have the maximum error in the order of 3 °C. The sole reason for this high difference is due to inaccurate prediction of mixed-layer depth. For example, the temperature profile on August 25, the bottom depth of epilimnion is approximately at 4 m (13 ft) for the experimental

`

results but simulation predicted it as 4.8 m (16 ft) which produced high variation in the thermocline region.

Nevertheless, this variation is inevitable because the epilimnion depth is more sensitive to wind speed, which varies in small range over a day. Therefore, the variation of epilimnion over a day is inherent. The simulation represents the temperature profile of a day simulated using average wind speed for the day.

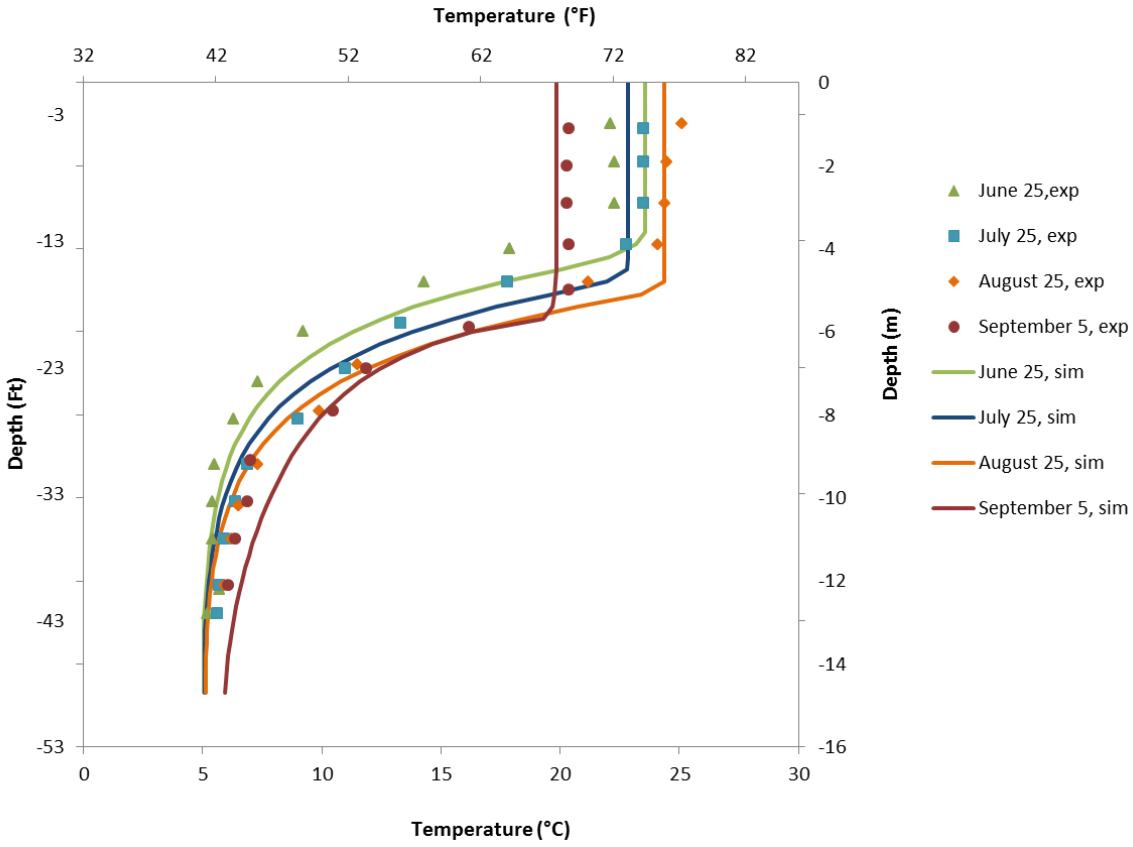

Figure 3-6 Comparison between the experimental and simulated temperatures for Ice Lake MN

`

3.5.2. Ice thickness validation

The research pond maintained by OSU in Stillwater OK is a small shallow pond with a surface area of 3 acres (1.2 Ha). The maximum depth of the pond at its full capacity is 3.81 m (12.5 ft). Ice thickness validation of OSU pond is shown in Figure 3-7. The model gives a reasonable match for the four experimental ice thickness measurements measured during the month of January and February 2011. The ice thickness is consistent with the trend of daily average air temperatures. The decreasing trend of ice thickness at the end of January 28 and January 29 is because of warm air temperatures of 9 °C and 10 °C. After January 30, there is sharp increase in the ice thickness and reaches the value of 5.2 in. (0.017 m) on February 3. This is because of sudden shift of warm air temperatures to freezing air temperature of -12 °C along with the snowfall of 2.4 in. (0.06 m). The snow mixed with the ice forms a slush layer that increased the ice thickness further.

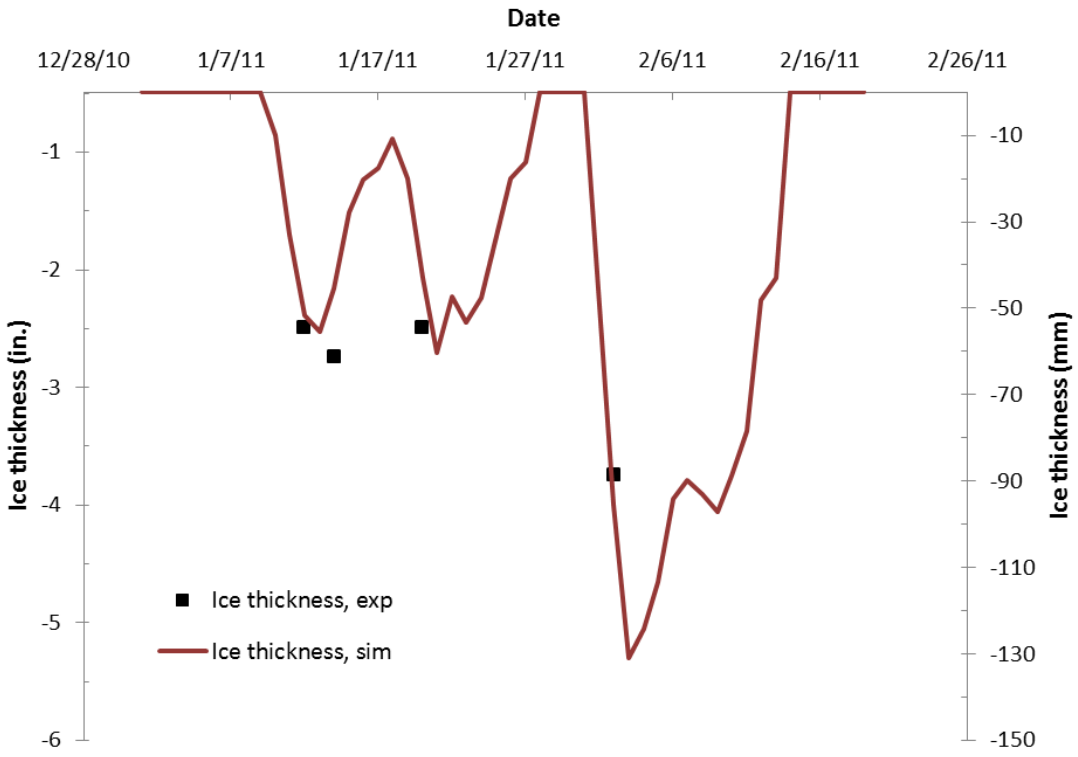

Figure 3-7 Ice thickness measurements compared with simulation results

`

3.5.3. Heat exchanger model validation

Two thermistor trees located in the deepest part of the OSU pond continuously record temperature data along the depth for every 15 minute intervals. One of the temperature trees is placed near the heat exchanger coils and the other is placed a certain distance downstream. Several experiments to calculate the amount of heat rejection to the pond by different heat exchangers with different geometric configurations have been conducted intermittently over a period of hours during the day.

The heat extraction tests are performed on a spiral-helical coil placed in an indoor test pool and subjected to a controlled environment. The test pool is of 4.3m (14 ft) in diameter and around 1.2m (4 ft) deep. The heat exchanger coil is suspended on a set of load cells to measure the buoyant force exerted during the ice formation around the coil.

The spiral-helical coil used in the validation both in the test facility, and in the OSU pond is made of high-density polyethylene plastic, and is 152.4 m (500 ft) long with a nominal diameter of ¾ inches (19.05 mm). The coil has an outside diameter of 2.4 m (7.9 ft) and inside diameter of 1.2 m (3.9 ft). The vertical and horizontal spacing set between adjacent coils are 2.63 inches (0.066 m) and 4.13 inches (0.0104 m). The supply and return temperatures were measured by thermistors embedded in the coil. The coil temperatures, heat exchanger loads and fluid flow rate were recorded at every 5 minutes.

The heat exchanger model is validated using the experimental results performed on a spiral-helical coil heat exchanger placed in an indoor test pool. The validation of the ExFT predicted by the model with the experimental data is shown in Figure 3-8 and the buoyancy force validation is shown in Figure 3-9. Unlike a lake, the temperature of the test pool varies greatly in response to the heat exchanger loads. With continuous heat extraction and with low pool temperatures ice formation occurs on the surface of the coil. With continuous heat extraction the

`

coil ice thickness increases, which increase the coil buoyancy force (phase I in Figure 3-9). With further increase in coil ice thickness, overlapping of ice between adjacent coil segments occurs. This overlapping increases the convective resistance, further reducing the coil heat transfer, which results in increased ice formation (phase II in Figure 3-9). The heating mode in the coil is reversed to melt the ice around the coils (phase III in Figure 3-9).

The heat exchanger model takes in the hourly averaged heat exchanger loads and pool temperature data as inputs to calculate the ExFT and coil ice thickness. The heat exchanger coil is divided into number of segments of equal length. For the calculation of the overlapping angle, the model assumes each coil turn as a separate segment. Since, the overlapping of ice around the adjacent coils reduces the convective heat transfer, the external convective heat transfer coefficient calculated using Hansen (2011) correlation is reduced by introducing a penalty function. The penalty to the heat transfer coefficient is given by

$$h_{o,effective,j} = h_{o,j}(1 - Penalty) \tag{70}$$

Where,

$h_{o,effective,j}$ is the exterior convective heat transfer coefficient for the j'th coil segment during the overlapping of ice [W/m^2]

$h_{o,j}$ is the exterior convective heat transfer coefficient for the j'th segment obtained from Hansen (2011). *Penalty* is the penalty coefficient for the segment which depends on the number of overlapping ice segments

The equation to calculate the penalty coefficient is obtained based on the sensitivity analysis,

$$Penalty = 0.187 \bullet (Number \quad of \quad overlapping \quad segments) \tag{71}$$

`

With the above assumptions, the model predicted ExFT closely matches the experimental temperature values as shown in Figure 3-8. The model slightly over predicts buoyancy force and predicts formation and complete melting of ice around the coils several hours before (18 hours before the initial ice formation and 9 hours before for the actual complete ice melt) than what is observed in the experiment, as shown in Figure 3-9. Overall, it follows a similar profile and exhibits the three phases approximately in the same time.

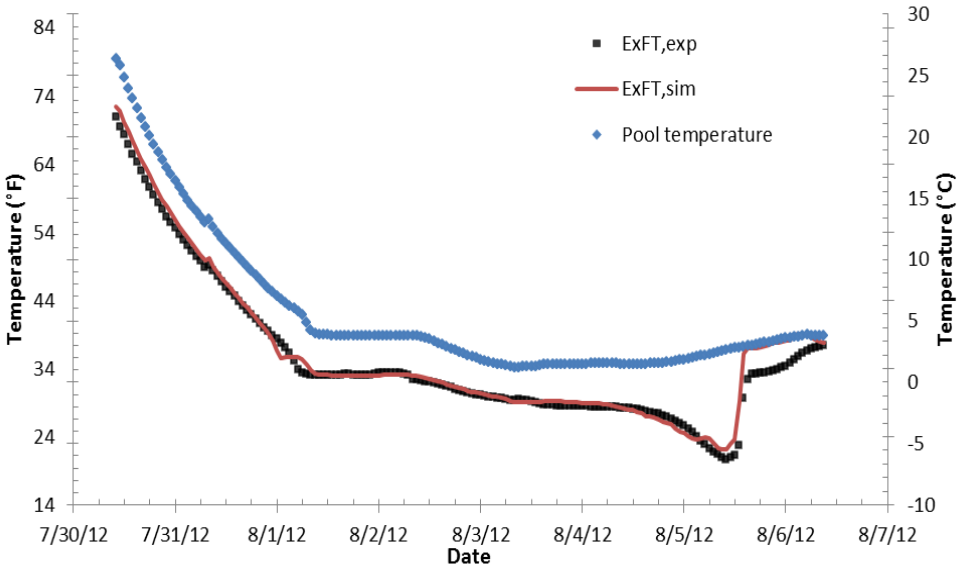

Figure 3-8 Comparison of the model and experimental ExFT for the spiral-helical coil heat exchanger placed in a test pool

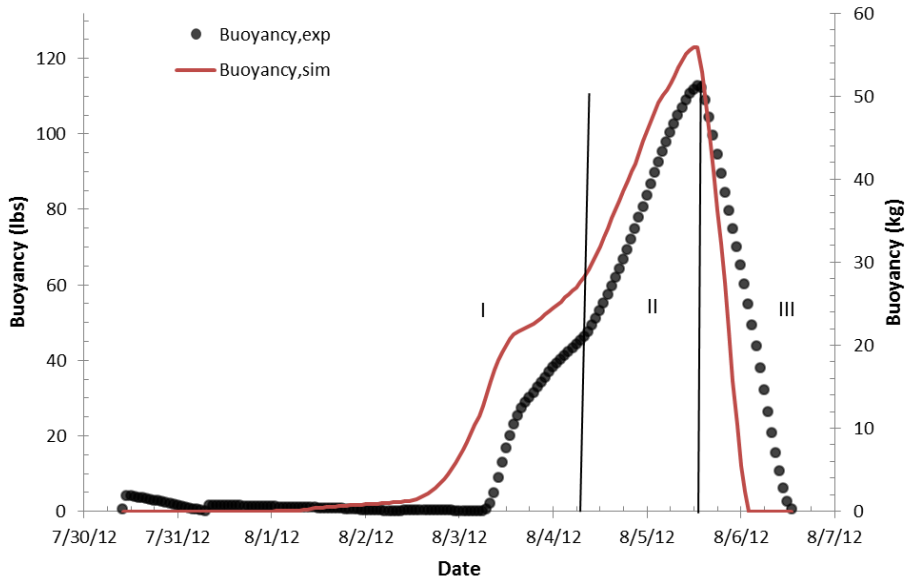

Figure 3-9 Experimental and model predicted buoyancy comparison

3.5.4. Validation of the SWHE model when coupled with the lake model

So far, we have validated the lake model and SWHE model and have presented the plots separately. In an effort to reconcile the two models, the validation of coupled model is discussed in this section. The validation of the SWHE model with the lake model is performed for the experimental results obtained with the spiral-helical coil tested in the research pond maintained by OSU. The comparison between the model predicted and experimental ExFT is shown in

Figure 3-10. The lake model runs on a daily time step while the heat exchanger model is modified to run on an hourly time step. The steep rise and fall of the ExFT predicted by the model is in response to the availability of the heat exchanger loads and change in the available daily averaged pond simulation temperatures. The ExFT predicted by the model closely matches with that of the experimental results. The slight under prediction between the model and the experimental ExFT is due to the slight difference between the simulated and actual pond temperature values.

`

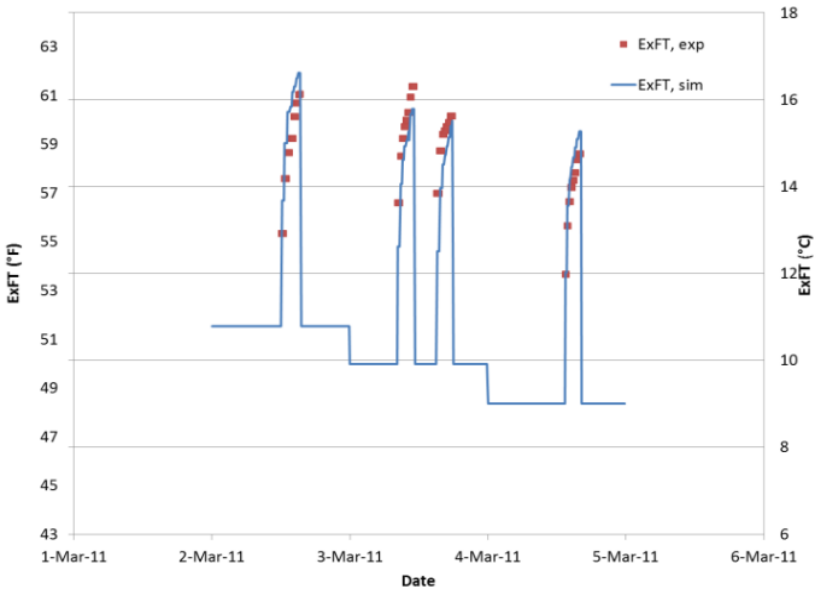

Figure 3-10 Comparison of the model and experimental ExFT for a spiral-helical coil heat exchanger

`

4.

DEVELOPMENT OF STAND-ALONE FORTRAN MODEL

4.1. Introduction

FORTRAN 90 is selected as the programming language to develop a lake model because of its flexibility in developing modular structure and requires less computational time. The FORTAN model can be divided into four different sections. 1) The first section consists of few basic subroutines that act as an interface between the user inputs and the lake model. These subroutines are used to establish the fundamental things needed to run the lake model and SWHE model. 2) The second section is the subroutines pertinent to lake model and 3) the third section is the drive routine for heat exchanger simulation. The lake model and heat exchanger model subroutines are implemented within two different loops such as time-step loop and iteration loop. 4) The fourth section consists of output subroutines which collects and write the simulated results to the separate .csv files.

A brief description of each of these sections is presented below. The significant portion of the FORTRAN implementation is that the lake and SWHE simulations are solved simultaneously at every time step. The heat of rejection or heat of extraction calculated by the heat exchanger simulation at the daily time step are passed to the lake model simulation at the same time step. Similarly, since both the models are implemented in the iteration loop, the lake model also passes the iterative, updated temperatures of the lake to the SWHE model to simulate the heat transfer rate and the exiting fluid temperatures. The FORTRAN model also has an option of turning off the heat exchanger so that we can evaluate the undisturbed lake temperatures.

`

The main driver subroutine controls the entire simulation of lake model and SWHE model. The main module calls every other subroutines and functions. '*Main driver'* is the core module which calls in every other subroutines and functions and controls the controls the entire simulation. Each subroutine is developed as a separate f90 module. The work of individual subroutines such as get the input, initialize, simulate and print the output is directed by the main driver routine. The data access between the individual subroutines is handled by passing the data in and out as arguments. By this way, a new subroutine to enhance the model can be easily added in the future.

The main driver routine consists of two major simulation loops namely day loop and the iteration loop. The day loop is the time step loop which drives the simulation for every daily time step and the iteration loop is used for the temperature convergence and surface ice thickness convergence. The maximum limit of the iteration loop is set as 100. However, as far as tested the maximum number of iterations needed by the lake model to reach the convergence is around 25.

4.2. Basic Subroutines

Table 4-1 lists the basic subroutines of the FORTRAN model, which sets the platform for the lake model simulation. The model starts with '*CALL GetInput'* that reads in all the input values specified by the user in the text file *'INPUTPARAMETER.txt'*. Input file is the simple commaseparated text file and its screen image is shown in Figure 4-1.

`

Table 4-1 Basic subroutines of the FORTRAN model

Basic subroutines
GetInput
NumOfSimDays
MaxNumOfLayersCalc
BathymetryCalc
WeatherData
Initialization

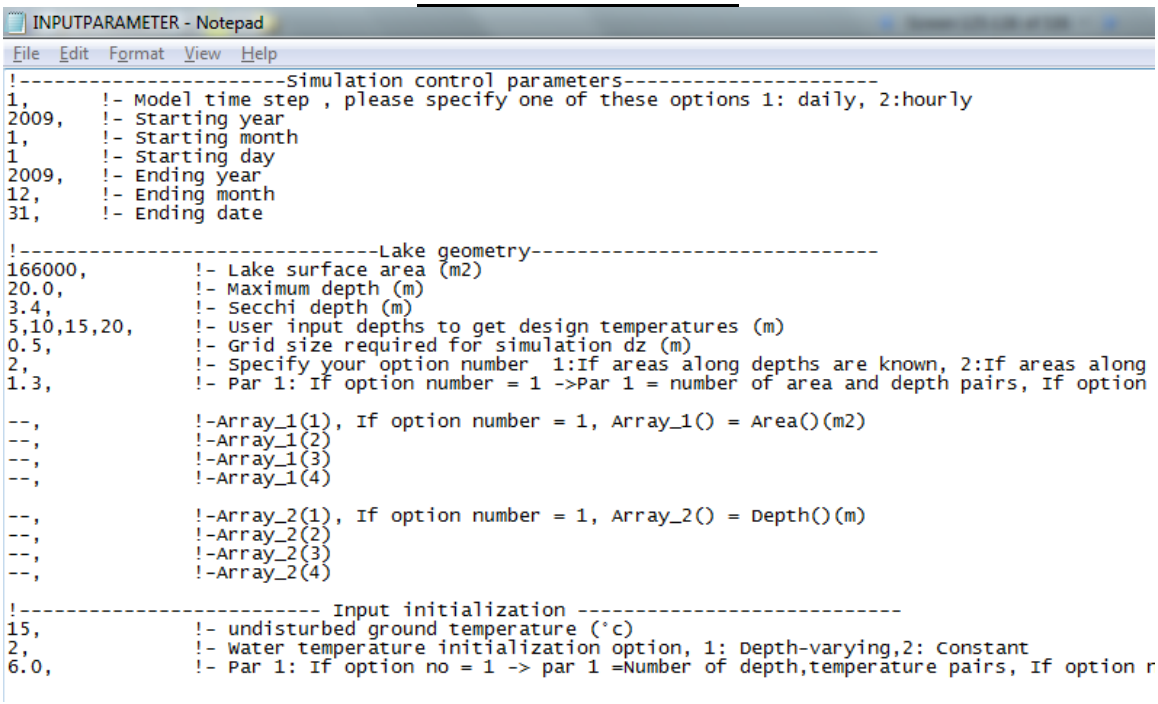

Figure 4-1 Screenshot image of 'INPUTPARAMETER.txt' file

The input parameter file consists of several sections such as bathymetry inputs, initialization inputs, weather data option, sub-model selection, heat exchanger inputs, antifreeze type and heat pump inputs.

Weather data input

The weather data input has two options through which user can input either actual weather data or typical meteorological file (TMY). The widely available TMY weather file format is the EnergyPlus weather files (EPW) which is used by most of the energy simulation

`

programs and this is used in the lake model. The EPW file named *'in.epw'* is given as an input to the lake model. This file consists of 8760 hours of various meteorological data of a typical year.

Actual weather data option gives users an advantage of evaluating more accurate lake temperature profiles. *'actual_weather_input.txt'* is the text file, which consists of daily average actual weather data. The data includes air temperature, solar radiation, relative humidity, wind speed, cloud cover and snow cover. Figure 4-2 shows the snippet of weather data input section. The first line is the user option to select either TMY or actual weather data.

```
! ------------------------------------ Weather data -------------------------------
1,                              !- Specify the weather data option- 1: TMY3, 2: Actual
in.epw,                         !- Specify the name of EPW weather file
actual_weather_input.txt,       ! - Specify the name of actual weather file
```

Figure 4-2 Weather data input section in 'INPUTPARAMETER.txt' file

Antifreeze input

The antifreeze properties are implemented in FORTRAN as individual function in a separate module called *Antifreeze Properties.* Antifreeze is required to avoid freezing of the heat exchanger fluid in colder climates. Propylene glycol, Ethylene glycol, Methyl alcohol, and Ethyl alcohol are the four antifreeze solutions for which the properties are written in the lake model simulation. User has to select the type of antifreeze and the percentage of concentration. Based on this the properties are calculated which includes dynamic viscosity, thermal conductivity, density and specific heat. Figure 4-3 shows the screen image of antifreeze inputs in the input text file.

```
! ---------------------------------Secondary coolant properties----------------------
1,              !-Type of Antifreeze: 0:None, 1: Propylene glycol, 2: Ethylene glycol
                !- 3: Methyl alcohol, 4: Ethyl alcohol
32.0,           !- Percentage concentration by weight
```

`

Figure 4-3 Antifreeze input section in 'INPUTPARAMETER.txt' file

Heat pump inputs

The last section of the input parameter file is the heat pump coefficients as shown in Figure 4-4. These values are the coefficients of curve-fit equations implemented in the heat pump model. The coefficients are calculated from the manufacturer's data, which is used in the curve fit equations in the heat pump model. The curve fit equations are the functions of entering fluid temperatures that calculate heat of rejection and heat of extraction.

```
! ----------------------------------Heat pump input--------------------
3,              !- Number of absorbed and rejected coefficient pairs

0.589369,               !- Array_1(1), Array_1() = Cabs()
0.004374,               !- Array_1(2)
-0.000022,              !- Array_1(3)

1.163194,               !- Array_2(1), Array_2() = Crej()
-0.001118,              !- Array_2(2)
0.000026,               !- Array_2(3)
```

Figure 4-4 Heat pump coefficients section in 'INPUTPARAMETER.txt' file

The detailed discussion of rest of the inputs related to lake bathymetry and initialization temperatures are presented in Chapter 5.

The *'NumOfSimDays'* routine calculates the simulation period according to the user specified simulation starting and ending day, month and year. The output of this routine controls the day loop in the main simulation.

'MaxNumOfLayersCalc' subroutine calculates number of water layers in the lake according to user defined maximum depth of the lake and grid size. The grid size input represent the desired vertical resolution of the outputs. The subroutine is used to define the uniform grid points in the vertical direction of the lake thereby dividing the lake into several horizontal water

`

layers. The lake temperatures and every other properties of water are calculated for each horizontal layer separately in the lake model.

'BathymetryCalc' subroutine is the most important routine from the perspective of lake model simulation. It takes in the bathymetry inputs such as surface area, maximum depth and volume development parameter and calculates the area and volume distribution of each horizontal water layer starting from the surface until the bottom of the lake.

'*WeatherData'* routine reads in the TMY weather data or actual weather data according to the user option. For TMY option, this routine process the 8760 hourly values from '*in.epw'* file and converts all them to appropriate daily values.

'Initialization' subroutine initializes the water temperature profile for the first day of simulation based on either constant or variable temperature profile. In addition, the lake sediment temperatures at the bottom of the lake are also initialized to the ground temperature input.

4.3. Lake Model Subroutines

Table 4-2 summarizes the subroutines that are used in the lake model simulation. The main functional of each subroutine is explained below in this section.

`

Table 4-2 List of subroutines related to lake model simulation

Lake model subroutines
Surface_Flux
Sediment_Heat_Flux
Calc_init_Eddy_diffusion_coeff
Heat_flux
TDMA_coefficient
Temp_and_density_Calc
UnstableDensities
SurfaceIceMelting
Ice
Mixing_layer
Calc_eddy_diff_coeff
Turnover
Convergence_check

Subroutine Surface_Flux:

Calculates the net heat flux at surface of the lake due to shortwave radiation, longwave radiation, convection and evaporation.

Subroutine Sediment_Heat_Flux

This routine solves for the sediment layer temperatures and calculates the heat flux between the water and the sediment layer

Subroutine Calc_init_Eddy_diffusion_coeff

Calculats initial eddy diffusion coefficients for all the water layers of the lake. The eddy diffusion coefficients are calculated seperatedly for ice covered and ice free conditons.

Subroutine Heat_Flux

Calculates the amount of heat gain by the water layers below the surface due to attentuation of solar radiation. The amount of solar radiation penetrated to the sub surface depends on the Secchi depth of the lake, which is a user input. During open water season the heat flux remaining after absorption at the surface is exponentially attenuated to the depth of the lake.

`

During ice cover period the heat flux reaches the water layer depends on albedo of ice. The incoming radiation melts the ice cover first and remainng radiation in expoenentially attenuated toward the depth of the lake.

Subroutine TDMA_coefficient

The mathematical coefficients alpha, beta, gamma and delta pertain to TDMA matrx are calculated. These coefficients are calculated for each water layer and at each timestep, which leeds to the calculation of temperatures of the respective layers.

Subroutine Temp_and_density_calc

Water layer temperatures and densities are calculated here in this subroutine based on TDMA coefficients. The density is calculated as a function of temperature.

Subroutine UnstableDensities

This routine checks for the presence of unstable density which is the condition of higher density water layer above the lower density water layer. If such condition occurs, water layers with unstable density profiles are mixed completely with the first stable layer below the unstable layers. This is handled in the subroutine by numerically mixing the unstable adjacent water layers i.e. by calculating volume weighed average temperatures of unstable water layers which represents the uniform average density mixed water layers.

Subroutine SurfaceIceMelting

Calculates the amount of ice melted on the surface of the lake and thus the net thickness of the ice on the lake surface. The top surface of the ice is melted by the heat flux due to solar radiation. The bottom surface of the ice melts due to the conductive heat transfer between the ice and the water

`

Subroutine Ice

The ice formation on the lake surface is simulated with this subroutine. The routine is triggered when the air temperatures goes below freezing and calculates the initial ice thickness formed during the start of ice-in period. In addition, it also calculates the increase in ice thickness if enough cool conditions prevail.

Subroutine Mixing_layer

This routine calculates the mixing layer thickness (epilimnion depth) by comparing the available kinetic energy from the wind and potential energy in the lake. The water layers are mixed until whole turbulent kinetic energy is spent on lifting every layer below epilimnion to mix with epilimnion.

Subroutine Calc_eddy_diff_coeff

The eddy diffusion coefficients are calculated for each water layer and at each time step based on the user defined eddy diffusion sub-model.

Subroutine Turnover

Lake turnover is numerically handled in the subroutine by fixing a constraint of 3.98 °C (T_{maxrho}) to a surface water temperature. If $T_{surface} > T_{maxrho}$, then all the layers below the surface whose temperature jumped over 3.98 °C including the surface layer are set to 3.98 °C. The energy gained by this process is distributed exponentially to the water column in a same way as shortwave radiation is attenuated

Subroutine Convergence_check

The convergence check subroutine checks for temperature convergence and ice thickness convergence between the iteration loops. If the convergence reached the results are updated for current time step and if not the iteration loop is continued until the convergence is reached. A

`

convergence criterion for lake temperature is set as 0.01 °C and for ice thickness, it is set as 0.01 mm.

4.4. SWHE model subroutines

Table 4-3 summarizes the list of subroutines related to the simulation of surface water heat exchanger model

Table 4-3 List of SWHE model subroutines

SWHE model subroutine
AvgPond_Temp_Dens_calc
HeatExchanger_driver
Heat_Exchanger_Freezing
Heat_Exchanger

Subroutine AvgPond_Temp_Dens_calc

This routine calculates the average lake temperature at the depth of the heat exchanger. It first determines the water layers between the user defined minimum and maximum depth of heat exchanger. Then, the temperatures of all these water layers are averaged. The average temperature value output from this routine is directly passed to the heat exchanger routine.

Subroutine HeatExchanger_Driver

The heat exchanger driver is the main routine from the perspective of SWHE simulation. It consists of '*Heat_Exchanger_Freezing'* and *'Heat_Exchanger'* routines. It has an outermost iteration loop just for the convergence of SWHE results. Through this iteration loop, entering and exiting fluid temperatures are converged. In addition, this subroutine contains heat pump model, which determines the heat of rejection or heat of extraction from the building loads using a curve fit equations.

`

Subroutine Heat_Exchanger_Freezing

The heat exchanger model predicts the exit fluid temperatures (ExFT), entering fluid temperatures (EFT) and heat transfer rate in daily time step. The calculations in this subroutine are for ice-free (on the surface of the heat exchanger) conditions. The algorithm for four types of SWHE's namely spiral-helical, flat spiral, vertical-horizontal slinky coil and flat vertical plate heat exchangers are implemented in this subroutine.

Subroutine Heat_Exchanger

This subroutine calculates the fluid temperatures and heat transfer rate under ice formation on the surface of the heat exchanger. The model also calculates the buoyancy force in the heat exchanger during freezing.

4.5. Output Subroutine

The converged values of each time step are stored in an array and passed to the output subroutine when the end day of simulation is reached. This routine prints the results in .csv format. The output results include water temperatures, ice thickness, exiting and entering fluid temperatures, and buoyancy force of the heat exchanger. An example screen image of output temperatures are shown in Figure 4-5

`

	A	B	C	D	E	F	G	H	I	J	K	L	M	N	O	P	Q
1	Layer	days															
2			1	2	3	4	5	6	7	8	9	10	11	12	13	14	
3	1	0	0	0	0	0	0	0	0	0	0	0	0	0	0	0	
4	2	0.5	3.38	3.04	2.86	2.74	2.61	2.53	2.45	2.39	2.33	2.3	2.26	2.21	2.14	2.1	2.
5	3	1	3.97	3.94	3.78	3.65	3.52	3.42	3.33	3.25	3.18	3.12	3.07	3.02	2.97	2.93	2.
6	4	1.5	3.97	3.94	3.95	3.93	3.9	3.83	3.77	3.72	3.67	3.62	3.58	3.53	3.48	3.44	3.
7	5	2	3.98	3.97	3.95	3.93	3.9	3.96	3.96	3.93	3.9	3.87	3.84	3.82	3.78	3.76	3.
8	6	2.5	3.98	3.97	3.97	3.98	3.97	3.97	3.97	3.97	3.96	3.97	3.95	3.97	3.97	3.95	3.
9	7	3	3.99	3.97	3.98	3.98	3.98	3.97	3.97	3.97	3.98	3.97	3.97	3.98	3.97	3.95	3.
10	8	3.5	4	3.98	3.98	3.98	3.99	3.98	3.98	3.98	3.98	3.98	3.99	3.98	3.97	3.97	3.
11	9	4	4	3.99	3.99	3.98	3.99	3.98	3.98	3.98	3.98	3.99	3.99	3.98	3.97	3.98	3.
12	10	4.5	4	3.99	4	4	3.99	3.98	3.98	3.98	3.98	3.99	3.99	3.98	3.97	3.98	3.
13	11	5	4	3.99	4	4	4	3.99	3.98	3.98	3.99	3.99	3.99	3.99	3.99	3.98	3.
14	12	5.5	4	3.99	4	4	4	3.99	3.99	3.99	3.99	3.99	3.99	3.99	3.99	3.99	3.
15	13	6	4	4	4	4	4	3.99	3.99	3.99	3.99	3.99	3.99	3.99	3.99	3.99	3.
16	14	6.5	4	4	4	4	4	3.99	3.99	3.99	3.99	3.99	3.99	3.99	3.99	3.99	3.
17	15	7	4	4	4	4	4	3.99	3.99	3.99	3.99	3.99	3.99	3.99	3.99	3.99	3.
18	16	7.5	4	4	4	4	4	3.99	3.99	3.99	3.99	3.99	3.99	3.99	3.99	3.99	3.
19	17	8	4	4	4	4	4	4	3.99	3.99	3.99	4	4	3.99	3.99	3.99	
20	18	8.5	4	4	4	4	4	4	3.99	3.99	4	4	4	4	4	4	
21	19	9	4	4	4	4	4	4	4	4	4	4	4	3.99	3.99	3.99	3.
22	20	9.5	4	4	4	4	4	4	4	4	4	3.99	3.99	3.99	3.99	3.99	3.
23	21	10	4	4	4	4	4	4	4	4	4	3.99	3.99	3.99	3.99	3.99	3.
24	22	10.5	4	4	3.99	4	4	4	4	4	3.99	3.99	3.99	3.99	3.99	3.99	3.

Figure 4-5 Excel .csv file of output water temperatures

4.6. Model Algorithm

The complete structure of the model along with the subroutines are illustrated with a simple algorithm given below.

Start – daily time step loop

Start – Iterative loop

1. Read model inputs, weather data file and building loads.
2. Calculate surface heat fluxes, sediment heat fluxes and dissipated heat flux to the water column.
3. Calculate the initial vertical eddy diffusion coefficient (k_z) for the entire water column.

Start – heat exchanger iterative loop

`

4. Read model inputs, lake temperatures at heat exchanger depth and building loads.

5. Estimate initial values for heat exchanger EFT and ExFT for the first iteration

6. Check for the formation of ice on the heat exchanger surface

If ice formation occurs

7. Calculate the heat transfer, EFT and ExFT and buoyancy force based on ice-on-coil model

If no ice formation occurs

8. Calculate the heat transfer, EFT and ExFT based on the heat exchanger model.

9. Check for the convergence of EFT and ExFT values.

End - heat exchanger iterative loop

10. Calculate the temperature and density of every water layer in the water column using TDMA algorithm.

11. Identify and rectify the unstable density layers.

If no ice cover

12. Calculate the wind induced mixing and the epilimnion layer thickness.

13. Calculate the hypolimnion eddy diffusion coefficient.

14. Initiate turnover algorithm, if condition for turnover exists.

If ice cover

If $T_a < T_f$ (condition for freezing)

`

15. Calculate the ice surface temperature.

16. Calculate the ice growth by congelation.

17. Accumulate new snow fall and calculate the formation of snow-ice

If $T_a \geq T_f$ (condition for melting)

18. Calculate the heat flux to melt the snow and ice layers from the top.

19. Calculate the bottom melt of ice by heat diffusion from the water layers.

20. Calculate the updated temperature values using TDMA algorithm.

21. Recheck and rectify the unstable density layers.

22. Check for temperature and ice thickness convergence.

End - Iterative loop

23. Print outputs to the respective files.

End – daily time step loop

`

5.

SURFACE WATER HEAT PUMP SYSTEM MODEL IMPLEMENTATION IN ENERGYPLUS

5.1. Introduction

The objective of the work presented in this chapter is to discuss about the implementation of the surface water heat pump system simulation model in EnergyPlus environment. The model implementation can effectively replace the existing EnergyPlus shallow pond model developed by Chiasson et al. (2000) . The lake model couple with SWHE model developed as a stand-alone FORTRAN is implemented as a separate module for SWHP system in EnergyPlus. Furthermore, the structure of the SWHP system module and the input/output parameters of the lake model are explained here in this chapter.

Chiasson et al. (2000) developed the pond model in EnergyPlus as a supplemental heat rejecter for ground source heat pump systems. This is a shallow pond model, which is based on lumped parameter approach. It is a very simple model, which considers the pond itself a single node and calculates the bulk temperature of the pond. It neglects the spatial variations in lake temperatures across the depth of the lake, which makes the model not suitable for deep lakes. Chiasson et al. (2000) model used a surface heat balance to predict the water temperature. The heat exchanger model coupled with the pond model to predict the exiting fluid temperatures of

`

slinky coil. This work compares the simulation results with the heat rejection results experimentally measured in rectangular shallow ponds which produced a maximum of 5.2% difference. Chiasson et al. (2000) used Dittus-Boelter equation for inside convection coefficient and Churchill and Chu (1975) straight pipe correlation for outside convection coefficient.

On the perspective of the application of SHWP systems, the significant phenomenon, which the model should simulate, is the temperature stratification of the lakes. Therefore, the detailed lake model and the surface water heat exchanger model were developed initially as a standalone in FORTRON 90 and have been implemented in EnergyPlus.

The major functions of the new SWHP system program are

- Based on user input regarding the physical characteristics and location of the lake, the model is simulated to predict the daily lake temperatures across the depth, though which the temperatures are known at heat exchanger depth.
- Once the lake temperatures are predicted near SWHE, the SWHE model simulates the heat transfer between the heat exchanger and the lake to find the exiting fluid temperatures.
- In addition, depending on the building cooling load or heating load SWHE determines whether the heat should be rejected or extracted from the lake.

5.2. Handling Time-Step

The critical part of implementation is connecting the lake model module to EnergyPlus stems from the fact that most of the EnergyPlus models are based on shorter time-step but the lake model is based on daily time step. The shortest user defined time-step in EnergyPlus in one minute. EnergyPlus simulations are based on variable adaptive time step for the interaction between the thermal zones and HVAC components for updating system response. The program

`

itself determines the variable time step required. The interactions between zones and the environment are calculated based on user defined constant time step (EnergyPlus 2012a). Since the lake model is a daily time step model, some modifications are required with the implementation to trigger the lake model only once in a day. However, the SWHE model should run according to the system time step. In this manner, the following points summarizes the general outline of how the time step issue is handled in EnergyPlus implementation process.

- Lake model is simulated first at the start of every day and calculates the lake temperature profile for the day
- SWHE model makes use of the lake temperatures for the current day and calculates heat transfer rate to/from the lake and heat exchanger exiting fluid temperatures (ExFT) according to the user defined time-step.
- In addition, when the last time step of a day is reached, SWHE model calculates the amount of energy rejected/extracted from the lake for the day by adding up all the energy transferred at each time step.
- This accumulated energy is supplied to the lake model in order to calculate the lake temperatures for the next day that may increase or decrease the next day's lake temperatures depending on rejection or extraction of heat.

In short, lake simulation lags by a day in building simulation. The SWHP system simulation begins with the lake model for each simulation day and continues to run SWHE model for rest of the day. This is repeated for all the days of simulation. The lake temperature variation over a day is generally low except near the surface of a lake. Also, the actual change of lake temperatures from day to day is relatively small. Therefore, the energy consumption differences caused because of the lag in lake model by a day should be negligible.

`

The program starts with the calculation of lake temperature profile which is the most significant part of simulation. Then, the program switches to the SWHE calculation subroutine. The algorithm keeps track of the iterations for each time-step and the converged value of heat transfer to/from the lake is calculated for every user-defined time-step. Once it tracked the last time-step of a day, it estimates the accumulated heat rejection/extraction for a day, which is the sum of energy transferred for every time-step.

The boundary temperature for heat exchanger for any time step is the average lake temperature near the neighborhood of the heat exchanger calculated by the lake model. Since, the lake model runs only for a day, SWHE model assumes daily average lake temperature near the heat exchanger for every time-step within a day.

The accumulated heat rejection/heat extraction may have a little effect on the next day lake temperatures and thus guarantees the energy balance in the simulation. Figure 5-1 shows how the lake model and SWHE model are coupled with each other also it explains the way the daily time step and system time step are handled in EnergyPlus.

`

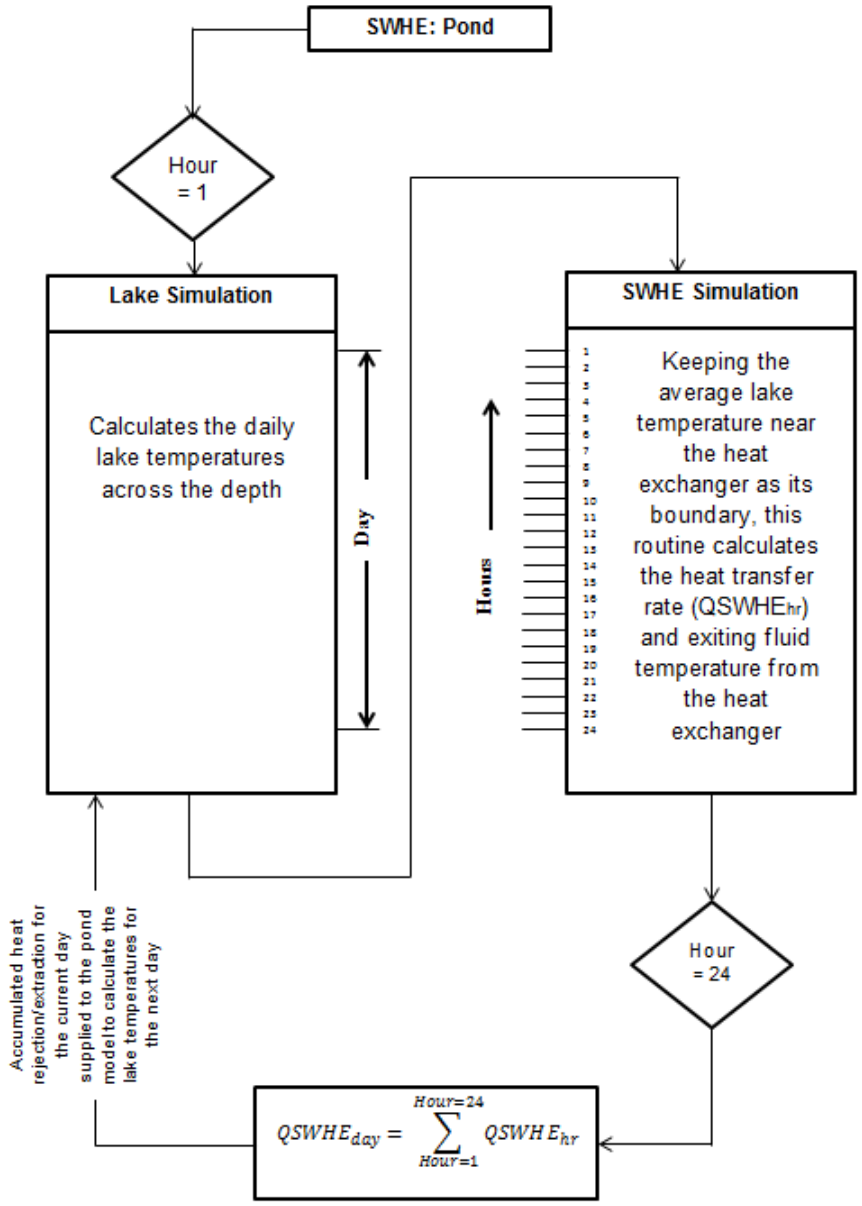

Figure 5-1 Flowchart of operating process and implementation of SWHP system in EnergyPlus

The source code implemented in EnergyPlus executes two phases of SWHP simulation, lake model and surface water heat exchanger model. The lake model predicts the lake temperatures whereas the SWHE model predicts the heat transfer rate and exiting fluid temperature. As an overview, the SWHP system module performs certain calculations which includes

`

- Heat transfer takes place between the atmosphere and surface
- Heat diffusion and heat transfer in the water column
- Heat transfer between the lake and the sediments
- Ice formation/melting on the surface of the pond
- Heat transfer between the heat exchanger and the lake

5.3. Lake Model Implementation

EnergyPlus is an integrated simulation environment whereby the major parts, zone, system and plant are solved simultaneously based on fundamental heat balance principles. The surface water heat exchanger implemented in EnergyPlus is connected to the supply side of a condenser loop that in turn connected to the plant supply side loop with heat pump as the primary equipment.

The lake model has been implemented in EnergyPlus as a component of condenser loop like vertical ground loop heat exchanger, cooling tower etc. and can be configured on the condenser supply side. The data structures of the lake model are written in separate EnergyPlus module. The model from FORTRAN 90 was translated to EnergyPlus with formatting, writing conventions, calling conventions, subroutine definitions, variable definitions, initialization and output routines that conform to the EnergyPlus code standards. The EnergyPlus programming standard are followed in developing the input files. Specifically, there are two files Input Data Dictionary (IDD) and Input Data File (IDF) are developed for the implementation of lake model in EnergyPlus. All the inputs associated with this model are given under the object name of '*SHWP: Pond*'. The inputs needed to run the lake model are discussed later in this section.

`

On the perspective of input data, one of the objectives of the simulation programs like EnergyPlus is to have inputs to which design engineers have access. The lake model is developed in such a way it requires minimal data and less computation time. Within EnergyPlus environment, the lake model algorithm is handled in the exact manner as the stand-alone FORTRAN except the way SWHE is coupled with the lake model.

Initially, EnergyPlus model starts to get input and initialization of lake model. The initializations include lake temperature, ground temperature intializations and generating appropriate grids according to the user defined grid size and lake maximum depth. The main calcualtion routine is then called which contains SWHE and lake model as two different components because of different time-steps. At the starting hour of each day, the lake model is called to simualate the temperatures at every depth of the lake. Each time the lake model is executed, the temperatuers are stored in a separate variable in order to use that to calcuate the lake temperatues for the next time step. The lake temperatuers for the current day are calculated based on iteration loop implemented within the lake model subroutine. When this routine reaches converegence, it exits out of iteration loop and sweeps thorugh SWHE subroutine with updated lake water temperatures. Figure 5-2 is the flowchart which illustrates the iteration loop of the lake model implemeted in EnergyPlus.

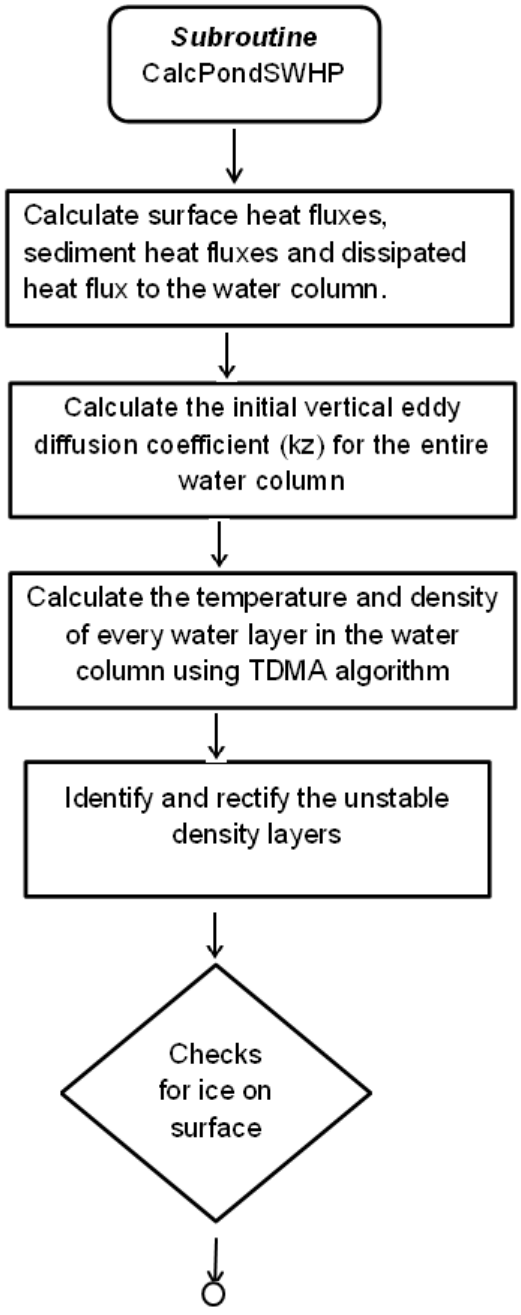
Subroutine
CalcPondSWHP
Calculate surface heat fluxes, sediment heat fluxes and dissipated heat flux to the water column.
Calculate the initial vertical eddy diffusion coefficient (kz) for the entire water column
Calculate the temperature and density of every water layer in the water column using TDMA algorithm
Identify and rectify the unstable density layers
Checks for ice on surface

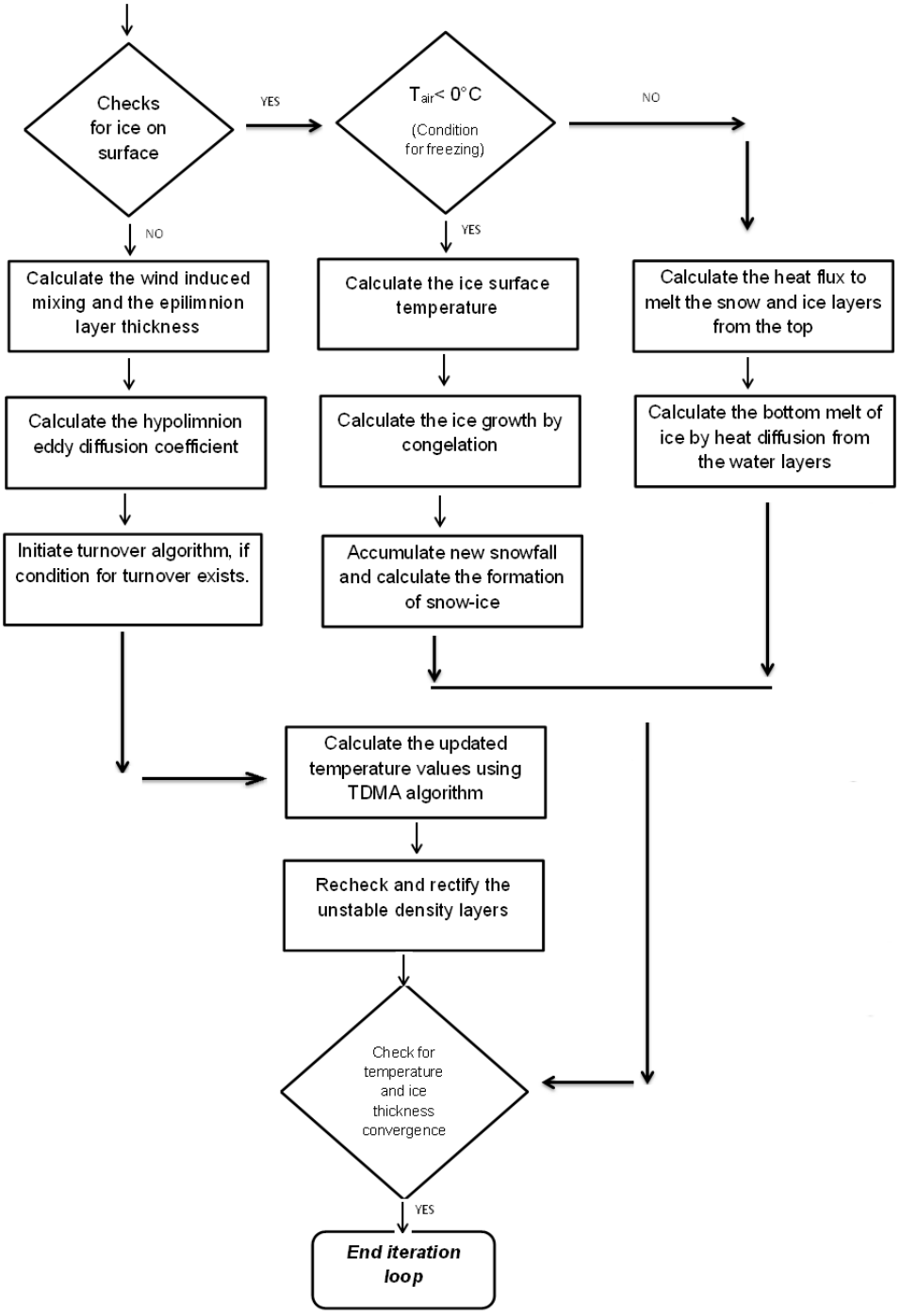

Figure 5-2 Iteration loop of the lake model implemented in EnergyPlus

`

1-D differential governing equation as explained as Equation (1) in section 3.2 adopted from Hondzo and Stefan (1993) solved in an iterative scheme for the simulation of heat transfer process in the lake model to calculate the lake temperatures across the depth. The properties of each layer are determined by the temperature values calculated. Layer thickness represents the resolution of temperature output based on user input. The horizontal surface area and the volume of each water layer depend on lake bathymetry and it is calculated from volume development parameter (V_d)

The surface heat transfer, sediment heat transfer, heat absorption and diffusion down the depth of the water column and mixing depth are calculated within the lake model subroutine. In addition, ice formation on the lake surface and ice melting are executed. Each mechanism has its own routines and is called within the lake model subroutine. The densities and specific heat capacities of water are calculated at various places in the module using the water property functions of EnergyPlus. The model attempts to simulate the continuous change of lake stratification in response to heat exchange with atmosphere at surface and heat transfer processes take place within the lake. The complete set of input data required to simulate the lake model is described in Table 5-1. What follows the table is the detailed discussion about the type of inputs a needed to run this lake model.

`

Table 5-1 Input data required to simulate the lake model

Input field
Lake Name
Lake Surface Area
Maximum Lake Depth
Volume Development Parameter
Secchi Depth
Grid Size
Type of initialization temperature profile
Initial Water Temperature
Initial temperature at Quarter-th Depth
Initial temperature at Middle Depth
Initial temperature at Three Quarter-th Depth
Initial temperature at the bottom
Initial Ground Temperature
Eddy Diffusion Model Type
Maximum Eddy Diffusion Coefficient
Surface Convection Model Type

Lake morphometric inputs

The lake morphometric inputs include lake surface area, maximum depth, Secchi depth and volume development parameter for the lake. In this, Volume Development parameter (V_d) is a constant which characterizes the shape of the lake basin. This constant is necessary to model the variations in area and volume with depth, which is very significant in modeling the temperature along the depth of the lake. This kind of approach in modeling lake bathymetry is adopted from Johansson et al. (2007). V_d is calculated as given in the equation below and it depends on the basin shape of the lake and it varies from 0.05 to 2; concave lake basin shape have $V_d > 1$ and the convex lake basin shape have $V_d < 1$.

$$V_d = \frac{Maximum\ Volume}{\frac{Surface\ area * Max\ depth}{3}} \tag{72}$$

`

Secchi depth is the measure of clarity of water; high Secchi depth indicates more clear water whereas low Secchi depth indicates cloudy or turbid water. Secchi depth is measured using Secchi disk. An example of Secchi disk measurement is shown in Figure 5-9 . This disk is lowered into the lake and the depth at which it is disappeared is Secchi depth. It is a measure of how far sunlight penetrates into the water column. Secchi depth is a function of time due to change in weather, lake usage, precipitation, lake level fluctuations, erosion of shoreline etc., The characteristic of low Secchi and high Secchi depth of the lake are explained in Table 5-2. If the lakes are maintained by any water quality monitoring program user can access Secchi depth data though their online sources. One such example is the 'Florida LAKEWATCH' lake water monitoring program which have Secchi depth data for the lakes in Florida (Florida Lakewatch 2013)

Table 5-2 Characteristic features for low and high Secchi depth

High Secchi depth	***Low Secchi depth***
Clear lake; Water transparency is more	High turbid lake; Water transparency is less
Sunlight penetration is more	Sunlight penetration is less
Low algae content	High algae content

`

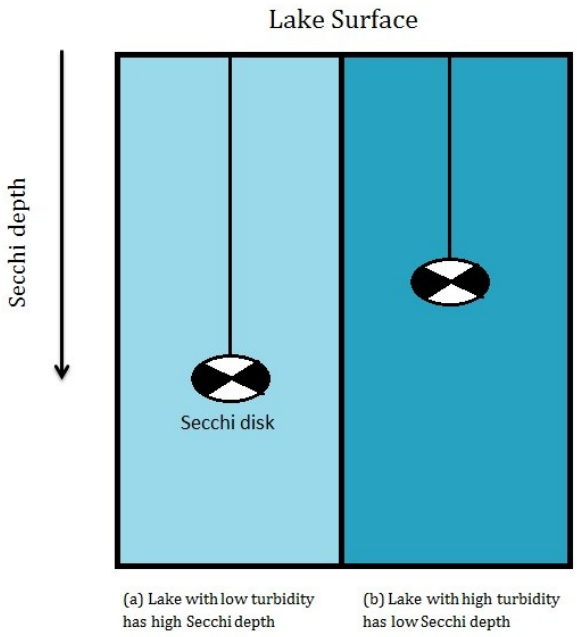

Figure 5-3 Secchi depth measured using Secchi disk

Initialization inputs

An initial lake temperature (usually considered as the lake temperature on January 1) is a required data for the start of the simulation. For variable temperature initialization profile user need to specify temperature vs. depth information. The user is directed to give the approximate lake temperatures at quarter-depth, middle depth, three quarter depth and the bottom of the lake. The undisturbed ground temperature is used to initialize the temperature of the sediment below the lake bottom, and serves as a lower boundary condition. The ground temperature initialization varies with every location.

Selecting sub models: Surface convection and eddy diffusion

In order to increase the versatility of the lake model to accurately predict the temperatures for various lake categories there are 7 different surface convection and evaporation

`

modelsBashyam et al. 2013b). These correlations were developed based on their experimental analysis ranging from swimming pools to small lakes.The temperature transport mechanism in a lake is predominantly controlled by the turbulent diffusion process resulting in the formation of eddies. The accuracy of prediction of lake temperatures is highly dependent on effective prediction of the eddy diffusion coefficient. Eddy diffusion coefficient is a function of depth and time. To calculate the eddy diffusion coefficient for different lake categories various sub-models are explained in Bashyam et al. (2013b). Based on the validation results, the recommended surface convection/evaporation and eddy diffusion models have been identified for each lake category as shown in Table 5-3.The recommended model combinations are set as default model combinations in EnergyPlus lake model.

The user has to select 'automatic' option to have a default recommended sub-model combination in the lake model. Or else, the user can select the appropriate models by themselves as analyzed and recommended for each lake category given in Table 5-3

Table 5-3 Recommended sub-models for different lake category

Lake category	Surface Area Ha(acres)	Recommended models	
		Surface Convection model	Eddy diffusion model
Small shallow ponds	≤ 5 (12)	Molineaux et al. (1994)	Gu and Stefan (1995)
Small lakes	5(12) - 100 (250)	Molineaux et al. (1994)	Imberger et al. (1978)
Medium sized lakes	100(250) - 1000(2500)	Molineaux et al. (1994)	Rohden et al. (2007)
Large lakes	>1000(2500)	Molineaux et al. (1994)	McCormick and Scavia (1981)

Grid spacing

The model predicts the temperature as a function of depth and time. The user-defined node spacing value determines the vertical resolution of the temperatures. The lake model does not account for variable grid sizing. The entire domain of the lake is divided into equal grid spacing and the temperatures are predicted for every node.

`

Weather data

Once the lake model has the required inputs from the user, it uses EnergyPlus weather files (EPW) to predict the daily lake temperatures across the depth. It should be noted that the special set of calculations are added to handle the calculation of daily average weather data. At the start of every day, the hourly weather data for the day is acquired and subjected to proper conversion to set the weather inputs for daily time step lake model. Through the lake model run, the lake model using daily weather data predicts the temperatures along the depth. With the temperatures at the HX depth are known, focus can be switched to the simulation of SWHE. The lake temperature simulated for a day is assumed as the lake temperature for every hour.

5.4. SHWE Model Implementation

The surface water heat exchanger model is separate routine '**SUBROUTINE HeatExchanger'**, which simulates heat exchanger submerged in the lake. It has been implemented in EnergyPlus as a plant component that is intended to be configured as a part of condenser loop. SWHP system runs in EnergyPlus by configuring the lake along with surface water heat exchanger as heat source/sink on the condenser loop and in turn, the condenser loop is connected to the plant loop with the heat pump as the primary equipment. SWHE model runs according to the system time step and predicts fluid temperature exiting the surface water heat exchanger and heat transfer rate given the time-varying entering fluid temperature and flow rate.

The HX data and fluid data are all now have been initialized and steps followed are to calculate exiting fluid temperature and heat transfer rate between the SWHE and the lake water. The inside and outside convection coefficients used in the further calculations are modeled as functions in the model. The routine, which consists of heat exchanger model, does not take into

`

account any heat transfer calculations when the ice is formed on the surface of the heat exchanger. There is a separate subroutine to account for 'ice-on-coil' model calculations. When the model reaches the entering fluid temperature below freezing, the program calls a separate routine '**SUBROUTINE HeatExchangerFreezing'.**

Table 5-4 Input details required for SWHE model

Input field
HX Fluid Inlet Node Name
HX Fluid Outlet Node Name
HX Fluid Name
HX Fluid Name
Pond Heat Exchanger Type
Outside coil diameter (m)
Horizontal spacing of a coil (m)
Vertical spacing of a coil (m)
Height of the flat plate (m)
Length of the flat plate (m)
Thickness of the flat plate (m)
Number of passes (m)
Hydronic Tubing Outside Diameter (m)
Hydronic Tubing Inside Diameter (m)
Number of tubing circuits (dimensionless)
Length of the tubing circuit (m)
Depth of the lake where the top of the HX is situated (m)
Depth of the lake where the bottom of the HX is situated (m)

The following input parameters are required for every SWHE type.

Spiral helical heat exchanger.

- Outside tube diameter in mm (in)
- Inside tube diameter in mm (in)
- Length of the hydronic tubing per coil in m (ft)

`

- Outside coil diameter in m (ft)
- Horizontal spacing between adjacent tubes in mm (in)
- Vertical spacing between adjacent tubes in mm (in)
- Volumetric flow rate in one coil in L/s (GPM)

Figure 5-4 shows the illustration of some of the input parameters for spiral helical heat exchanger.

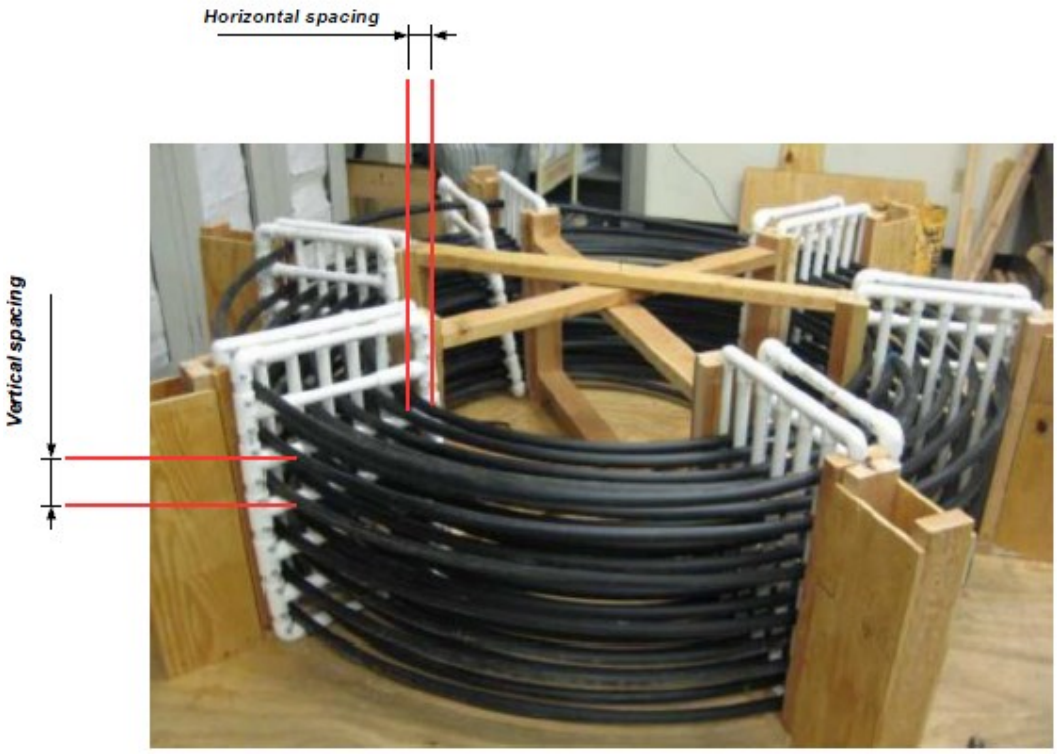

Figure 5-4 Illustration of a spiral helical coil and its input parameters (Courtesy: Hansen 2011)

The correlation used by the design tool to calculate the heat transfer coefficients for spiral helical coil has been tested for certain range of input parameters. The user input should be within the correlation parameters (Hansen 2011).

Effective range of input parameters

`

- 26.7 mm(1.050 in) < outside tube diameter < 42.2 mm(1.660 in)
- 21.8 mm(0.86 in) < inside tube diameter < 34.5 mm(1.358 in)
- Length of the hydronic tubing <= 152.4 m (500 ft)
- 38.1 mm(1.5 in) < horizontal spacing < 104.8 mm(4.125 in)
- 38.1 mm(1.5 in) < vertical spacing < 104.8 mm(4.125 in)

Horizontal spiral heat exchanger

- Outside tube diameter in mm (in)
- Inside tube diameter in mm (in)
- Length of the hydronic tubing per coil in m (ft)
- Outside coil diameter in m (ft)
- Horizontal spacing between adjacent tubes in mm (in)
- Volumetric flow rate in one coil in L/s (GPM)

Figure 5-5 shows the illustration of some of the input parameters for horizontal spiral heat exchanger

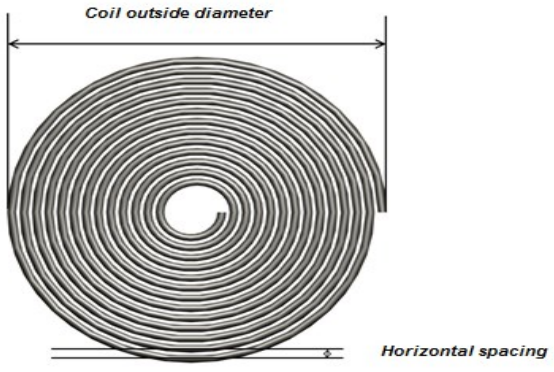

Figure 5-5 Illustration of a horizontal spiral coil and its input parameters

`

Vertical or horizontal slinky heat exchanger

- Outside tube diameter in mm (in)
- Inside tube diameter in mm (in)
- Total hydronic tubing length in m(ft)
- Outside coil diameter in m (ft)
- Volumetric flow rate in one coil in L/s (GPM)

Figure 6 shows the illustration of some of the input parameters for vertical or horizontal slinky heat exchanger

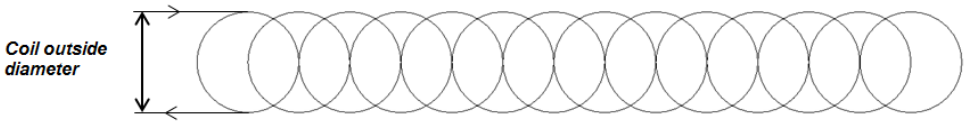

Figure 5-6 Illustration of the slinky coil input parameter

Flat plate heat exchanger

- Length of the plate in m (ft)
- Height of the plate in m (ft)
- Thickness of the plate in mm (in)
- Number of passes (-)
- Volumetric flow rate in one plate in L/s (GPM)

Figure 5-7 shows the illustration of some of the input parameters for flat plate heat exchanger

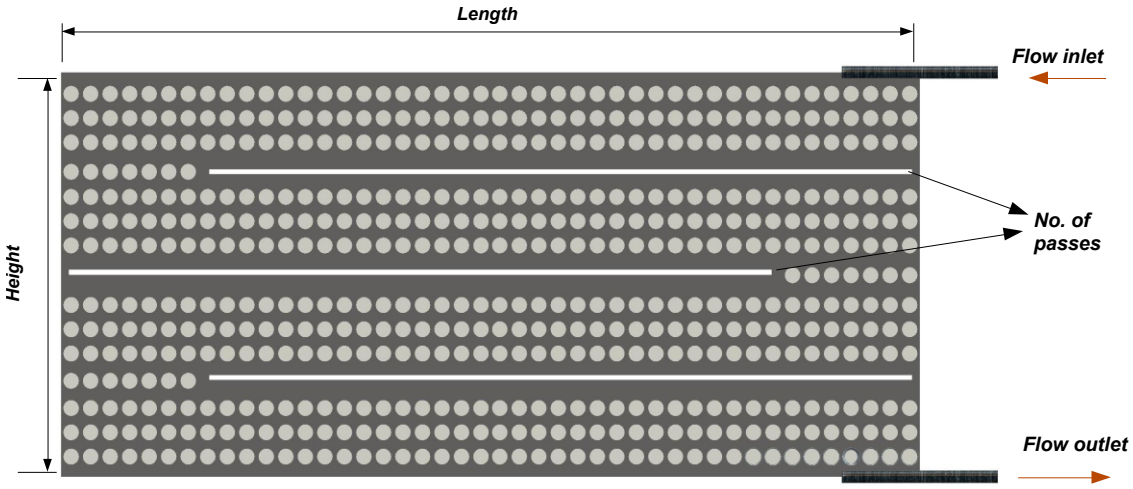

Figure 5-7 Illustration of a flat plate heat exchanger with input parameters

For every heat exchanger type, the user has to provide the minimum and maximum heat exchanger depth. Figure 5-8 shows the illustration of the minimum and maximum heat exchanger depths.

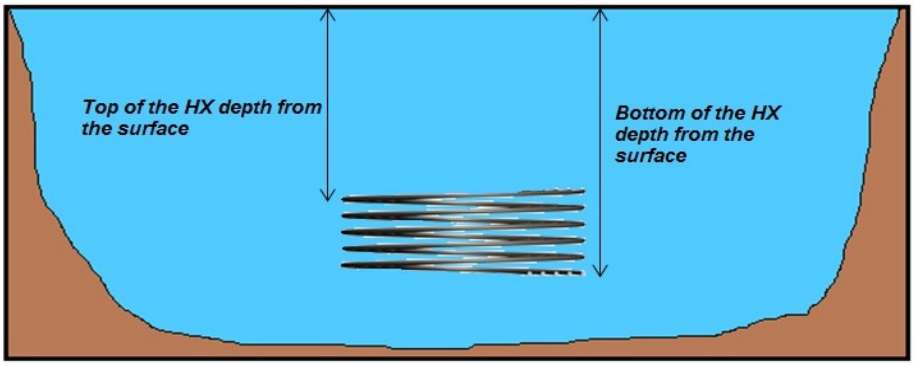

Figure 5-8 Illustration of the maximum and minimum heat exchanger depth

`

5.5. Model Structure

The framework of the lake model and SHWE model is shown in Figure 5-9. The module consists of several subroutines that are called from from other subroutines within the SHWP module. Major subroutines within the SWHP module are explained below

SimPondSWHP: This is the public subroutine which acts as an iterface between the plant loop equipment manager and all the routines involved in the lake model. This routine calls the other subroutine implemented in the SWHP module. It makes one time call to **GetPondSWHP** routine which reads all the lake model input from IDF file using input processor.

GetPondSWHP: The input data for SHWP sytem simulation which inlcues lake simulation and SHWE simulation are read by this routine and delievered to other routines in the module.

InitPondSHWP: An initialization routine, according to the input read, initializes the module variables for each time step

CalcPondSWHP: This is the main routine which consists of all the algorithms pertinent to lake simulation. It has various subroutines which includes the calculations explained in the model development section. It is called every day and updates the lake tempratures across the depth of the lake for every day.

CalcPondHX: It contains the heat exchanger algorithm to calculate the heat transfer rate and ExFT. It is called and the calcualtions are executed according to the system time step.

UpdatePondSWHP: After simulation of lake model it updates the value of lake temperatures also after heat exchanger simulaton it updates the outlet node properties, which inlcude the heat exchanger exiting fluid temperature and mass flow rate.

`

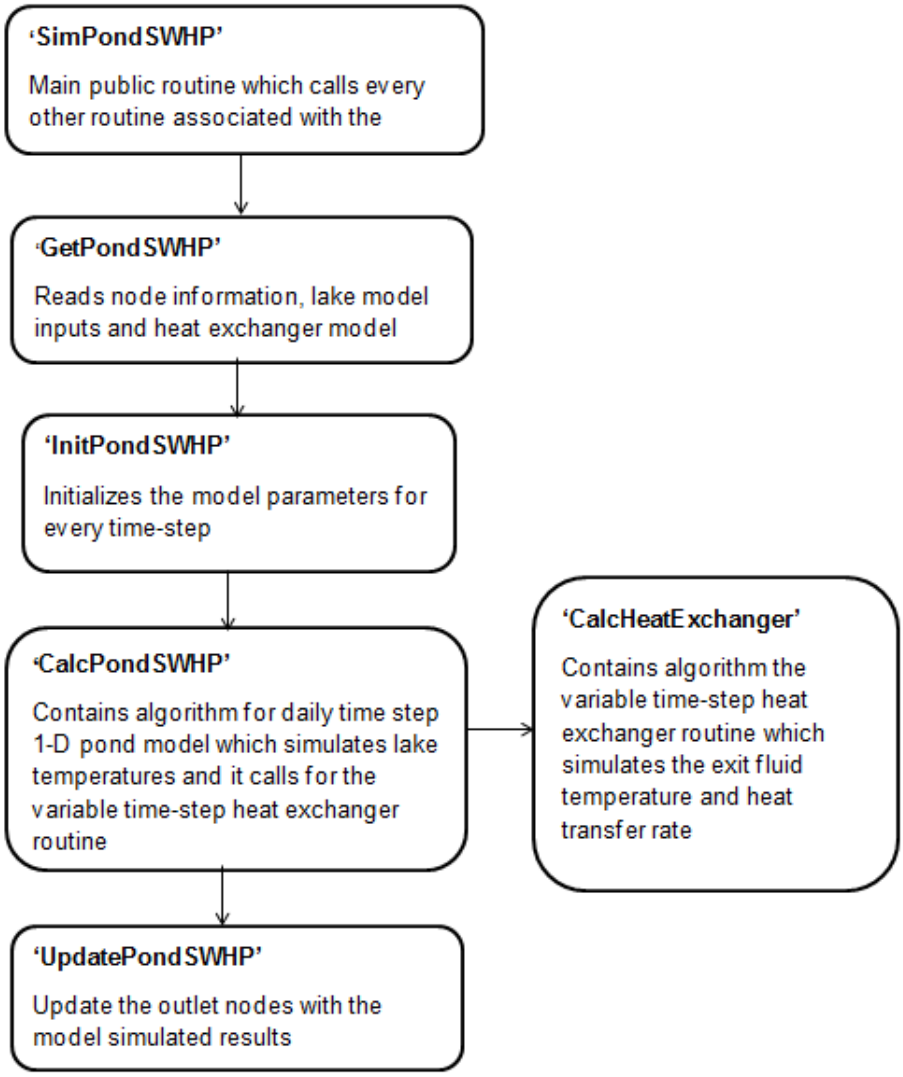

Figure 5-9 Framework of the lake model implemented in EnergyPlus

5.6. EnergyPlus Code Changes

'**PondSWHP**' is the new module developed in EnergyPlus and '**SimPondSWHP'** is the main routine which calls every other subroutine connected to the pond simulation. There were also few changes in the other modules of EnergyPlus to accommodate the new model.

`

5.6.1. Plant Loop Equipment

The plant loop equipment module has a subroutine which calls the different components of the plant loop by selecting the type of the component. There are few code changes in this module to facilitate the call of subroutine '**SimPondSWHP'**

5.6.2. Data Plant

This module defines the structure for various equipment of the plant loop. The parameter for equipment type and the parameter for the general equipment type is declared in this module. The parameter for the equipment type is assigned as 60 (**'TypeofSWHtExchgPond')** and the parameter for the general equipment type is assigned as 20 (**'SURFACEWATERHEATEXCHANGER'**)for new lake simulation.

5.6.3. Plant Manager

This module allocates the branches, components in the plant loop and assigns the branch number and component number according to the equipment type and general equipment type, which module serves as driver for the lake simulation

5.7. Error Handling

The error handling programming is also updated separately for the new module implemented in EnergyPlus. The error handling codes catches the typical typo errors in the input files and also user incorrect inputs. For instance, if the depth of the heat exchanger depth specified is higher than the maximum depth of the lake an error is triggered. The appropriate error message and error type is specified to the user through the error handling routines of EnergyPlus manager.

`

5.8. Discussion of results

The lake temperatures predicted by the lake model implemented in EnergyPlus is validated for Lake Washington. It is a large size and deep lake. Lake Washington (47°36'34" N, 122°15'33" W) is located close to Lake Sammamish and it is the largest lake in King County, Washington with a surface area of 8700 Ha (21500 acres) and a maximum depth of 65 m (214 ft). The experimental measurements of the lake is obtained from King County (2012) and compared with the simulation temperatures. The results are simulated with the sub-models Rohden et al. (2007) and Molineaux et al. (1994) . This combination was selected as the best model combination for large size lake category as explained in Bashyam et al. (2013b).

Figure 5-10 to Figure 5-13 shows the comparison results of temperature profiles for few days of summer season. The temperature profiles show strong stratification during summer and this temperature profile persists for most part of the year. The maximum differences around 10 m depth are mostly due to the small differences in predicted epilimnion depth. Aside that, the temperatures at every other depth predicted by the model matches well with the experimental measurements.

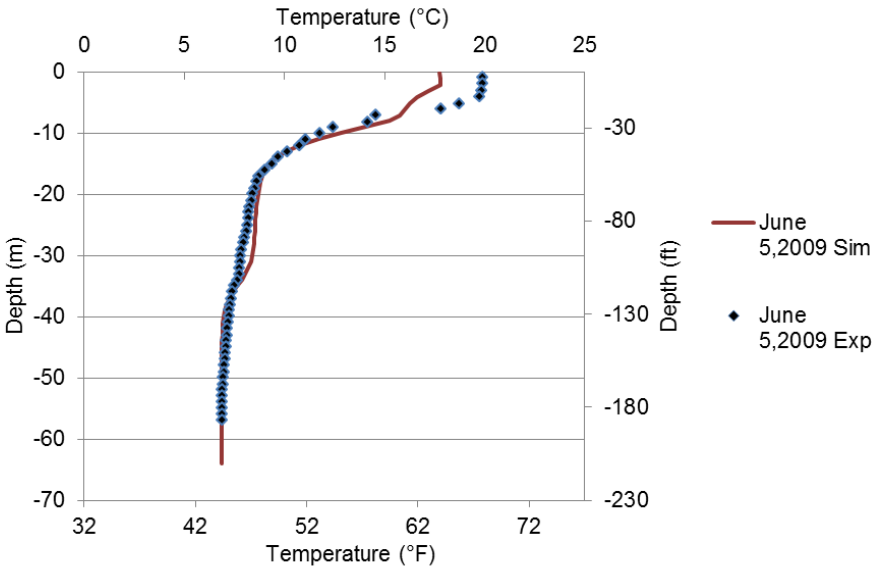

Figure 5-10 Comparison of experimental and simulated temperatures of Lake Washington on June 5, 2009

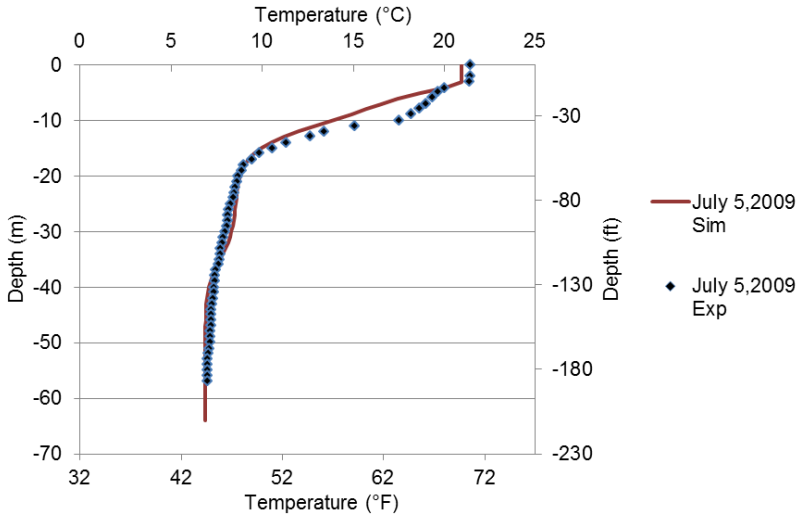

Figure 5-11 Comparison of experimental and simulated temperatures of Lake Washington on July 5, 2009

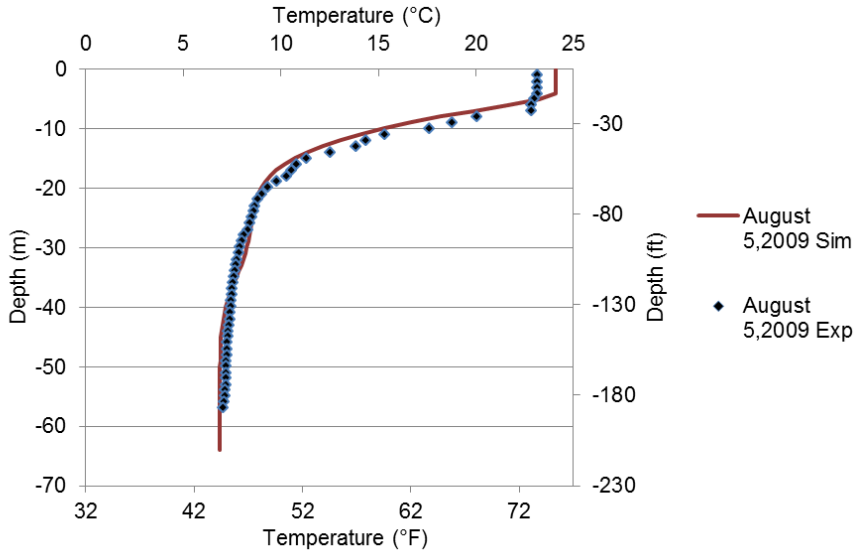

Figure 5-12 Comparison of experimental and simulated temperatures of Lake Washington on August 5, 2009

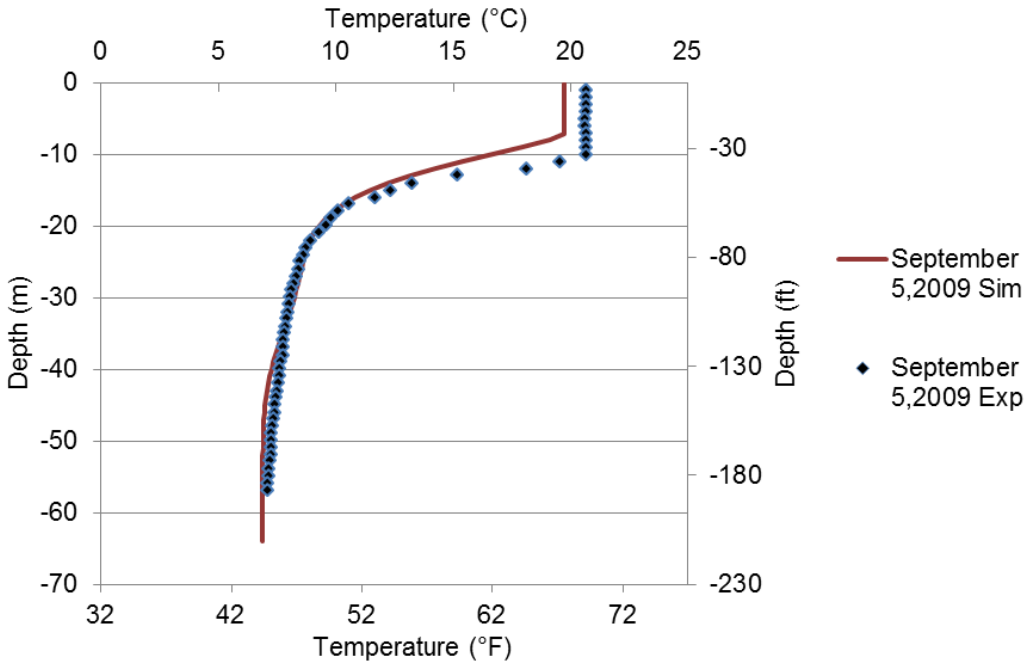

Figure 5-13 Comparison of experimental and simulated temperatures of Lake Washington on September 5, 2009

`

5.9. EnergyPlus Documentation

The new model implementation in EnergyPlus is updated with two EnergyPlus documents. Input/output reference that explains to the user about inputs needed to run the model and discusses about where it can be accessed from. In addition, the document also discusses about the output variable of the simulation. Engineering reference is the document which gives information about the model features, underlying assumptions and model limitations.

5.10. Computation time

As the model implementation in the EnergyPlus distribution includes the compiled version of the model the speed would be much high. The lake model by itself takes a reasonable amount of computation time. However, for the grid spacing in the order of 0.1 m, which is relatively too small for deep lakes, the lake model runs for higher computation time. The best way to balance the accuracy and the computational time is to change the grid size to better suit the types of lakes. The user is recommended to simulate with 0.1 m grid size for shallow ponds and 0.5 m grid size for every other deep lakes.

The ice-on-coil model is expected to increase computation time due to the calculations based on segments of the heat exchanger, and in fact, it does. However, for the conditions where there is no risk of freezing on the heat exchanger surface, the SWHE model runs for short computational time.

`

6.

ANALYSIS TO DEVELOP GUIDELINES FOR MINIMUM RESERVOIR SIZE

6.1. Introduction

The SWHP system removes heat from a lake and supplies it to the conditioned space in a building during heating mode. In cooling mode the process is reversed where the heat is extracted from the conditioned space of a building and rejected to a lake. In many cases, the lake temperatures will not be affected on a noticeable level. However, it is possible that high heat rejection or extraction rates could adversely affect the lake temperatures. The purpose of this chapter is to provide such information as a part of design guidance of SWHP systems.

When we use lake as a heat source or heat sink, the lake temperatures may be affected on a noticeable level. Therefore, the most significant question is to decide on how much heat can we reject or extract from a lake without affecting the thermal stability of a lake. The purpose of this chapter is to provide such information as a part of design guidance of SHWP systems.

In a cooling dominated building, heat rejection is more than heat extraction over a year. If ground is used as a heat source/sink for a cooling dominated building, the ground temperatures are likely to increase over several years because of imbalance between heat rejection and extraction. Similarly, the lake temperatures are also affected over time because of high heat rejection or extraction. The change in lake temperatures may not be the same from the surface to

`

the bottom of a lake. Since heat escapes through evaporation at the surface, the surface temperatures are less affected than the sub-surface temperatures of a lake. High heat rejection can de-stratify a lake and thus undesirably increase the lake temperatures at the depth of heat exchanger. This could lead the lake temperatures to exceed the design lake temperature limit and in turn have a significant impact on the heat transfer rate. Thus, the lake temperatures rise provides inadequate cooling to a building.

The lakes in very cold climates could be frozen at the surface and thus have coldest water below the ice surface. Figure 6-1 shows the simulated temperature profile on the day of maximum ice thickness of 41-acre (16.6 ha) lake, which is 20 m (65 ft) deep. It can be seen that the temperature immediately below the ice surface is the lowest in the lake and the highest temperature of the lake 2.9 °C (37 °F) at the bottom of the lake. Also, under frozen surface conditions, the heat transfer from the sediment is important.

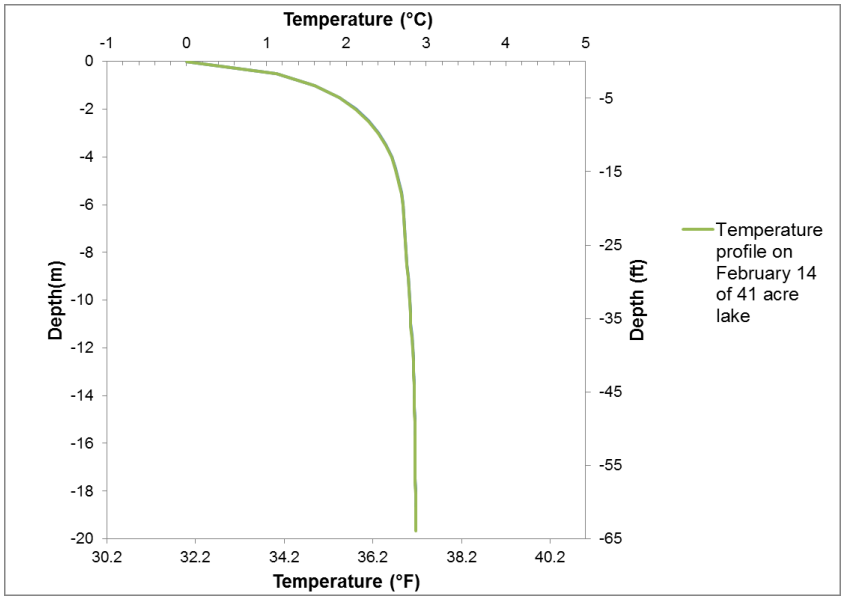

Figure 6-1 Undisturbed lake temperature profile on the day of maximum ice thickness (February 14) of the 41-acre lake

`

Despite low temperatures the lakes can still be used to provide adequate heating. However, the special set of problem arises if the heat extraction rate significantly reduces the lake temperatures. Since the lakes in cold climates already have very low heat content, high heat extraction rate reduces the lake temperatures to near-freezing temperatures (Davin et al. 1981). This in turn increases the risk of formation of ice on the surface of the heat exchanger. The ice formation affects the heat transfer rate between the heat exchanger and a lake and provides inadequate heating. Notably, in shallow lakes, extracting heat from very low near-freezing temperatures of lake is a difficult task.

The results of this part of this work will tell us how much temperature change can be expected for various heat rejection and extraction rates. The main objective of this part of the thesis is to develop guidelines for maximum lake sizes for SWHP applications to ensure acceptable system performance. In other words, the analysis is to find how much heat can be rejected or extracted from the lake without affecting the maximum and minimum allowable design temperatures of the lake.

6.2. Background

To test rigorously the effects of heat rejection and extraction on lake temperatures would require an experimental set up of two side-by-side identical lakes. This seems highly infeasible for anything larger than a small pond because driving one of the lakes to failure with very high heat rejection or extraction rates would require very large energy source.

Studies have been made on predicting the maximum and minimum lake sizes by means of developing a lake model. Pezent and Kavanaugh (1990) develop the lake model to simulate lakes as a heat source or sink. The main objective of their work was to develop a lake model and to analyze the variation of lake temperatures with heat rejection or extraction rates. Since the model was focused on the simulation of lakes in hot and humid climates like in southern region of

`

United States, the model did not account for ice formation on the surface. The temperatures are simulated with 3-zone model; epilimnion, metalimnion and hypolimnion thickness are specified by the user as the input to the model and does not account for wind mixing and turbulent diffusion process in the lakes. The increase in lake temperatures are analyzed by rejecting the cooling loads into the lakes. In this work, based on their three zone lake model, they concluded that the stratification of shallow lakes of 6 m (20 ft) deep is destroyed for loads more than 15 tons per acre (130 kW/ha). For large lakes of 12 m (40 ft) deep Pezent and Kavanaugh (1990) concluded that de-stratification occurs at approximately 200 tons per acre (1738 kW/ha). Pezent and Kavanaugh (1990) work also analyzed the temperature change of shallow lakes during heat extraction scenario. Their work concludes that 5 tons (17.6 kW) of heat extraction from the shallow lakes in southern warm climates does not reduce the lake temperatures by a noticeable level.

Feng et al. (2012) calculated the increase in the water temperature due to heat rejection through an analytical approach. This approach assumes all the heat rejected to the surface layer of known depth and increase in surface temperature is calculated based on changes in heat and mass transfer at the surface. This does not account for storage of heat below the lake surface or the effects of stratification. In the case of heat extraction from an ice-covered lake, most of the energy comes from the sediment, and the cumulative amount of energy that can be extracted vs. time cannot readily be determined with an analytical solution.

Apart from these approaches, the only consistent approach with the developed lake and SWHE model is the one-dimensional numerical analysis. However, a critical constraint on what can be done with this model is with the handling heat rejection or heat extraction. Three different ways of distributing the heat in a lake are proposed and the analysis is performed based on the three HX sub models, yet no one are readily verifiable from existing experimental data. The three heat exchanger sub models are discussed in the next section.

`

6.3. Methodology

The specific question is related to what happens to the heat that is rejected to the lake, or, conversely, how is the cold water created by heat extraction dissipated or transported through the lake? Consider the following possibilities:

The simple answer is that in a one-dimensional model the heat extraction or rejection only directly affects the layers at which the heat is being extracted or rejected and the lake model will take care of the transport. (this option is referred to as "HX sub-model 1" in the next paragraph). In addition, this would make sense if the heat were somehow transported laterally throughout that particular layer. However, consideration of the physics leads to the conclusion that it is far more likely that, under heat rejection conditions, a buoyant plume will transport the heat upwards in the lake. Under heat extraction conditions, depending on which side of the maximum density point the lake and the plume are, the buoyant plume might go upwards or downwards.

Accordingly, let us look into two "limiting case-type" models. The first is the model already described, "HX sub-model 1" and this model would be the limiting case where buoyancy effects are negligible. The second, referred to below as "HX sub-model 2" determines the direction of the buoyant plume. It the plume is upwards, all of the energy rejected is transported to the top surface. (Or, the "cold" is transported upwards for heat extraction cases with upward plumes.) If the plume is downwards, all of the "cold" is transported to the bottom of the lake. The transported energy is then subject to diffusion, surface convection, etc. if at the top layer, or diffusion and conduction to/from the sediment if in the bottom layer. This would be the limiting case where viscous drag on the plume is negligible.

Another simple model splits the difference between the two limiting cases. "HX sub-model 3" determines the direction of the plume, then distributes the heat uniformly in the layers between the heat exchanger and the surface (for upward plumes) or in the layers between the heat

`

exchanger and the bottom (for downward plumes). By "uniformly" the distribution is proportional to the volume in each layer. Therefore, in this case, for an upward plume, the surface layer would still receive more energy than lower layers with smaller cross-sectional areas. Having developed three possible models for how the heat or cold might be transported from the heat exchanger through the lake, what follows is the brief study for a strip mall building (dominated by heat rejection) and an apartment building (dominated by heat extraction).

In the absence of experimental validation, the best that can be done at present is to use the existing models to make a best estimate of how much heat extraction or rejection can cause a small effect (here 1°C and 2°C maximum changes are investigated) as well as how much heat rejection can de-stratify the lake.

Rather than short-term impact of building loads on the lake, the temperature changes in the lake are quantifiable or significant over a course of time. Thus, the analysis is started with the calculation of hourly building loads for a year. Clearly, different building loads will have different load profiles, so the results are likely to be different when buildings other than strip mall used for heat rejection and apartment building used for heat extraction. Also, annual building load profiles are reduced here to a maximum heat rejection rate or heat extraction rate in order to characterize the loading.

The temperature variation depends on morphological parameters such as lake size, depth and volume and on climatic conditions to which the lakes are exposed. Therefore different lakes sizes have been analyzed by placing it in multiple locations in United States. The crucial task is to select the 'best' one of these sub models and to give the maximum lake sizes for heat rejection and extraction. Three different lakes with different sizes and depths are used for the analysis. Table 6-1 gives the surface area, maximum depth and the depth at which the heat exchanger is placed.

`

Table 6-1 Lake sizes and depths used for the analysis

Lake	Lake Size Ha (acres)	Maximum depth m (ft)	HX Depth m (ft)
3 acre pond	1.2 (3)	3.8 (13)	1.5 (5)
41 acre lake	17 (41)	20 (66)	15 (50)
4580 acre lake	1853 (4580)	75 (245)	15 (50)

6.4. Case Study 1: Heat Rejection

For most continental US climatic conditions, commercial buildings are cooling dominant. Such type of building is more suitable for heat rejection analysis because such cooling loads are more likely to adversely affect lake temperatures. A commercial strip mall building was chosen for estimating the increase of lake temperature due to heat rejection. The total area of the building is 2090 m^2 (22,500 ft^2). The loads are adjusted upwards by increasing the number of buildings. For each combination of building and location, the cooling and heating loads for every hour is predicted from the annual building simulation in EnergyPlus (DOE 2012).

The strip mall building is simulated for different locations, which includes Phoenix, AZ, Atlanta, GA, Seattle, WA and Indianapolis, IN. The locations are selected based on the climatic conditions. Phoenix, AZ for its extremely hot climate, Atlanta, GA for its hot and humid climate, Seattle, WA for its warm moderate climate and Indianapolis, IN for its continental climate that features both hot summers and cold winters. The peak hourly cooling load and the average load on the peak cooling day of the strip mall building in all four different locations are summarized in Table 6-2

`

Table 6-2 Maximum hourly and maximum daily average cooling loads of the strip mall located in different locations

Strip mall locations	Max Cooling load (Hourly)		Max Cooling load (Averaged over a day)	
	kW	tons	kW	tons
Phoenix	78	22	35	10
Atlanta	46	13	28	8
Seattle	20	6	8	2
Indianapolis	25	7	11	3

The stand-alone FORTRAN lake model developed as a part of this project, which is explained in Task 5, is used for the analysis. Appropriate initial conditions, lake bathymetry and Secchi depth of the lakes are given as input. The simulations for heat rejection are carried out for two years and second year lake temperatures are used for the analysis. The hourly heating and cooling loads of the building are read from the text file. Since the lake model is a daily time step model, the loads are averaged over a day and passed to the surface water heat exchanger subroutine.

The subroutine starts with the calculation of heat rejection in cooling mode and heat extraction in heating mode through a simple heat pump model developed along with the SWHE model. The heat pump model consists of a curve fit equations developed from the manufacturers data, which calculates heat rejection and extraction. The heat exchanger subroutine calculates the heat transfer rate between SWHE and the lake for a day and supplies it back to the lake model. The 1-D numerical lake model accounts for SWHE convective heat transfer mechanism based on the selection of 'HX sub-models'.

`

6.4.1. Heat exchanger coil sizing

The SWHE model was set up to simulate with HDPE spiral helical heat exchanger. The length of the one coil is 152.4 m (500 ft). Table 6-3 lists the dimensions of the spiral helical coil heat exchanger. Both the analysis of heat rejection and extraction are performed with the spiral helical coils of similar dimensions. The flow rate of the heat exchanger fluid (water) for both the heat rejection and extraction cases is 0.5 kg/s (8 GPM).

Table 6-3 Dimensions of the spiral helical coil heat exchanger

Parameters	Dimensions
Outer diameter of the tube	26.7 mm (1.05 in)
Inner diameter of the tube	21.8 mm (0.86 in)
Length of the heat exchanger tube	152.4 m (500 ft)
Outside diameter of the coil	1.98 m (6.5 ft)
Inside diameter of the coil	1.4 m (4.6 ft)
Horizontal spacing between the coils	105 mm (4.125 in)
Vertical spacing between the	105 mm (4.125 in)

Before analyzing with the stand-alone FORTRAN model, the length of the coil is sized for each climatic condition using a SWHE design tool developed in Excel VBA as a part of this project. The tool runs the lake model to predict undisturbed lake temperatures at the heat exchanger depth and then simulates SWHE model for heat transfer rate and exiting fluid temperatures of heat exchanger. Final output of the design tool gives the optimum number of coils needed for each respective location and building type. It adjusts the number of heat exchanger coils so that the peak entering fluid temperatures to the heat pump remains within the user defined limits. The reader is referred to Task 9 for the detailed explanation of design tool.

6.4.2. HX sub-model 1

The temperature increase in 41-acre (16.6 ha) lake is first tested with sub-model 1 using the loads of a strip mall building located in Phoenix, AZ. The heat rejection per acre is increased to the maximum of 68 tons/acre (591 kW/ha) by increasing the number of buildings. The

`

temperature profiles on the day of maximum cooling load (July 8) for different heat rejection rates are shown in Figure 6-2

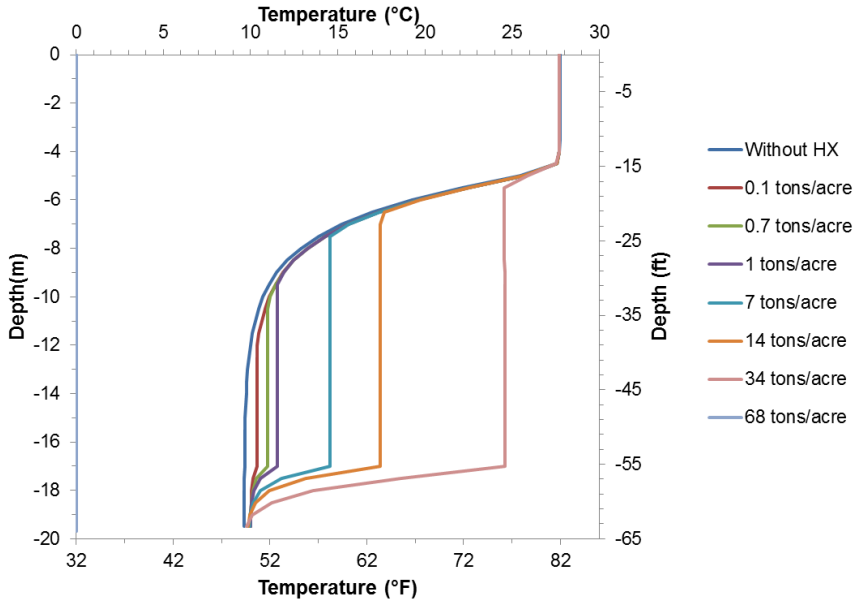

Figure 6-2 Temperature profiles on the day of maximum cooling load of a 41-acre lake located in Phoenix, AZ obtained using HX sub-model 1

Figure 6-2 clearly shows that the heat rejected into the lake using this sub model adversely affects the temperature profiles of the lake. At heat exchanger depth of 15 m (49.2 ft), the undisturbed lake temperature is 10 °C (50 °F), which rises to 24.6 °C (76.3 °F) for 68 tons of heat rejection per acre (591 kW/ha). However, there are no noticeable differences in the surface temperatures. This is because sub-model 1 is fairly simple model that distributes the heat to only the water layers at the depth where the heat exchanger is placed. The lake model then transports heat to the water layers above and below by means of mixing which takes place through unstable density differences. Since the sub model assumes that the heat input from the heat exchanger stays at the certain depth, the temperature rise in the lake is poorly predicted. Due to this reason

`

and, also because the analysis of the model is likely to give high unreliable temperature change, the model is left out from further analysis.

6.4.3. HX sub-model 2

Figure 6-3, Figure 6-4 and Figure 6-5 shows the temperature profiles on the day of maximum cooling load of 3-acre (1.8 ha) pond, 41-acre (16.6 ha) lake and 4580-acre (1854 ha) lake. All the plots are the results simulated in Phoenix, AZ using HX sub-model 2. As already discussed, HX sub-model 2 transports all the heat rejected to the top surface of the lake. Since the transported energy is subjected to convection and evaporation losses at the surface it can be seen from the plots that the surface temperature increase is very little even for higher heat rejection per acre. In 4580-acre (1854 ha) lake, the maximum temperature rise of 1.7 °C is observed at the surface for 123 tons/acre (1069 kW/ha) of heat rejection. For shallow pond in Figure 6-3, the temperature difference between the surface and bottom of the pond is very less. The pond temperature profiles remains almost de-stratified and the temperature increase is constant from the surface to the depth of the lake. For deep lakes as shown in Figure 6-4 and Figure 6-5, there is no thermocline destruction and there is no temperature rise at the depths below the surface even for the loads 68 tons/acre (591 kW/ha) for 41-acre lake and 123 tons/acre (1069 kW/ha) for 4580-acre lake.

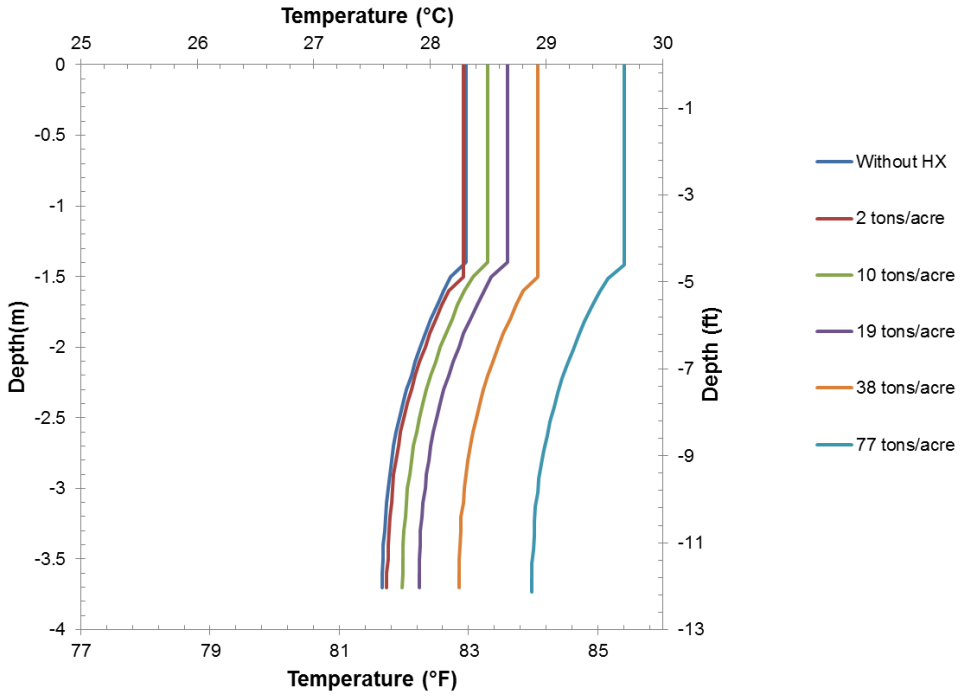

Figure 6-3 Temperature profiles on the day of maximum cooling load of a 3 acre pond located in Phoenix, AZ obtained using HX sub-model 2

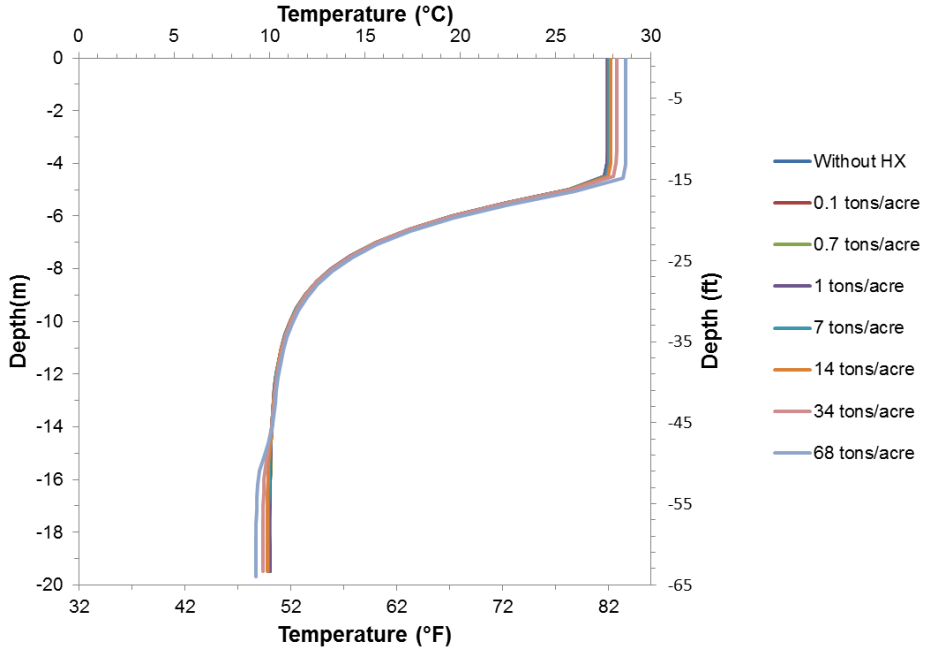

Figure 6-4 Temperature profiles on the day of maximum cooling load of a 41-acre lake located in Phoenix, AZ obtained using HX sub-model 2

`

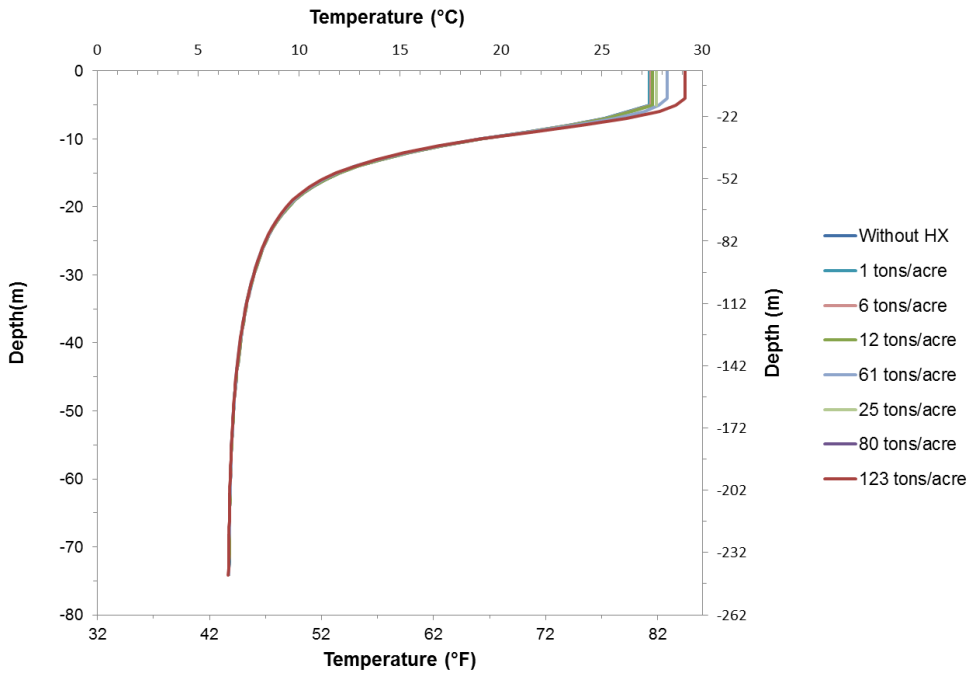

Figure 6-5 Temperature profiles on the day of maximum cooling load of a 4580-acre lake located in Phoenix, AZ obtained using HX sub-model 2

6.4.4. HX sub-model 3

To illustrate the heat distribution of HX sub-model 3, the temperature profiles for various heat rejection rates on peak cooling load day for the lakes located in Phoenix are plotted. Figure 6-6 shows small stratification is destroyed for 38 tons/acre (330 kW/ha) for shallow small size pond and it remains de-stratified for further increase in cooling loads. For 41-acre lake (Figure 6-7) and 4580-acre lake (Figure 6-8), approximately 68 tons/acre (591 kW/ha) and 123 tons/acre (1069 kW/ha) partially destroyed the stratification. Shallow lakes tend to de-stratify quickly when compared to deep lakes.

As already discussed HX sub-model 3 determines the direction of plume and distributes the heat uniformly in all the layers above/below the heat exchanger depth. In a combination of heat extraction and downward plume, the sub-model extracts heat uniformly from the layers

`

below heat exchanger depth. As we can see in Figure 6-7 and Figure 6-8, the temperatures are significantly decreased below 16 m (52 ft) in 41-acre lake and below 20 m (66 ft) in 4580-acre lake due to significant amount of heat extraction

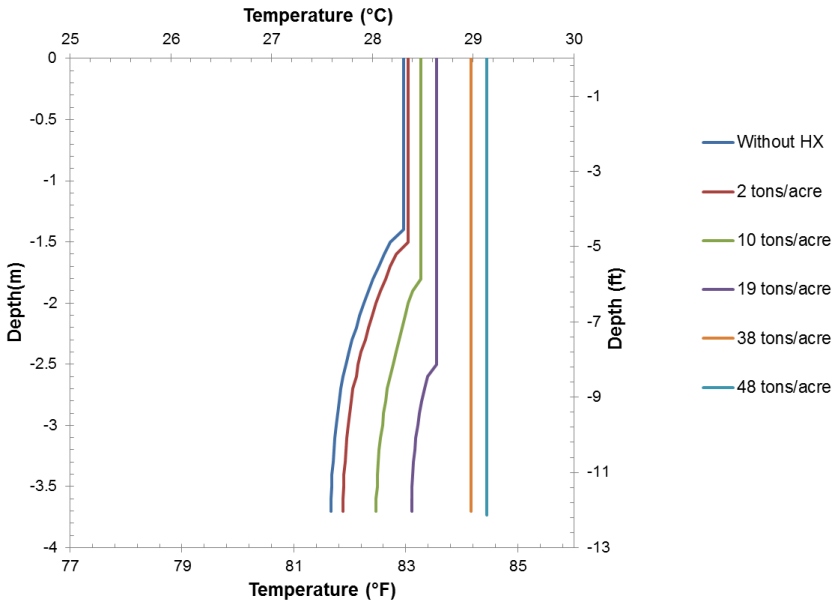

Figure 6-6 Temperature profiles on the day of maximum cooling load of a 3 acre pond located in Phoenix, AZ obtained using HX sub-model 3

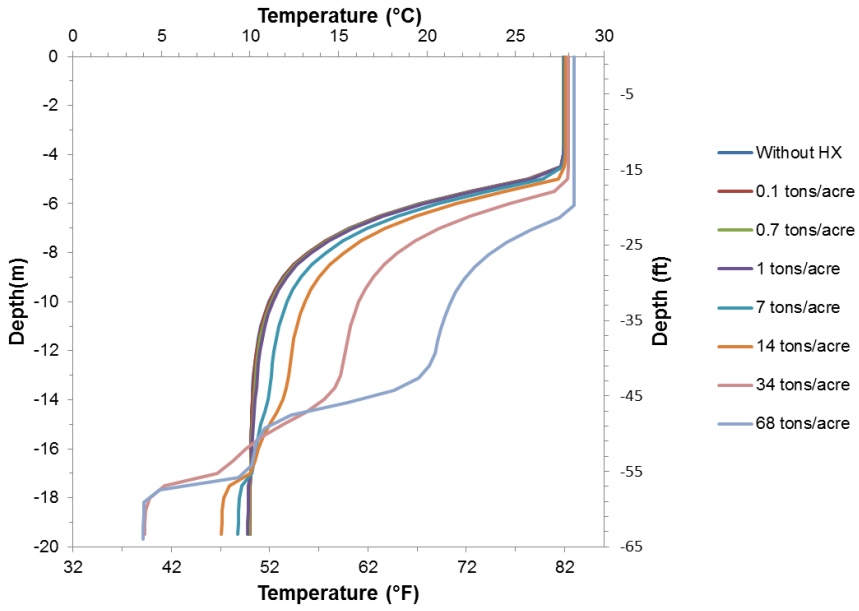

Figure 6-7 Temperature profiles on the day of maximum cooling load of a 41-acre lake located in Phoenix, AZ obtained using HX sub-model 3

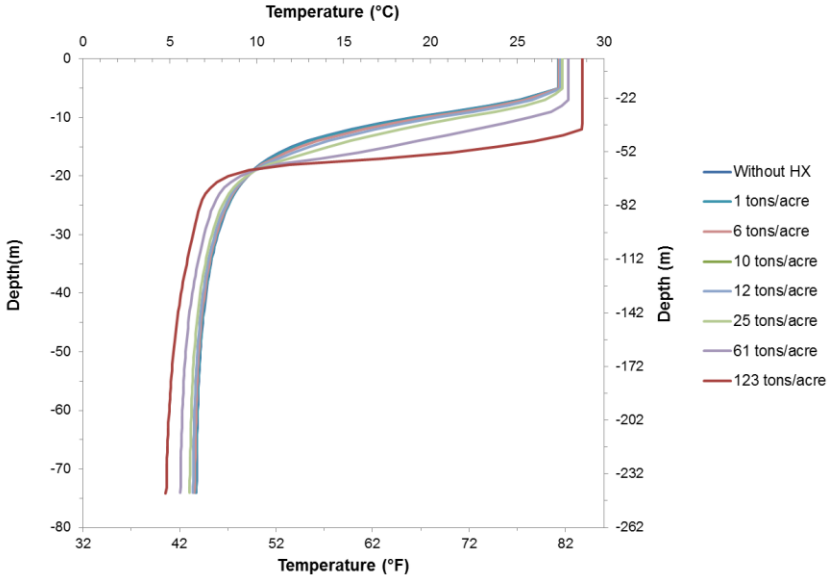

Figure 6-8 Temperature profiles on the day of maximum cooling load of a 4580-acre lake located in Phoenix, AZ obtained using HX sub-model 3

`

6.4.5. Results and discussion

As far as we know, there are no standards for acceptable temperature change in lake. Therefore, we have looked into the following criteria

- Halfway through de-stratification
- 1°C and 2°C maximum change on the day of peak cooling load
- 0.5°C and 1°C mean lake temperature change on the day of peak cooling load

The loads for which the temperature profile is half-way through de-stratification is considered as the maximum capacity of the lakes. This is the point where the lake temperatures are half way between undisturbed and completely de-stratified cases. This is illustrated through an example as shown in Figure 6-9. As can be seen in the figure, the heat rejection rate of 162 tons/acre almost stratified the lake till 16 m (52 ft) depth and for 68 tons/acre the temperature profile is approximately half-way between undisturbed (Without HX) and stratified cases.

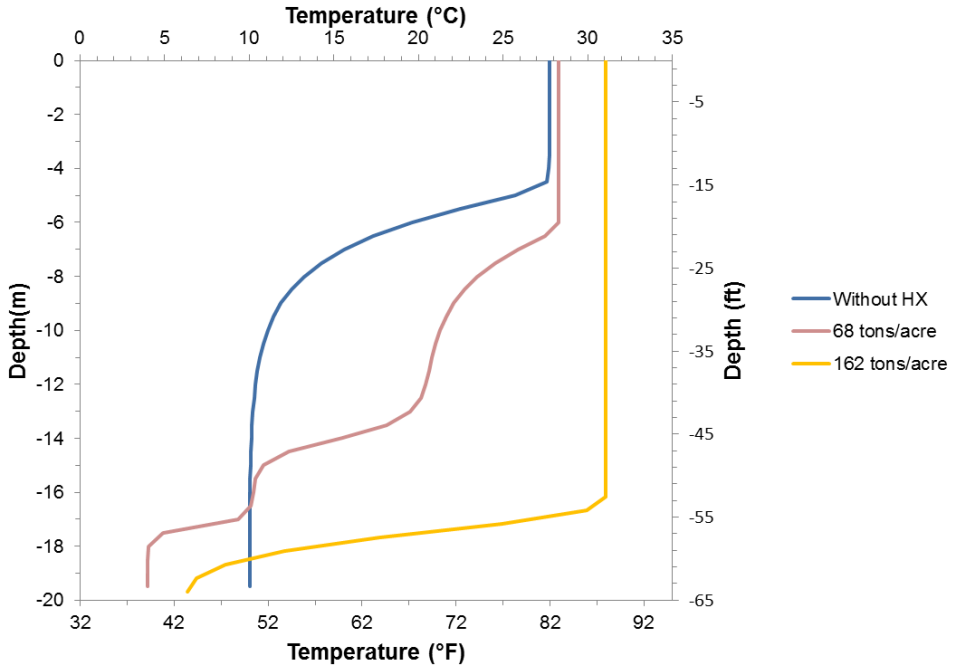

Figure 6-9 Illustration of half way through de-stratification through the temperature profiles on load of a 41-acre lake located in Phoenix, AZ obtained using HX sub-model 3

`

Condition 1: Halfway through de-stratification

The heat rejection rates summarized in Table 6-4 are the values at which the temperature profile is half way through de-stratification and it is different for each lake and location combination. Using HX Sub-Model 3, general conclusions can be drawn as for 41 acre (16.6 ha) lake significant de-stratification occurs approximately at 61 tons/acre (530 kW/ha) and for 4580 acre (1854 ha) lake, significant de-stratification occurs approximately at 121 tons/acre (1051 kW/ha).

Table 6-4 Heat rejection rates allowable for the partial destruction of stratification determined using HX sub-model 3

	3 acre pond	41 acre lake	4580 acre lake
Location	kW/Ha (tons/acre)	HX-3 kW/Ha (tons/acre)	HX-3 kW/Ha (tons/acre)
Phoenix	330 (38)	591 (68)	1069 (123)
Atlanta	391 (45)	530 (61)	1138 (131)
Seattle	295 (34)	547 (63)	1242 (143)
Indianapolis	278 (32)	626 (72)	1051 (121)

Condition 2: 1°C and 2°C maximum change on the day of peak cooling load

Furthermore, the recommendation of maximum heat rejection rate based on rise of lake temperatures by 1°C and 2°C are analyzed. Table 6-5 and Table 6-6 lists the allowable heat rejection rate for different lakes that will give a maximum lake temperature increase at all depths of 1°C and 2°C.

`

Table 6-5 Recommended heat rejection rate allowable for the maximum rise of lake temperature by 1°C (34 °F)

	3 acre pond		41 acre lake		4580 acre lake	
Sub Model	HX-2 kW/ha (tons/acre)	HX-3 kW/ha (tons/acre)	HX-2 kW/ha (tons/acre)	HX-3 kW/ha (tons/acre)	HX-2 kW/ha (tons/acre)	HX-3 kW/ha (tons/acre)
Phoenix	417 (48)	165 (19)	591 (68)	61 (7)	695 (80)	87 (10)
Atlanta	295 (34)	148 (17)	521 (60)	87 (10)	565 (65)	113 (13)
Seattle	382 (44)	156 (18)	547 (63)	139 (16)	591 (68)	400 (46)
Indianapolis	269 (31)	130 (15)	391 (45)	200 (23)	626 (72)	70 (8)

Table 6-6 Recommended heat rejection rate allowable for the maximum rise of lake temperature by 2°C (36 °F)

	3 acre pond		41 acre lake		4580 acre lake	
Sub Model	HX-2 kW/ha (tons/acre)	HX-3 kW/ha (tons/acre)	HX-2 kW/ha (tons/acre)	HX-3 kW/ha (tons/acre)	HX-2 kW/ha (tons/acre)	HX-3 kW/ha (tons/acre)
Phoenix	1077 (124)	669 (77)	1242 (143)	122 (14)	1277 (147)	156 (18)
Atlanta	877 (101)	321 (37)	1043 (120)	165 (19)	1138 (131)	226 (26)
Seattle	678 (78)	304 (35)	930 (107)	209 (24)	1095 (126)	799 (92)
Indianapolis	608 (70)	269 (31)	782 (90)	313 (36)	1129 (130)	243 (28)

The tons/acre required to rise the lake temperature by 1 °C is always higher for HX sub-model 2 than HX sub-model 3. This is because in sub-model 2, the surface layer alone receives the heat energy and it is subjected to convection and evaporation losses. Whereas the HX sub model 3, in addition to surface layer, the model build more heat over the summer at the layers below the surface too. Therefore, during heat rejection the lakes tend to heated up throughout the depth.

From Table 6-5, for HX sub-model 3 it can be seen that the tons/acre required to rise the temperature by 1°C for a 3-acre (1.8 ha) pond is higher than the other two lakes in the locations such as Phoenix, Atlanta and Seattle. This contrary is because the temperature rise of 1°C occurs

`

at the region of thermocline that is a high temperature gradient region, whereas the temperature rise for the shallow pond occurs in the stratified region. The 1 °C rise for 3-acre (1.8 ha) pond is approximately at the depth of 2.5 m (8 ft) for 19 tons/acre (165 kW/ha) cooling load (Figure 6-6). On the other hand, for a 41-acre (16.6 ha) lake the temperature rise by 1 °C is in the thermocline region at the depth of about 7 m (23 ft) for 7 tons/acre (61 kW/ha). Similarly, for 4580-acre (1854 ha) lake 1 °C rise is observed for 10 tons/acre (87 kW/ha) at 11 m (36 ft) depth

The heat rejection in a lake promotes upward mixing that would eventually increase the epilimnion depth for increase in heat rejection. The lakes with deep epilimnion tell us that the lakes are with higher heat storage capacity. We could observe 1 °C rise in thermocline region of deep lakes for relatively less heat rejection rate when compared to 3-acre (1.8 ha) pond. This can be attributed to the fact that thermocline temperatures changes rapidly for a small variation in epilimnion.

Condition 3: 0.5°C and 1°C mean lake temperature change on the day of peak cooling load

Table 6-7 and Table 6-8 give heat rejection rates for which the mass-weighted average lake temperature increases by 0.5°C and 1°C. 0.5°C increase in average lake temperature is observed for the heat rejection range from 7 tons/acre (61 kW/Ha) to 69 tons/acre (599 kW/Ha) and 1°C increase in average lake temperature is observed for the heat rejection range of 15 tons/acre (130 kW/Ha) to 91 tons/acre (791 kW/Ha)

`

Table 6-7 Heat rejection rates allowable for the rise of mass-weighted average lake temperature by 0.5°C

	3 acre pond	41 acre lake	4580 acre lake
Sub Model HX-3	kW/Ha (tons/acre)	kW/Ha (tons/acre)	kW/Ha (tons/acre)
Phoenix	165(19)	61 (7)	113 (13)
Atlanta	148 (17)	70 (8)	191 (22)
Seattle	374 (43)	104 (12)	599 (69)
Indianapolis	113 (13)	78 (9)	148 (17)

Table 6-8 Heat rejection rates allowable for the rise of mass-weighted average lake temperature by 1°C

	3 acre pond	41 acre lake	4580 acre lake
Sub Model HX-3	kW/Ha (tons/acre)	kW/Ha (tons/acre)	kW/Ha (tons/acre)
Phoenix	495 (57)	130 (15)	269 (31)
Atlanta	295 (34)	165 (19)	382 (44)
Seattle	617 (71)	269 (31)	791 (91)
Indianapolis	217 (25)	156 (18)	426 (49)

6.5. Case Study 2: Heat Extraction

The system with peak heat extraction is more critical than high heat rejection. During peak heating loads, if the lake temperature goes near freezing there is a risk of ice formation on the outer surface of the heat exchanger that affects the system performance. Therefore, it is important to analyze how much heat can be extracted from a lake. March 1 is selected as the starting day of simulation and it ran through the end of February. In this manner, the peak heat extraction would fall at the end of the simulation during February. Ice cover at the surface of the lake usually reaches its maximum amount during late February.

`

Similar to heat rejection analysis, heat extraction analysis is started with proper sizing of the coils. The spiral helical coil used in the previous analysis is also used here with same dimensions. Heat extraction analysis is performed using an apartment building in the locations Seattle, WA, Indianapolis, IN and Burlington, VT to analyze the maximum amount of heat that can be extracted from the lake. The climatic conditions of these three locations differ. Seattle is selected for its mild winter climate; Indianapolis and Burlington are selected for its continental climate with cold winters. The peak hourly heating load and the heating load averaged over the peak heating load day of an apartment building for all three locations is summarized in Table 6-9

Table 6-9 Peak heating loads for the apartment building

Apartment locations	Max heating load (Hourly)		Max heating load (Averaged over a day)	
	kW	MBtuh	kW	MBtuh
Burlington	71	242	53	180
Seattle	32	109	22	75
Indianapolis	65	222	46	157

The example plots of temperature decrease during heat extraction are shown in the next section for sub-model 2 and 3. Since, again, HX sub-model 1 is not analyzed because it would result in unrealistic temperature drop during heat extraction.

6.5.1. HX sub-model 2

Figure 6-10 to Figure 6-12 shows the temperature profiles of 3-acre (1.8 ha) pond, 41-acre (16.6 ha) lake and 4580-acre (1854 ha) lake for various heat extraction rates using HX sub-model 2 simulated in Seattle, WA. The undisturbed temperature profiles in all the plots shows almost de-stratified profiles on the day of maximum ice thickness formation. The highest temperature of shallow pond is around 1 °C and for deep lakes is around 3 °C. This de-stratified temperature profile is typical for most of the lakes in winter season.

`

Since the heat content of the shallow lakes is lower than the large lakes, the shallow lakes in the cold climates tend to freeze soon than the large lakes. There is ice formation on the surface of 3-acre pond and 41-acre lake during undisturbed condition itself. Nevertheless, for larger lakes, the peak heat extraction of 9042 MBtuh/acre (6548 kW/ha) causes the ice formation at the surface.

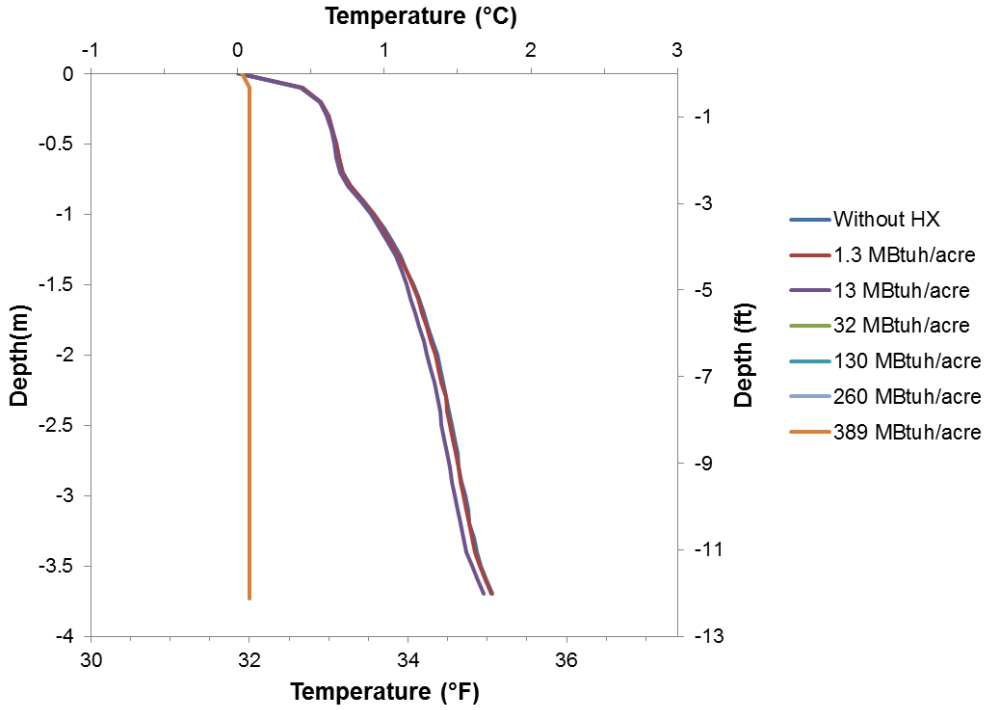

Figure 6-10 Temperature profiles on the day of maximum ice formation on the surface of a 3-acre pond located in Seattle, WA obtained using HX sub-model 2

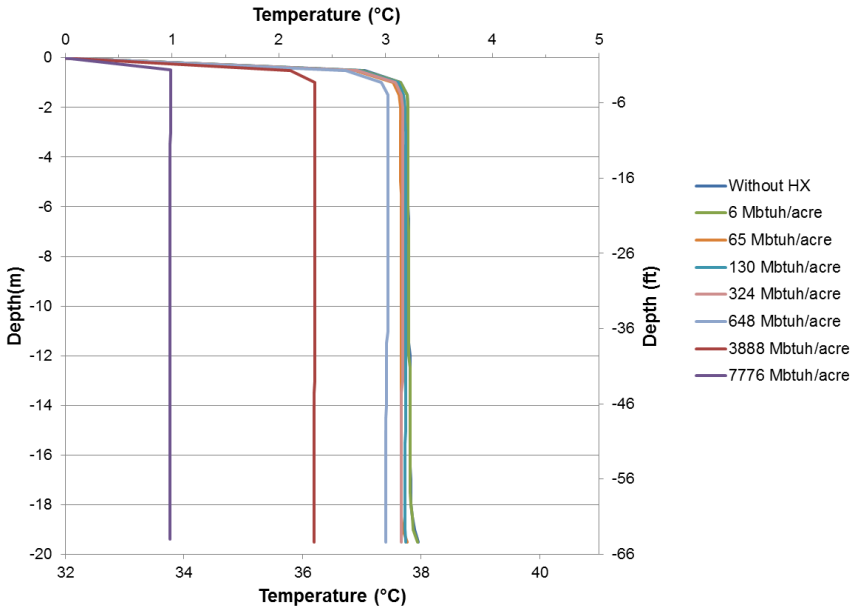

Figure 6-11 Temperature profiles on the day of maximum ice formation on the surface of a 41-acre lake located in Seattle, WA obtained using HX sub-model 2

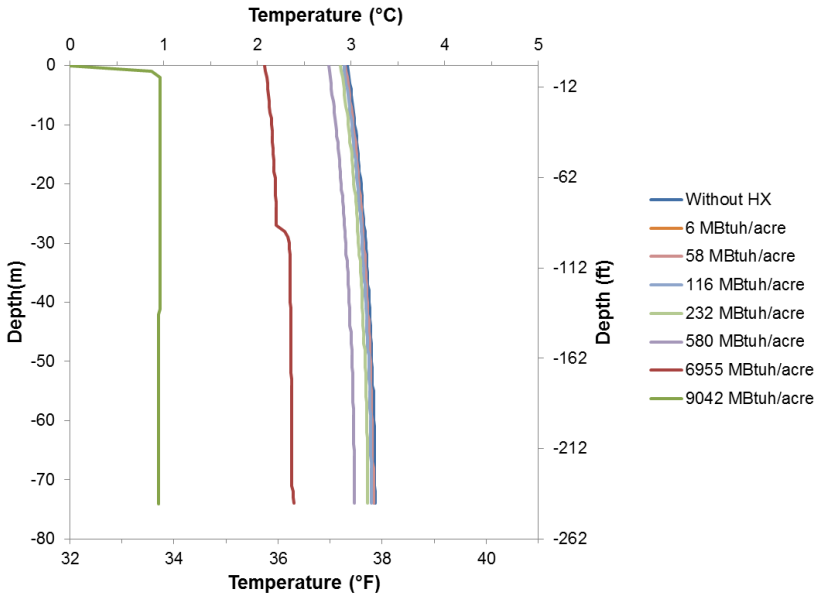

Figure 6-12 Temperature profiles on the day of maximum ice formation on the surface of a 4580-acre lake located in Seattle, WA obtained using HX sub-model 2

`

6.5.2. HX sub-model 3

Figure 6-13 , Figure 6-14 and Figure 6-16 shows the temperature plots for different lake sizes located in Seattle. Although, the temperature profiles are similar to HX sub-model 2, the drop in temperature is higher for HX sub-model 3 for same range of heat extraction rates. This is because HX sub-model 3 extracts heat from the water layers present below the surface and HX sub-model 2 extracts it from the bottom or surface depending on the direction of plume. For example, using HX sub-model 2 in 4580-acre lake, the maximum temperature drop for 232 MBtuh/acre (168 kW/ha) is almost negligible, which is less than 0.1 °C (Figure 6-12). On the other hand, using HX sub-model 3 in the same lake, the maximum temperature drop for 232 MBtuh/acre (168 kW/ha) is 0.9 °C (Figure 6-16).

In a 3-acre pond, the heat extraction rate of 26 MBtuh/acre (19 kW/ha) decreases the pond temperature to near-freezing temperatures. However, 0 °C does not indicate that the whole pond is frozen, it shows that the water temperatures are at near 0 °C. Figure 6-14 shows the ice thickness variation on February 19 for a 3-acre pond located in Seattle. The plot makes clear that the heat extraction rate of 26 MBtuh/acre (19 kW/ha) raised the ice thickness from 1.5 mm (0.06 in) to 44 mm (1.7 in) but not frozen the whole pond.

For 41-acre (16.6 ha) lake it requires around 529 MBtuh/acre (383 kW/ha) to decrease the lake temperature approximately from 3 °C to 1 °C as shown in Figure 6-15 . For 4580-acre (1854 ha) lake, it requires 1043 MBtuh/acre (755 kW/ha) to decrease the lake temperature approximately from 3 °C to 1 °C as shown in Figure 6-16..

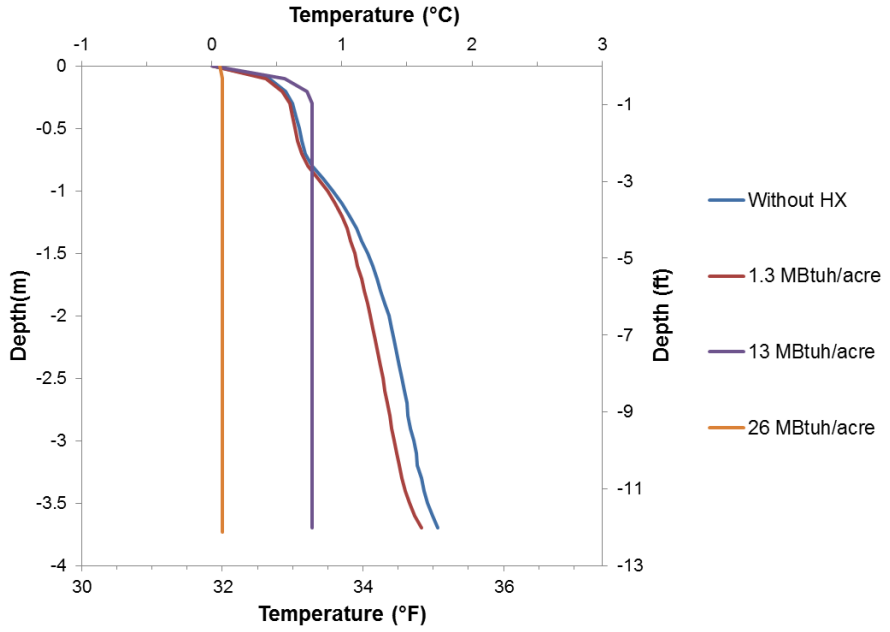

Figure 6-13 Temperature profiles on the day of maximum ice formation on the surface of a 3-acre pond located in Seattle, WA obtained using HX sub-model 3

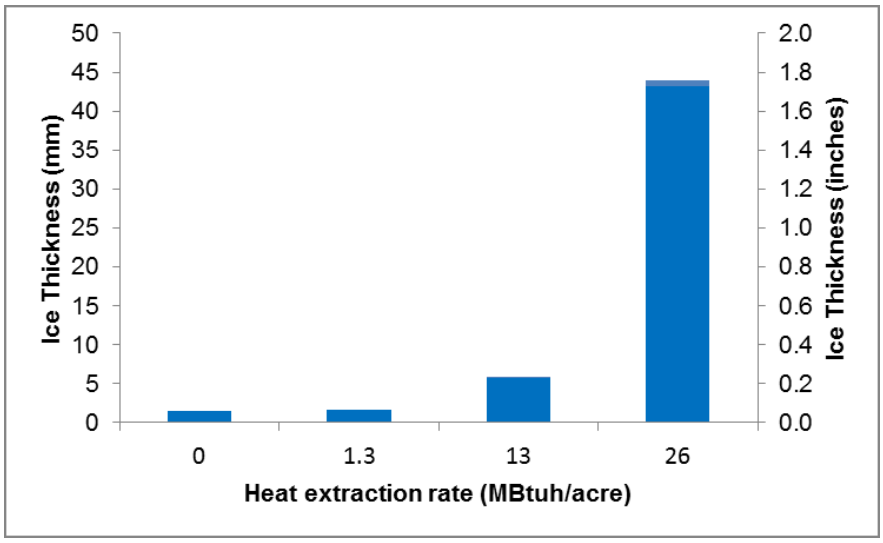

Figure 6-14 Ice thickness on February 19 of 3 acre pond located in Seattle, WA obtained using HX sub-model 3

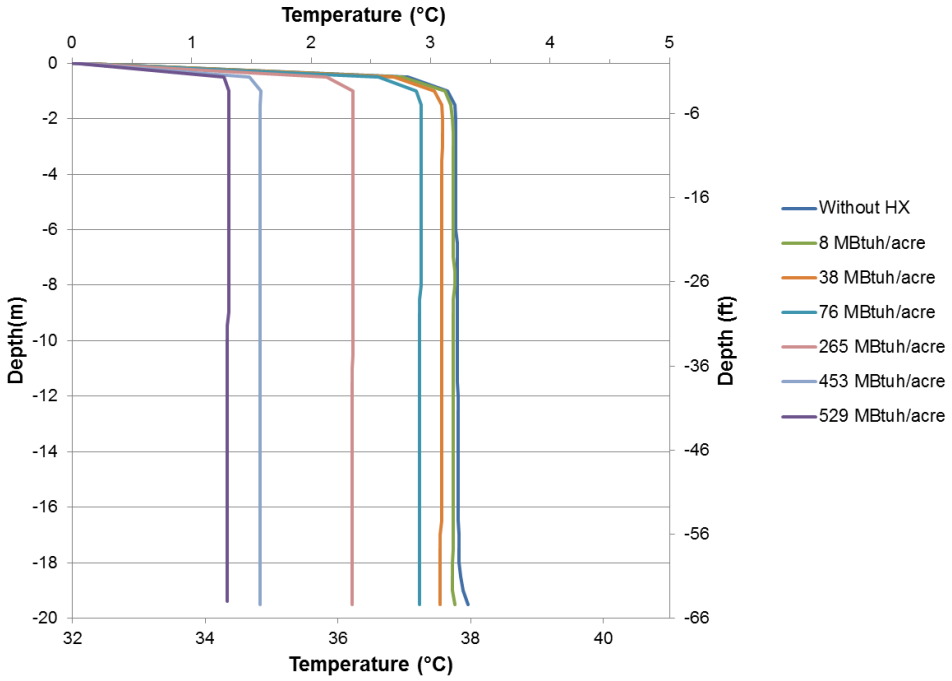

Figure 6-15 Temperature profiles on the day of maximum ice formation on the surface of a 41-acre lake located in Seattle, WA obtained using HX sub-model 3

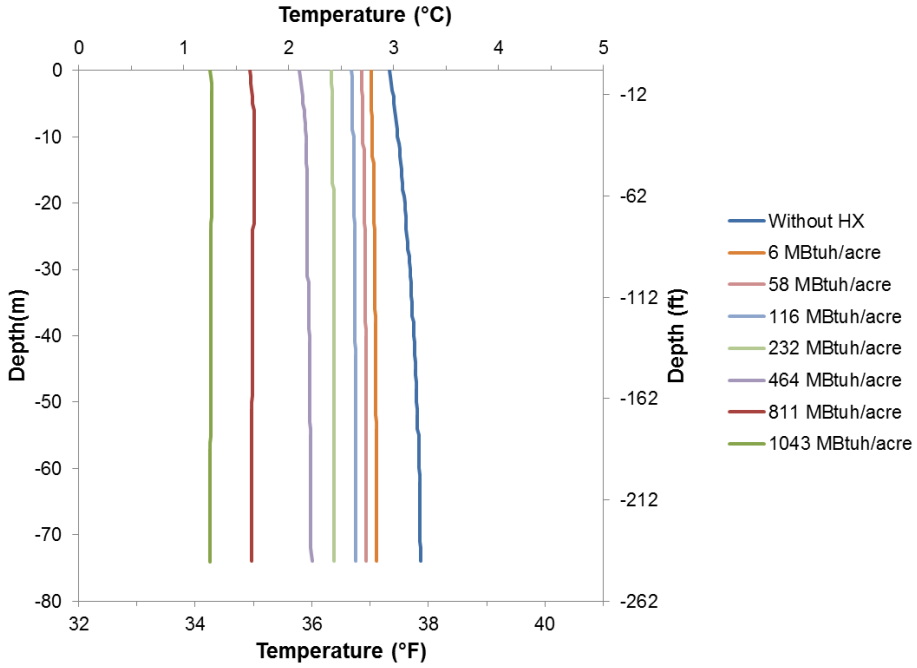

Figure 6-16 Temperature profiles on the day of maximum ice formation on the surface of a 4580-acre lake located in Seattle, WA obtained using HX sub-model 2

`

6.5.3. Results and discussion

Table 6-10 summarizes the maximum allowable heat extraction rates for 1°C drop in lake temperature for different lakes and locations. Similarly, Table 6-11 is for 2°C drop in lake temperatures.

Table 6-10 Recommended heat extraction rate allowable for the maximum drop of lake temperature by 1°C (34 °F)

	3 acre pond		41 acre lake		4580 acre lake	
	HX-2 kW/Ha (MBtuh/acre)	HX-3 kW/Ha (MBtuh/acre)	HX-2 kW/Ha (MBtuh/acre)	HX-3 kW/Ha (MBtuh/acre)	HX-2 kW/Ha (MBtuh/acre)	HX-3 kW/Ha (MBtuh/acre)
Seattle	188 (260)	9 (13)	2816 (3888)	192 (265)	5037 (6955)	336 (464)
Indianapolis	43 (60)	1.4 (2.0)	555 (767)	80 (110)	1869 (2581)	89 (123)
Burlington	131 (181)	1.3 (1.9)	692 (956)	83 (115)	4942 (6824)	112 (154)

Table 6-11 Recommended heat extraction rate allowable for the maximum drop of lake temperature by 2°C (36 °F)

	3 acre pond		41 acre lake		4580 acre lake	
	HX-2 kW/Ha (MBtuh/acre)	HX-3 kW/Ha (MBtuh/acre)	HX-2 kW/Ha (MBtuh/acre)	HX-3 kW/Ha (MBtuh/acre)	HX-2 kW/Ha (MBtuh/acre)	HX-3 kW/Ha (MBtuh/acre)
Seattle	282 (390)	19 (26)	5632 (7776)	383 (529)	6548 (9041)	755 (1043)
Indianapolis	107(148)	3 (4)	1388 (1917)	159 (219)	5341 (7375)	178 (246)
Burlington	-*	-*	1662 (2295)	194 (268)	7414 (10237)	247 (341)

* The SWHE had tube-center spacing of 104.7 mm (4.1 in) in and it frozen completely solid before the 2°C limit was reached

`

From Table 6-10 and Table 6-11, for 3 acre pond resulted in very low heat extracted rates per acre such as 2 MBtuh/acre (1 kW/ha) and 4 MBtuh/acre (3 kW/ha) in places like Indianapolis and Burlington using HX Sub-Model 3.

Since, the 3-acre (1.8 ha) shallow pond is frozen at the surface in cold locations like Indianapolis and Burlington its undisturbed lake temperatures are very low under the ice formation. Further cooling of pond due to heat extraction causes to ice thickness to increase and reduces the pond temperatures beneath the surface. Figure 6-17 to Figure 6-20 shows the temperature and ice thickness variation of 3-acre (1.8 ha) pond during high heat extraction in Indianapolis and Burlington.

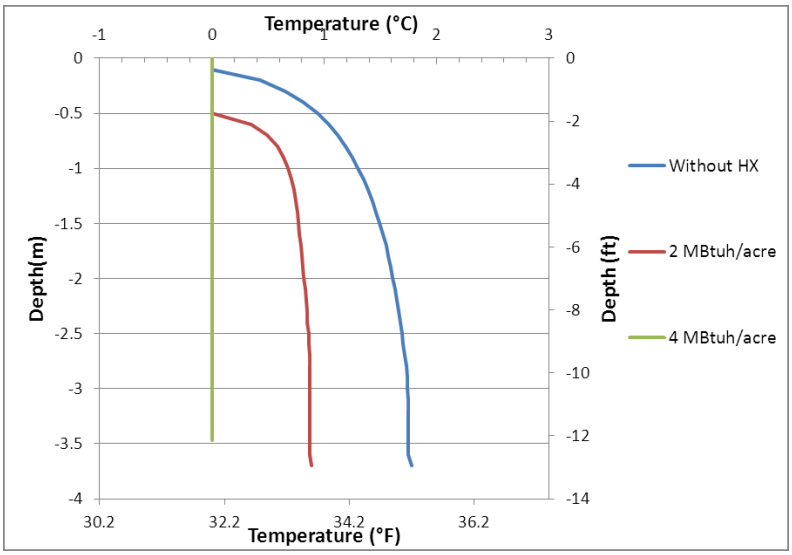

Figure 6-17 Temperature profiles on February 2 of a 3-acre pond located in Indianapolis, IN obtained using HX sub-model 3

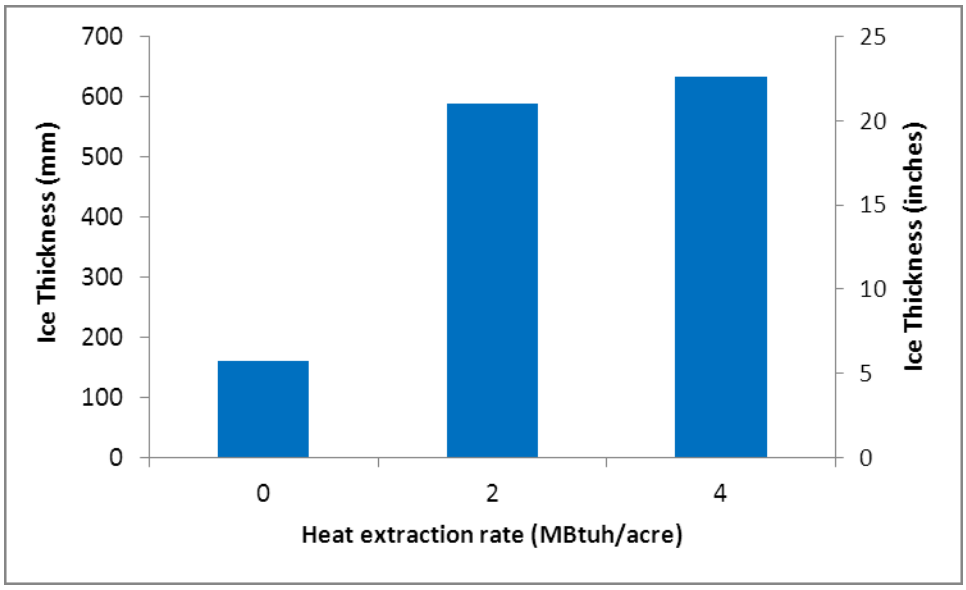

Figure 6-18 Ice thickness on February 2 of 3 acre pond located in Indianapolis, IN obtained using HX sub-model 3

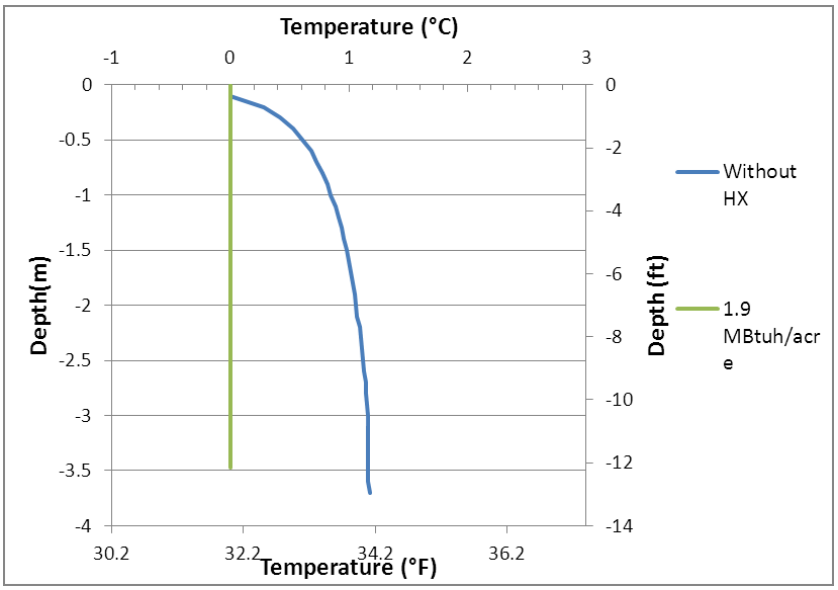

Figure 6-19 Temperature profiles on January 24 of a 3-acre pond located in Burlington, VT obtained using HX sub-model 3

`

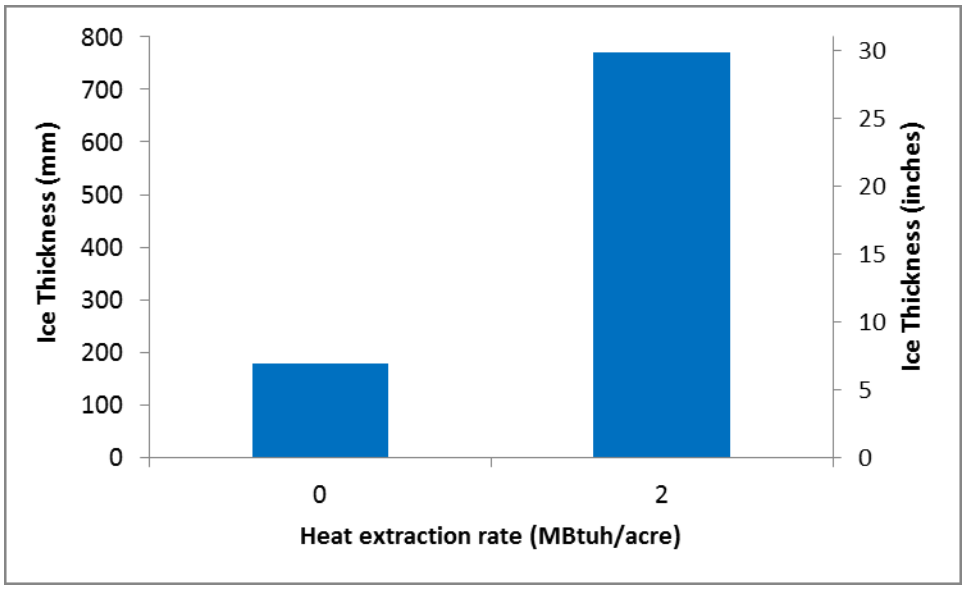

Figure 6-20 Ice thickness on January 24 of 3 acre pond located in Burlington, VT obtained using HX sub-model 3

The heat extraction rate per acre required to de-stratify a lake by destroying the small inverse stratification depends on the depth and meteorological conditions of the lake. For example, we can see from Figure 6-13, the de-stratification occurs at 13 MBtuh/acre (9 kW/ha) for a 3-acre (1.8 ha) pond in Seattle WA. However, for the same size pond located in Burlington VT, the de-stratification occurs for very small heating loads of 1.9 tons/acre (17 kW/ha) shown in Figure 6-19 . Noticeably the significant temperature decrease occurred in the whole lake where the water temperatures dropped from 1 °C to 0 °C. Since, the building loads for Burlington VT are more heating dominated; the combination of adequate cold conditions for low temperature profile and highest heating demand causes the pond temperatures to drop suddenly for low heat extraction rates.

Figure 6-20 show that 175 mm (7 inches) of ice thickness during undisturbed condition rises to 757 mm (30 inches) for 2 MBtuh/acre of heat extraction rate. The undisturbed pond temperature of 3-acre (1.8 ha) pond in Burlington VT is very low around 1 °C as shown in Figure

`

6-19. Therefore, we could not calculate the required heating rate per acre for the temperature drop of 2 °C. In these conditions, the water temperature dropped to the lowest possible and heat exchanger model could not model the freezing conditions of the heat exchanger because the ice thickness at the surface of the heat exchanger reaches its maximum amount that the model can predict.

6.5.4. Conclusions

The effect of heat rejection or extraction that cause the lake temperature variation of 1°C and 2°C is analyzed in this chapter using three different simplified HX sub models. Since HX sub-model 3 is a type which splits-the-difference between two limiting case type models (HX sub-model 1 and HX sub-model 2), HX sub-model 3 is selected here as the best to give design recommendations. A major limitation of this study is the results are based only on the simulations and there are no experimental data to validate the results. Based on the limited information, the results are presented for 4 different locations and 3 different lake types.

Heat rejection case

On looking at the results, we can say that the heat rejection rate is relatively sensitive to lake site particularly for 1°C and 2°C temperature variation. There is substantial difference depending on lake type and location and no definitive trend in the results related to either lake type or location. This makes it difficult to recommend a single heat rejection/extraction rate that suits for every case that has been analyzed. However, we could say from limited locations and lake types analyzed, a 1°C temperature increase in lake temperature is caused by a low heat rejection rate of 7 tons/acre to high heat rejection rate of 46 tons/acre. Similarly, a range for heat rejection rate that caused 2°C temperature rise is 14 tons/acre to 92 tons/acre.

The maximum allowable loading for specific lake/location is considered as the heat rejection rate at which the temperature stratification is completely destroyed for shallow ponds

`

and partially destroyed for large lakes. At this point of maximum loading, the lake temperature will be increased significantly from undisturbed lake temperatures. In all the three lake types analyzed, significant temperature de-stratification occurs approximately at the loads between 38 tons/acre and 143 tons/acre

Heat extraction case

From the 3 lake sites analyzed, Seattle WA requires relatively high heat extraction rates to cause specific temperature variation in a lake compared to other two locations. The results also points out that the heat extraction rate that cause a lake temperature drop of 1°C or 2°C, increases with lake size. Useful recommendation can be drawn from the results as a range of heat extraction rates. In this way, a range from 2 to 464 MBtuh/acre caused the lake temperature to drop 1°C and range of 4 to1043 MBtuh/acre caused the lake temperature drop to 2°C.

`

7.

DEVELOPMENT OF DESIGN TEMPERATURES FOR SURFACE WATER HEAT PUMP SYSTEMS

7.1. Introduction

The heat transfer between a surface water heat exchanger and a lake is driven by the lake temperatures at the depth where the heat exchanger is located. The annual maximum and minimum temperatures of a lake at the depth of a heat exchanger may be considered as the SWHP design temperatures. However, the peak cooling and heating loads may not be coincidence with the peak temperatures. A crucial point for an accurate design and energy analysis of a surface water heat pump system is a proper knowledge of the lake temperatures. Climate conditions, weather and bathymetry of a lake have prominent influence on the temperature characteristics of surface water bodies. The critical factors in designing SWHP system is the upper and lower limit of the heat pump entering fluid temperatures within which the optimum performance of the heat pump can be expected. Therefore, to select an appropriate heat pump system we must need to know the seasonal peak lake temperatures of winter and summer that in turn decides the inlet temperature range to the heat pump.

The data and procedures to design and analyze air source heat pump systems have been studied extensively over many years. ASHRAE (2009) contains a huge set of statistical temperature and humidity data for 5564 locations around the world including 1085 locations in

`

the United States. The data are available for both annual and monthly peak conditions. The monthly values are useful when the time of occurrence of annual peak load does not correspond to the occurrence of peak design temperature. However, for surface water bodies there are no equivalent data available. Only very limited water temperature data sets are available (Hattemer and Kavanaugh 2005) and year-to-year variations further complicate and limit the use of such historical data for design purposes. Despite growing interest in SWHP systems, there is a paucity of standard design data and procedures to aid engineers to efficiently design and analyze the system.

The main objective of this work is to develop an alternative approach to predict design temperatures, develop an easy-to-use database that can readily assist a HVAC design engineer to design a SHWP system. In this chapter, we analyzed three different approaches that could possibly generate design temperatures and developed contour maps of design temperatures determined from the best approach.

7.2. Background

The first step in designing a SWHP system is to determine the size of a heat exchanger that satisfy the building's cooling and heating load requirement. Heat exchanger coil sizing involves determining the coil length, diameter and number of parallel loops of coil, or in the case of flat plat heat exchanger sizing involves determining the sufficient surface area of the plate and number of plates required. The sizing of surface water heat exchanger depends on lake water temperature because the difference between this and the temperature of the heat exchanger fluid drives the heat transfer and controls the exiting fluid temperature (ExFT) of a heat exchanger. Thus, an accurate sizing limits the entering fluid temperature (EFT) to a heat pump within the prescribed value. In other words, significant part of designing a SWHP system is to determine

`

whether the system can actually satisfy the peak building loads between the optimal EFT limits of a heat pump and this is possible only if we know the lake temperatures at heat exchanger depth.

There have been only few works reported in the literature dealing with the sizing of a SWHE. Kavanaugh and Rafferty (1997) presented a series of design graphs for cooling and heating scenarios based on approach temperature to size spread/slinky coils and loose bundle coils. Spread/slinky coils are flattened, spread out horizontally with overlapping and loose bundle coils are retained with a band to hold the coils. They defined approach temperature as the temperature difference between the coil exit temperature and the lake temperature at the heat exchanger depth. By calculating an approach temperature from available lake temperature and desired coil exit temperature, adequate coil length can be read off from the appropriate graph. Nevertheless, there are certain assumptions such as flow rate per unit of heat rejected/extracted was constant 0.054 L/s-kW (3 GPM/ton) and minimum flow rate should remain turbulent inside the tube which limit the usage of the graphs

Hansen (2011) conducted several experiments on different heat exchanger types in 3-acre (12,000 m^2) pond located in Oklahoma, which is maintained by Oklahoma State University. The author arrived with correlations to calculate the outside Nusselt number and hence the outside convection heat transfer coefficient for five types of heat exchangers namely spiral-helical, spiral, slinky-type, loose bundled and flat vertical plate heat exchangers. Hansen (2011) also developed sizing graphs similar to Kavanaugh and Rafferty (1997) that gives SWHEs size per unit of heat transfer rate as a function of approach temperature. Figure 7-1 shows an example of sizing graph developed by Hansen (2011) for Minnesota scenario through which a design engineer can find ft/ton of coil required based on approach temperature for Minnesota region.

`

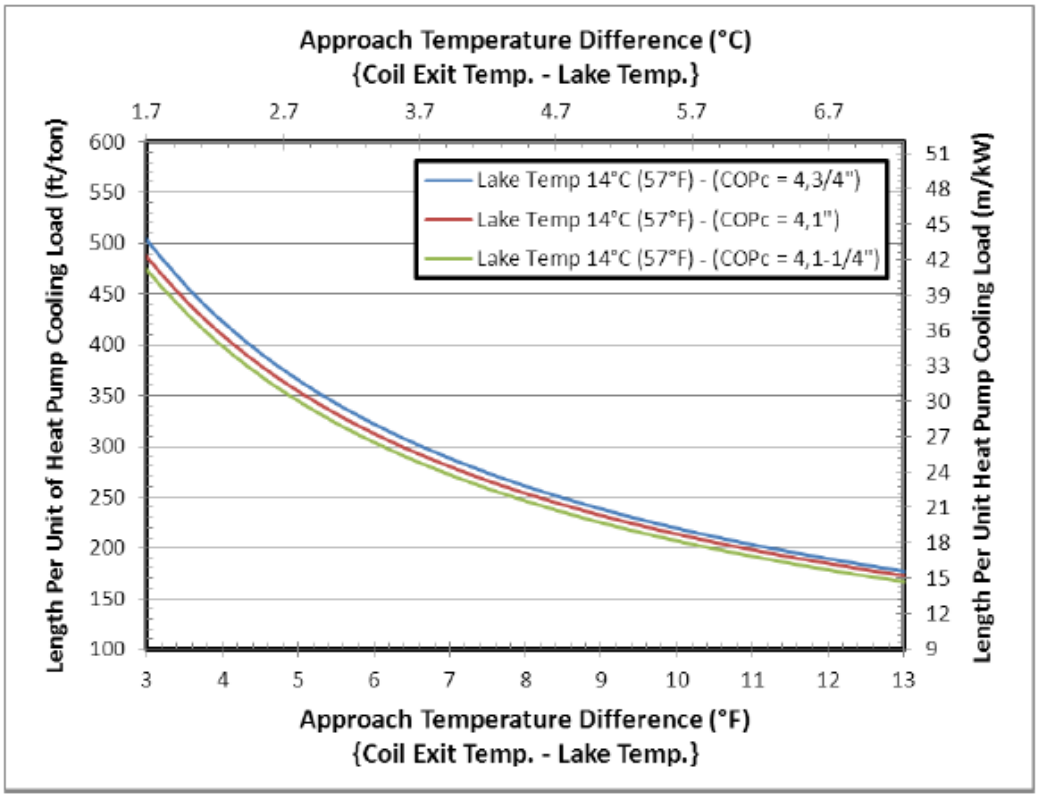

Figure 7-1: Minnesota scenario-sizing graph for spiral helical coil (Source:Hansen (2011))

In addition, he analyzed the sensitivity of spiral-helical coil length to the lake temperature variation. By utilizing the outside heat transfer coefficient correlation developed for spiral-helical coils, he performs set of simulation that determines the length per unit of heat rejection (ft/ton) for different lake temperatures ranging from 5°C (41°F) to 35°C (95°F). For this range of lake temperature, the SWHE loop varies from 11 m/kW (180 ft/ton) to 2.5 m/kW (30ft/ton). Thus, it makes clear that lake water temperature is a highly important to design a SWHP system design and perform analysis.

Other than heat exchanger coils, flat plate heat exchanger made of stainless steel or titanium. (e.g. "SlimJim®") is also an option for SHWP system. Watts (2010) provided an example of preliminary design selection of flat plate heat exchangers with the pond peak

`

temperatures of 27 °C (81 °F) in summer and 4 °C (39 °F) in winter. The design conditions specified are EWT to the heat pump limits of 32° C (90° F) and 1.7 °C (35° F), rated heat rejection and heat extraction of 22771 W (6.5 ton) and 10404 W (3 ton), and rated flow rate of 15 GPM. The internal calculations are not explained clearly, however, they calculated appropriate size as 2 m x 4.5 m (4 ft x 15 ft) and number of plates required as 6 for the specified design conditions. With the current design practices, the first thing we need to consider is the design lake temperatures to use in the design calculations.

Of particular relevance to this paper, Hattemer and Kavanaugh (2005) collected measured lake temperature data and provided us with set of temperature profiles for the lakes from 14 different regions across the United States. The geographical distribution is shown in Figure 7-2. Hattemer and Kavanaugh (2005) identified various agencies whose responsibilities are to maintain geological information and monitor lakes, waterways, and environment. They collected temperature data from the websites of such agencies, which includes USGS (2011), USACE (2011) , AASG (2011), EPA (2011), WOW (2011) and TVA (2011). In the instance, if there is no access to online data, they obtain data by contacting individual representatives of the agencies. The compiled and updated dataset comprises temperature profiles of 47 lakes of different sizes and depths (EIS 2012). The dataset of each lake contains 3 to 10 temperature profiles representing few winter and summer months. Generally, each temperature profile consists of measurements for every 1.5 m (5 ft) depth across the depth of a lake. The measurements of obtained data were made in the years 1999 to 2004 and the measurements of few Alabama lakes were made in 1959-60. The measurements are given only for sample days in a year and the dates are not mentioned in the database.

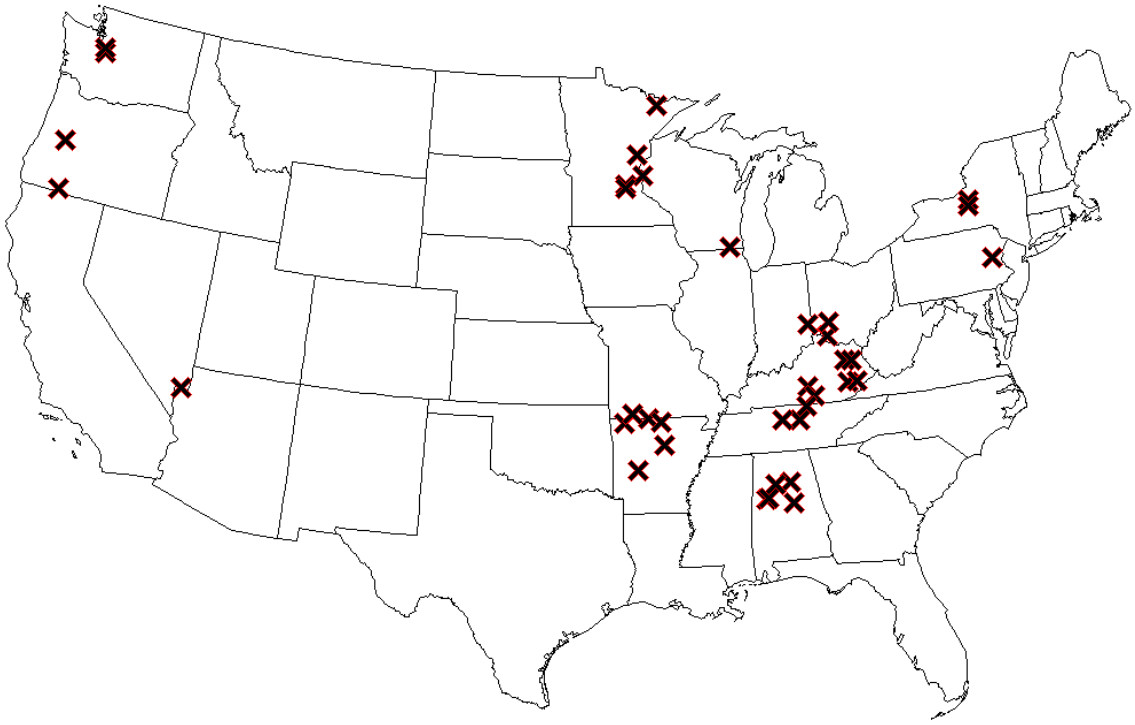

Figure 7-2 Geographical distribution of lakes found in Hattemer and Kavanaugh (2005)

The crucial aspect of year-to-year variation of lake temperatures makes the existing design temperature database subjected to some limitations. The data need to have enough measurements over time at a specific location to make a reliable judgment about design conditions. To illustrate this with an example, we obtained data for Ice Lake located in the city of Grand Rapids in Minnesota (45°18'55" N, 92°46'08" W) which has a surface area of 17 Ha (41 acres) and depth of 16 m (52 ft) to compare with corresponding data collected by Hattemer and Kavanaugh (2005). The type of data we obtained are, more than one year of daily or almost daily temperature measurements through spring, summer, and fall from water on web website (WOW 2011). They make measurements of lake water temperatures extensively over number of years and has been in operation since 1997. The temperature data available are on daily or near-daily basis for six years from 1998 to 2003. We compared the temperature profiles of Ice Lake for the month of October obtained from EIS (2012) database with experimental temperatures of Ice Lake

`

for the same month obtained from water on the web (WOW 2011). The daily measurements are obtained for the month of October for each year from 1998 to 2002 and plotted the maximum temperatures for the month at each depth in Figure 7-3. It shows clear distinction between Hattemer and Kavanaugh (2005) data and the experimental measurements varying year-to-year. For example, at 10 m (33 ft) depth there is a difference of 2°C (35°F) and at 8 m (26 ft) depth there is a difference of 4.7°C (40°F) between "October 2002 - Hattemer and Kavanaugh" and "October 2002 – WOW". In the epilimnion region at 4 m (13 ft) depth there is a difference of 8.1°C (46°F) between 'October 2002 - EIS (2012)' and 'October 1998 – WOW'. Similarly, minimum temperatures are plotted in Figure 7-4. This plot also shows difference between Hattemer and Kavanaugh (2005) data and the experimental minimum temperature. At 8 m (26 ft) depth, there is a difference of 1.9 °C (35°F) is observed between "October 2002 - Hattemer and Kavanaugh" and "October 1999 – WOW"

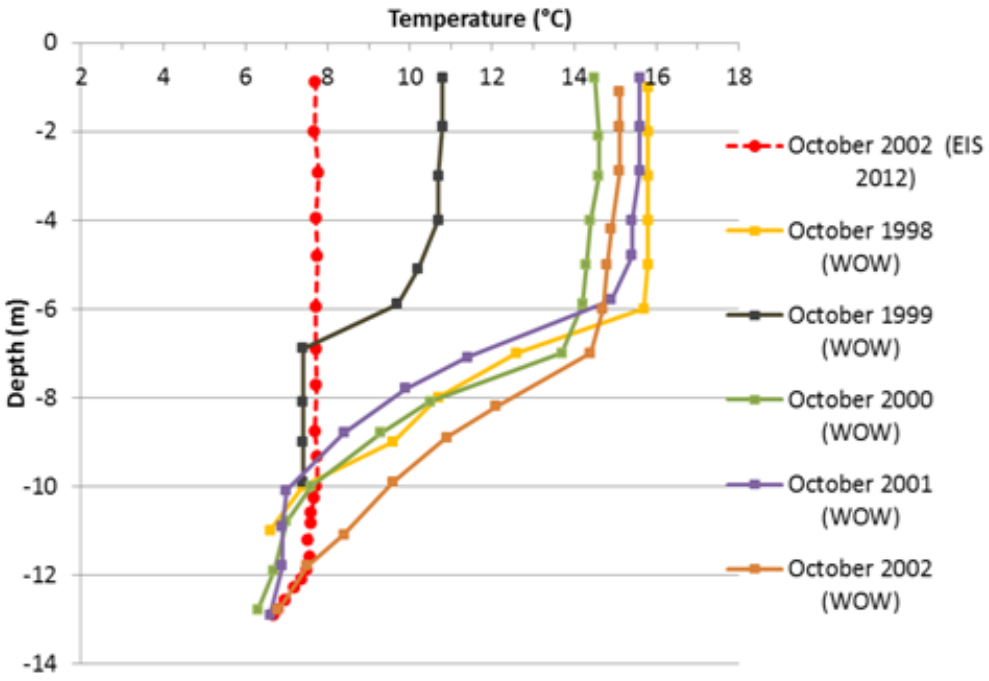

Figure 7-3 Comparison between EIS (2012) and experimental maximum temperatures of Ice Lake for the month of October

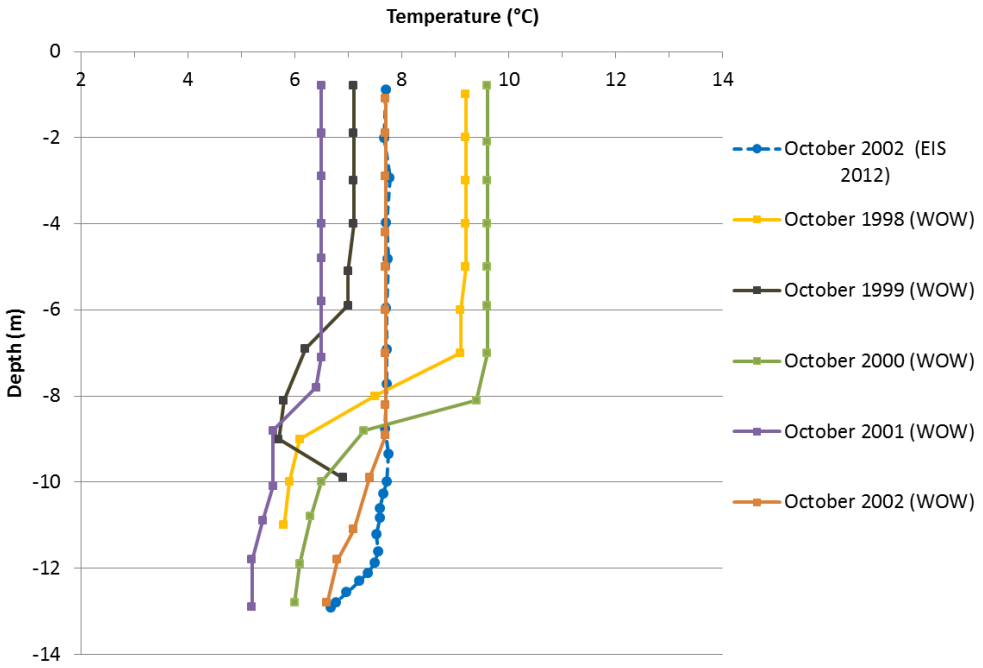

Figure 7-4 Comparison between EIS (2012) and experimental minimum temperatures of Ice Lake for the month of October

In addition, we compared the annual maximum temperatures of different years with the data obtained from WOW. The daily measurements provide a means to calculate the annual maximum temperature profile. Since these maximum temperature profiles are made up of maximum temperatures that occur on different days for different depths, they do not necessarily represent a specific day. Figure 7-5 shows maximum temperature profiles for six different years. Although they all follow the same trend, there are quite large year-to-year variations. There is a maximum temperature of 8°C (15°F) at the depth of 10 m (33 ft) and there is a maximum variation in the maximum temperature of 3 °C (5°F) at 6 m (20 ft).

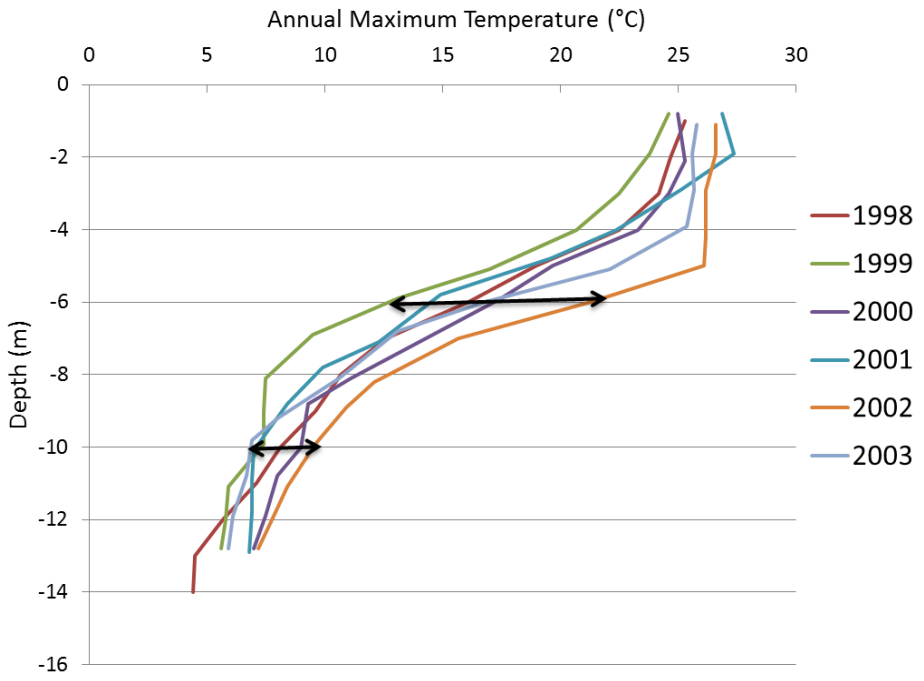

Figure 7-5 Variation of experimentally measured annual maximum temperature profile in Ice Lake, MN

In terms of helping to make a decision on annual maximum and minimum temperatures, reliable experimental data are invaluable; the existing temperature database is adequate only for systems built on one of these lakes. Nevertheless, from the above discussions, it can be seen that the existing design temperature database have some limitations when year-to-year variation of lake temperature is of interest

Moreover, it leaves us with the question of what if a system is to be built on any other lakes that are not in the database of Hattemer and Kavanaugh (2005). For example, there are 11,378 lakes in the size range of 25 acres to 247 acres in the United States as estimated by Lehner and Döll (2004). The measured data set covers only certain lake sizes, locations and limited to certain period. Since each lake is unique, the measured data alone are rarely sufficient and it makes difficult for an engineer to make a decision on likely minimum and maximum water

`

temperatures. It would seem, therefore, that further investigations are needed to develop an approach to estimate lake temperatures for potential SWHP sites.

7.3. Design Temperature Data Collection Approaches

Three different approaches namely water-temperature-data-driven approach, meteorological-data-and-model-driven approach and satellite-data approach are investigated to find the lake temperatures and develop a database. The data provided by each approach is analyzed and best approach is developed based on how helpful the data is to a design engineer to make a decision on annual maximum and minimum temperatures.

7.3.1. Water-temperature-data-driven approach

The first approach is based on retrieval of lake temperature data from possible online sources and this is the extension of Hattemer and Kavanaugh (2005) approach . We explored different websites of agencies pertinent to water quality monitoring. These websites provide information about real-time and historical water temperature data of various water bodies. Through this search, we have located the temperature data sets in different websites and collected different types of water temperature data that includes spot measurements, measurements across depth and continuous measurements for years. The temperature measurements continuously made for years and along the depth of a water body is a kind of comprehensive data set that is more useful in developing a database. Perhaps, the spot measurements like in the surface or at any of the depth are of interest but not suitable for design temperature database since they may not meet the distribution characteristics discussed below.

The majority of currently available data sets can be grouped into two categories ‘generally useful’ and ‘indirectly useful’. ‘Generally useful’ data can provide extensive characterization of lake temperatures from the perspective of certain things such as

`

- Geographical distribution of data: The data obtained would have to cover a wide range of locations so that users of a database could either interpolate or find a location and water body in the database that is close enough for design purposes.

- Temporal distribution of data: In order to be generally useful, there needs to be enough measurements at a specific location to make a reliable judgment about design conditions

- Spatial distribution of data: SWHE may be placed at a range of depths. The data would need to contain measurements at multiple depths so that the design temperatures at specific depths would be available. A surface measurement or any spot measurements at a depth alone is of limited usefulness as the temperature change across the depth is significant as shown in Figure 7-5. Nevertheless, it might be possible to use spot measurements at the surface or at any depth to calibrate another model.

- Body-of-water-size distribution: In order to be generally useful, we would need data from a range of lake sizes.

- Availability in digital form: In order to be generally useful, it needs to be feasible to extract the data. Some sources in Michigan (MichiganDEQ 2011), consist of scanned bit images of handwritten or typewritten notes on temperature profiles measured at certain times. Although it might be feasible to extract some of the data for validation purposes, it would simply not be feasible to extract the entire data set or even a broad coverage for the state of Michigan.

The data that do not possess any of the distributions said above is categorized as 'indirectly useful'. Despite their incomprehensive features and individual limitations, the lake temperature measurements can serve to validate another approach or be used as a part of another approach.

`

Starting with USGS (USGS 2011) which is nation's largest organization that provides related information about the natural resources have access to temperature data of various types of water bodies like streams, lakes and reservoirs. These data are available for each state across the nation. In USGS, a distinction is made and the surface water bodies are classified based on the physical features, size and shape. A breakdown by water type of sites with measurements of any type is shown in Table 7-1. They are characterized by the site name, so we have separated creeks, streams and brooks, even though there may be no physical difference between them

Table 7-1 Breakdown of water type of sites - USGS

Type	Count
Rivers	1084
Creeks	708
Lakes	50
Reservoirs	20
Bay	36
Pond	4
Streams	44
Ditch	32
Canal	15
Brook	19

While the temperature measurements are geographically wide spread across the United States, most of the measurements are made for running water. There are only 74 sites that are lakes, reservoirs or ponds that is our prime interest. Of these most of them are surface water temperatures and only very few temperatures are measured at certain depths. For instance, Lake Houston located 15 miles northeast of Houston, Texas has a maximum depth of 14 m (45 ft) and four temperature measurements at depths of 0.3 m (1 ft), 1.8 m (6 ft), 3.6 m (12 ft) and 5 m (16 ft).

Water-on-the-web website WOW (2011) maintained by University of Minnesota which contains much better temperature data. Using a remote automated moving temperature sensor,

`

temperature profiles were collected for 14 lakes in Minnesota, New York, Washington, Nevada, and Texas. It has comprehensive temperature data across depth and for most number of days in a year. Of the 14 lakes, 7 lakes have temperature data for more than 250 days in a year, 3 lakes have data for almost 200 days per year and 4 lakes have data set for less than 100 days in a year. Therefore, while this data source has good temporal and spatial distributions of data, it has very limited geographical distribution.

Another source with limited geographical distribution is the Tennessee Valley Authority from which the data available for 13 different reservoirs located in the eastern part of Tennessee (TVA 2011). The source has temperature profile data across depth available for less than 10 days in a year particularly for summer days and lacking in both temporal as well as geographical distribution.

As a part of their major lake-monitoring program, the King County Department of Natural Resources and Parks in the state of Washington has lake temperature data for two major lakes, which are Lake Washington and Lake Sammamish. Both of the lakes are located east of Seattle in King County, Washington. In addition, they also have measurements of meteorological parameters of the location where the lakes are situated. Lake temperatures are measured and recorded at each meter from the surface by King County's sampling station in the lake. The buoys are still active and the historical temperature datasets are available till date can be retrieved from their website (King County 2012).

Other sources of water temperature data investigated are Lake Base Gleon (Lakebase 2011), Michigan DEQ (MichiganDEQ 2011), and U.S. Environmental Protection Agency - STORET data (EPA 2011). However, such data are often lacking from a standpoint of geographical, temporal or spatial distributions, constraining the amount to be included in large-scale design temperature database. Michigan Department of Environmental Quality has number

`

of bit-image scans that has temperature data for the lakes in Michigan. Several of those reports have spot measurements of temperature for a single day or several days. In a similar way, though STORET data are available for many locations they are surface measurements.

Therefore, through online retrieval we can get satisfactory lake temperature data for only very few lakes. As far the analysis of online data sources, the retrievable data would not lead to a generally useful data because the data are very sparse from either a geographical or a temporal standpoint. Furthermore, most of the data are spot measured and it is unavailable for various depths. Having said this, several of the above resources most notably the water on the web website, contains data which can be categorized as indirectly useful that can be used for validation of lake models which are discussed later in this paper in the model-driven section.

7.3.2. Satellite-data approach

The retrieved data from online databases through water temperature data driven approach were not enough to make a useful design temperature database. Therefore, for second approach we used satellite measurements to estimate surface temperatures. There are limited numbers of paper where estimation of surface water temperatures from satellite data has been attempted.

Fisher and Mustard (2004) used Landsat 5 TM (Thematic Mapper) and Landsat 7 ETM+ (Enhanced Thematic Mapper+) thermal images for measuring the sea surface temperatures. Their study area encompasses the southern coast of New England centered on Narragansett Bay. *In situ* water surface temperatures of 9 different locations are obtained from the records available from National Oceanic and Atmospheric Administration (NOAA), National Data Buoy Centre (NDBC), NOAA Physical Oceanographic Real-Time System (PORTS) and the NOAA National Estuarine Research Reserve System (NERR). 53 Landsat images of the study area between the years 1984 and 2002 were obtained. The images were corrected for cloud contamination using a Climatology algorithm they developed, which corrects the temperatures based on the blended

`

contemporary and historical *in situ* data of that location. An overall standard deviation error between satellite measured and in situ measured temperatures resulted from this study was 1.56°C (34.8°F) during summer and 1.2°C (34.1°F) during winter.

Wloczyk et al. (2006) used Landsat 7 ETM+ imagery to measure surface temperatures. The study area consists of Lake Stechlin, 12 small lakes and the coastal zones of the Baltic Sea in North East Germany. 9 satellite images encompassing the entire study area were selected covering the time span from February to November 2000. The Atmospheric correction was performed on those images using 'ATCOR' model. In situ temperature measurements was performed at one site location in Lake Stechlin, one site each for all the 12 smaller lakes and at eleven different sites in the coastal zones of the Baltic Sea. The difference between the satellite derived lake surface temperatures with respect to the *in situ* temperature measurements for Lake Stechlin and the 12 smaller lakes showed an RMS error of 1.4°C (34.5°F) and 2.2 °C (35.9°F) respectively. RMS error of 1.6°C (34.8°F) was obtained with respect to the *in situ* bulk temperatures in the coastal zones of the Baltic Sea.

Schneider and Mauser (1996) used Landsat 5 TM thermal images for lake surface temperature measurement on Lake Uberlingen in Germany. They acquired 21 Landsat images of Lake Uberlingen between 1987 and 1994 and all the images were obtained between the months from May to August. The atmospheric impact on thermal radiation is modeled using 'Lowtran 7'. Lowtran 7 model over-predicts the water surface temperatures. Comparing the in situ temperature measurements on Lake Uberlingen with the satellite measured temperatures yielded an RMS error of 0.53°C (32.9°F)

From the literature review, it is known that reasonably accurate surface temperature measurement is possible. To get the temperature from a satellite image we downloaded the Landsat image for the specific site, used a graphical interface tool to visually locate the lake in

`

each image, determined the correct pixel of the image, and applied the atmospheric correction to obtain the temperature values through a series of calculations.

Landsat 7 with the ETM+ (Enhanced Thematic Mapper Plus) sensor was launched on April 15, 1999. The objective of Landsat 7 is to provide high quality visible and infrared images of all landmass and near coastal areas on the earth while orbiting at an altitude of 705 km. The ETM+ instrument is a fixed, eight band, multispectral scanning radiometer capable of providing high resolution imaging information of the earth's surface. The different bands have different uses, but we are particularly interested in Band 6, which lies in the thermal infrared region of the spectrum (10.4-12.5 μm). Bands 1 to 5 and 7 have a spatial resolution (pixel size) of 30m (99 ft); Band 6 has a spatial resolution of 60m. Since February 2010, the images of Band 6 have been resampled to the resolution of 30m (99 ft).

The ETM+ sensor measures the amount of Spectral intensity in $W/m^2 \cdot Ster. \mu m$ emitted from the surface and transmitted through the atmosphere. Spectral intensity can be defined as the rate at which the radiant energy of the surface is emitted at the wavelength λ to the atmosphere, per unit area of the emitting surface, per unit solid angle about the direction of emission, and per unit wavelength interval $d\lambda$ about λ. In theory, the surface temperature of a black body could be estimated with Planck's law knowing the total emission in Band 6. In practice, though, the 705 km of atmosphere absorbs some of the surface emission, so the results should be corrected with an atmospheric model.

To validate this approach, the experimental measurements for the Arkansas River at Tulsa, Oklahoma are obtained from USGS and compared with temperature obtained through the satellite image. We used software called Global Mapper to extract the pixel values. The pixel values are converted to surface radians and then to temperatures using standard NASA equations described in the Landsat handbook. These temperature values are compared with experimental

`

data without including the atmospheric correction. Hence, the resulted temperatures from the process without atmospheric corrections are only the erroneous surface temperatures that could not be useful to develop a detailed database. In addition, there are some practical difficulties in processing large quantities of satellite data for a large number of lakes to extract the corresponding pixels. Though atmospheric correction may be the most important task of this approach, we have not attempted to develop this approach further on considering number of reasons, including the fact that even developing a database of temperatures at the surface of a water body would require an effort beyond the scope of this project and even then, success would be uncertain. Figure 7-6 shows that there are some significant differences where the satellite measurements falls outside the daily range measured in situ

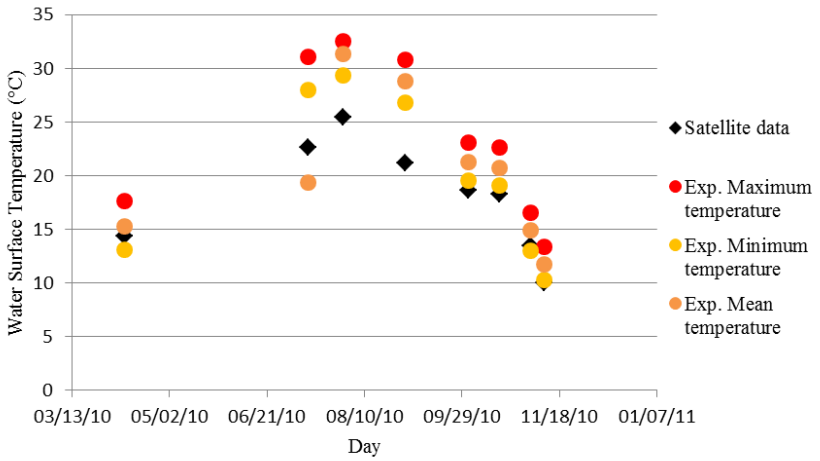

Figure 7-6 Satellite data measurements and experimental measurements of Arkansas River on different days

7.3.3. Meteorological-data-and-model-driven approach

Weather data is one of the significant inputs to the lake model since the meteorological parameters drive the major heat transfer mechanisms in the lake. Therefore, it is necessary to identify a weather file format, which is accurate and suitable to generate design temperatures throughout the world. Broadly speaking, there are two types of hourly weather data available for

`

simulation purposes, namely “actual” weather data for multi-years and weather data for a typical year.

Integrated Surface Hourly (ISH) database developed by National Climatic Data Center (NCDC) is the largest multi-year database. The database contains hourly meteorological observations from the period of early 1900, recorded from 20,000 stations located throughout the world. Multi-year’s ISH data can be accessed from single integrated database through a web interface and can be converted into a compatible format to use in the lake model. However, there are some constraints in acquiring complete actual weather data sets for locations in either the continental United States or worldwide. Actual weather data has significant numbers of ‘gaps’ that require expertise and time to fill. Neither the expertise nor the time were available for this project.

U.S. National Renewable Energy Laboratory (NREL) combined with NCDC and developed a dataset of actual hourly weather data and solar data called Solar and Meteorological Surface Observational Network (SAMSON) (NCDC 1993). The station record begins in the year 1961 and it contains 30 years of actual weather data until 1990. The dataset is divided geographically into eastern, central and western U.S. and it contains data for 213 stations across United States. Despite the fact that the dataset includes multi-years actual weather data, it is not suitable for developing a database because of less number of locations in United States and the database cannot be extended worldwide. However, the data can be used for comparing purposes. Therefore, an alternative approach is to consider typical meteorological year (TMY) type data, one of the earliest weather data developed by NCDC. These are hourly solar radiation and meteorological data derived from measured weather data of longer period of time (1948–1980) collected from different sources and represents the typical year of a specific location excluding the peak year conditions (Wilcox and Marion 2008).

`

NREL developed TMY2 and TMY3 that represents the further advancement of TMY dataset respectively. TMY3 was developed from measured meteorological values from 1991 to 2005 and modeled solar values and available for 1020 locations across United States. Similarly, several other sources provide typical weather data for the locations across the world are Canadian Weather for Energy Calculations (CWEC) for Canada, Chinese Standard Weather Data (CSWD) for China etc.,

EnergyPlus Weather (EPW) weather files are developed by U.S. Department of Energy intended to be used in EnergyPlus building simulation program (EnergyPlus 2012). EPW weather files are developed from various sources depending on the location. EPW files are available for 1042 locations in the United States, 71 locations in Canada, and more than 1000 locations in 100 other countries in the world. EPW file represents data set of hourly values of air temperature, solar radiation, wind speed, humidity, atmospheric pressure and cloud cover data that represents long-term typical weather conditions over a year. Therefore, from the above discussions, it is obvious that EPW files would certainly be more desirable and have the potential to generate worldwide database. Thus, meteorological-data-and-model-driven approach uses EPW weather data and our experimentally validated lake model to predict the design lake temperatures. Although, we can extend this approach for various locations in the world, as a preliminary testing we limited our work to generate design temperatures only for continental United States. Overall, from the analysis of three different approaches we can conclude only the model-driven approach has the high potential to develop design temperatures database. Substantially, we can develop design temperature database from this approach that possesses all the distribution characteristics.

7.4. Model testing

After the lake model validation, it appeared to be predicting the lake temperatures correctly. However, the model is tested for initial condition independence before proceeding with

`

design temperature prediction. The initial conditions of the lake model represent the constant initial temperature profile for the first day (January 1) of simulation. Different initial condition scenarios are tested for a 41-acre lake by placing it in Shreveport, Louisiana and Minneapolis, Minnesota. These locations are selected as a representative warm and cold places based on the annual average air temperature.

By using TMY weather file, the lake model predicted maximum and minimum temperatures at every depth for different initial temperature conditions. If the model were operating correctly, there would be no difference in the design temperature prediction for different initial conditions. Figure 7-7 and Figure 7-8 shows the annual maximum and minimum temperature profiles of the 41-acre lake located in Shreveport, LA. Figure 7-9 and Figure 7-10 represent the maximum and minimum temperature profiles of the 41-acre lake located in Minneapolis, MN. From Figure 7-7 and Figure 7-9 it can be seen that for different initial conditions the maximum temperatures below 6 m depth varies significantly. Similarly, there are significant differences between in the minimum temperatures for different initial conditions in Figure 7-8 and Figure 7-10

The minimum temperature dependence on initial temperatures is less when compared to the dependency of maximum temperatures but still the differences remain. These plots tell us the problem of convergence in the lake model. The incorrect input of initial temperatures could lead to wrong design temperatures because the temperatures are not converged for one year simulation.

The convergence limitation in a one year simulation does not completely eliminate the possibility of the model-driven approach, but it introduces another thought of running the simulations for two years, which allows the lake temperatures to converge in second year. Again, the model is tested for series of initial conditions for the same locations and lake. Figure 7-11

`

through Figure 7-14 shows that even with the extreme initializations of lake temperature, the model converges, though higher computation time is required by the simulation. Therefore, the model is allowed to run for two years and the design temperatures are calculated based on the second year lake temperatures.

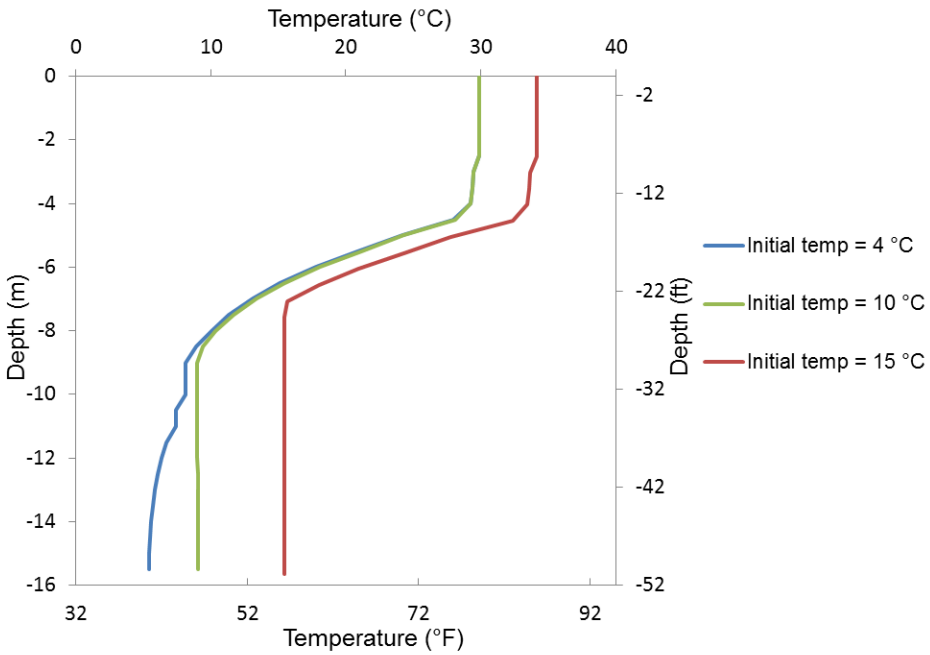

Figure 7-7 Annual maximum temperature profiles for different initial conditions of the 41-acre lake located in Shreveport, LA

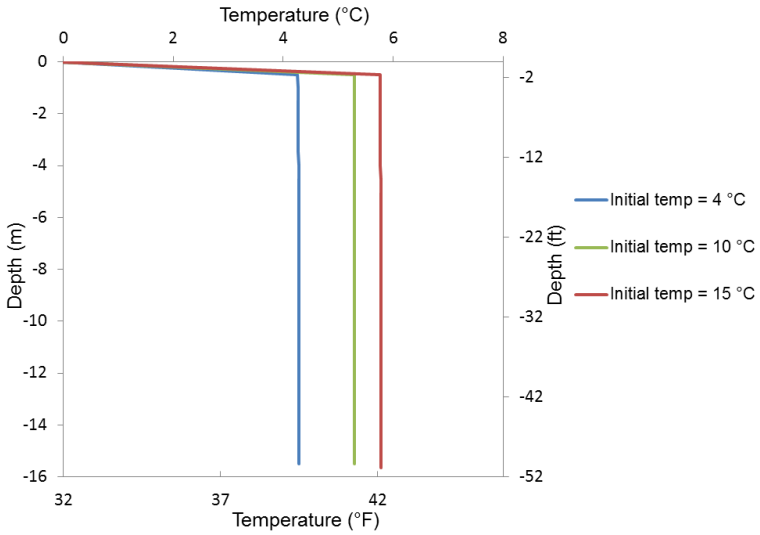

Figure 7-8 Annual minimum temperature profiles for different initial conditions of the 41-acre lake located in Shreveport, LA

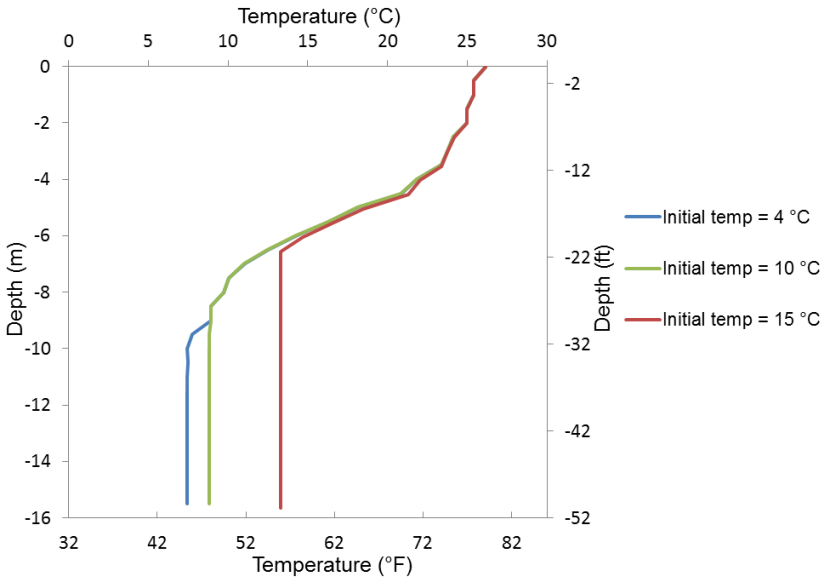

Figure 7-9 Annual maximum temperature profiles for different initial conditions of the 41-acre lake located in Minneapolis, MN

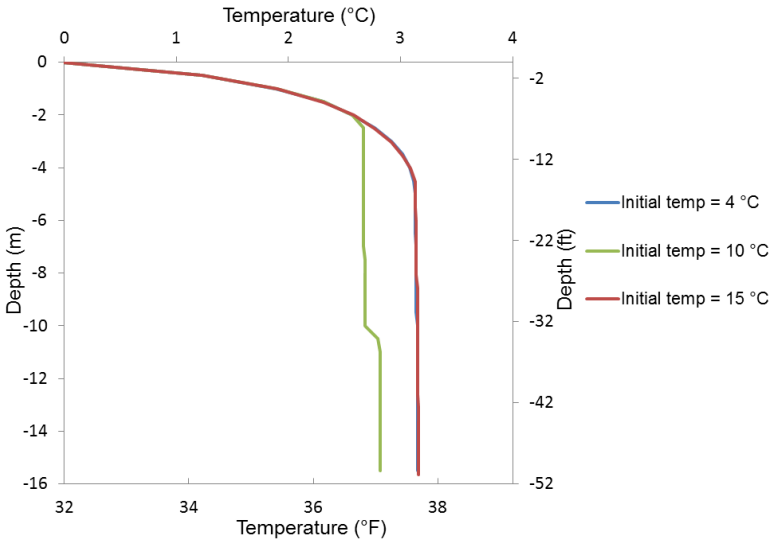

Figure 7-10 Annual minimum temperature profiles for different initial conditions of the 41-acre lake located in Minneapolis, MN

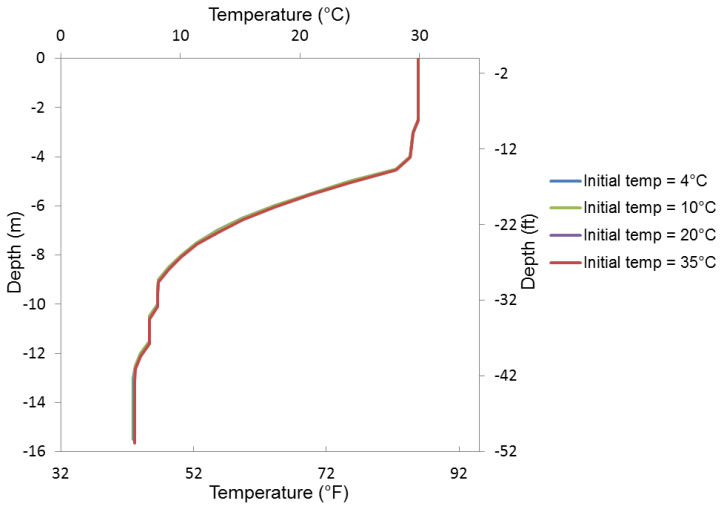

Figure 7-11 Annual maximum temperature profiles for different initial conditions of the 41-acre lake located in Shreveport, LA

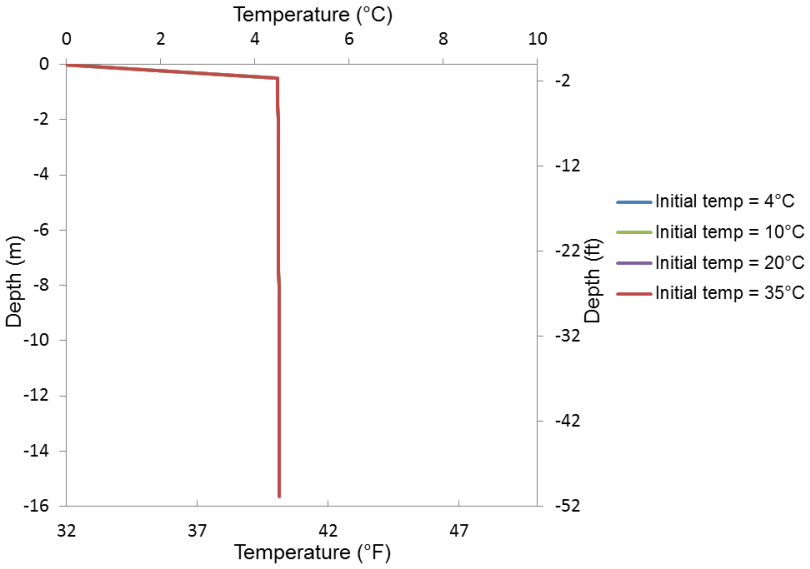

Figure 7-12 Annual minimum temperature profiles for different initial conditions of the 41-acre lake located in Shreveport, LA

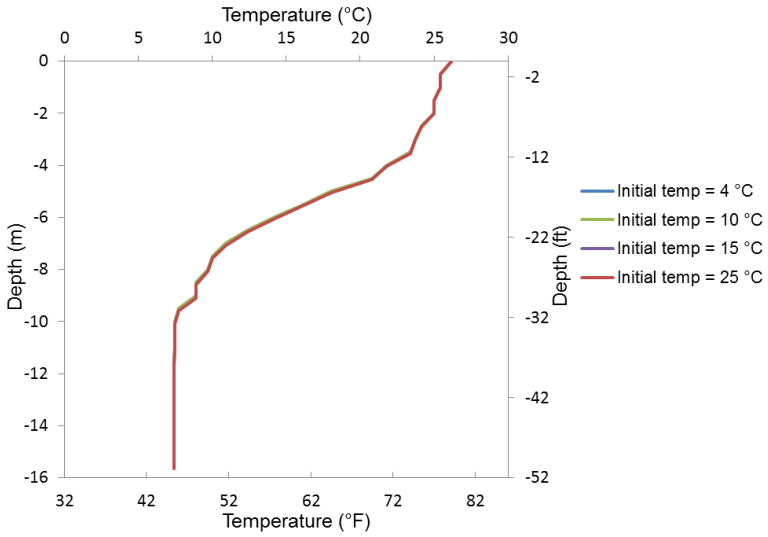

Figure 7-13 Annual maximum temperature profiles for different initial conditions of the 41-acre lake located in Minneapolis, MN

`

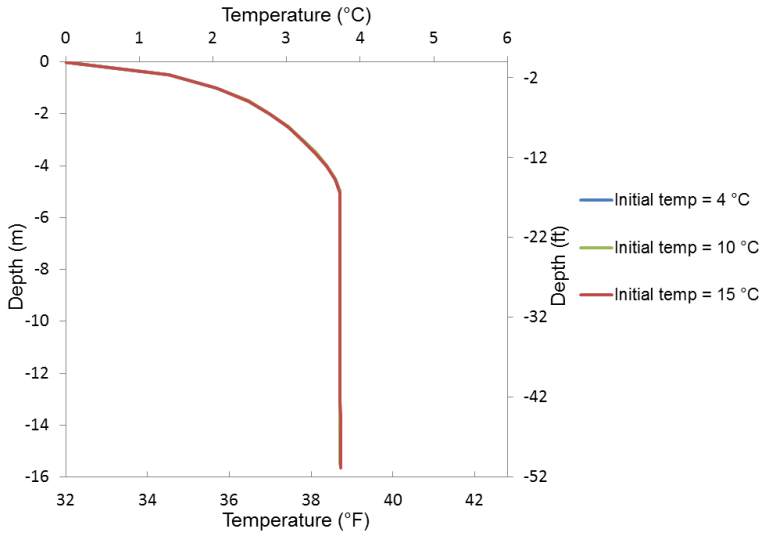

Figure 7-14 Annual minimum temperature profiles for different initial conditions of the 41-acre lake located in Minneapolis, MN

7.5. Development of model-driven approach

7.5.1. Uncertainty analysis in the model

After the lake model has been developed comprehensively to derive minimum and maximum lake temperatures as a function of depth, we begin by quantifying the error associated with the model to determine how well the lake model can predict the design temperatures. The degree of uncertainty the model has by itself is investigated through a statistical analysis, which compares the model predicted peak temperatures with experimental measurements.

Rather than representing the uncertainty by a single value, the goal of the statistical approach is to predict '95% prediction interval'. The upper and the lower bound of a confidence interval can represent the level of uncertainty associated with the prediction of design temperatures. A narrow confidence interval represents that the model is predicting with high accuracy. The upper bound of a confidence interval is the desired temperature that should be added to the maximum temperatures predicted by the model and in the case of minimum temperatures, the lower bound temperatures are added.

`

It is worth noting that the analysis is performed for maximum temperatures alone, based on the difference between the annual maximum temperatures predicted by the model at each depth and annual maximum temperatures at corresponding depth calculated from the experimental data. Since, we do not have adequate winter month experimental temperatures; the model uncertainty in predicting minimum temperatures is not analyzed. However, we anticipate that the model uncertainty in the case of minimum temperatures might be less because we are using small grid sizes here in the model simulations.

To isolate the uncertainty, which may result by using typical meteorological weather, we used actual weather data in the calculation of model uncertainties. The experimental temperatures measurements needed for the analyses are collected from the sources such as WOW (2011) and King County (2012). In addition, the physical dimensions, including lake surface area, volume and maximum depth are also collected from these online databases. The brief summary about these sources are already discussed before in water temperature data driven section. Unfortunately, there are only few datasets available, which comprises of near-daily temperatures (measured at least once in a day) to compute the annual maximum temperatures. Five different lakes were chosen for the analysis, based on the range of near-daily experimental temperatures available for multiple years.

1. OSU pond is a shallow pond located in the city of Stillwater, Oklahoma. The pond has a surface area of 1.2 Ha (3 acres) and depth of 3.8 m (12 ft).
2. Ice Lake located in the city of Grand Rapids in Minnesota which has a surface area of 17 Ha (41 acres) and depth of 16 m (52 ft)
3. Otisco Lake is located at the eastern end of the Finger Lake District, southwest of Syracuse, New York. Otisco Lake, the seventh largest in size of the eleven Finger Lakes, which has a surface area of Otisco Lake 760 Ha (1878 acres), and a maximum depth of 20 m (66 ft)

`

4. Lake Sammamish located east of Seattle in King County, Washington. The surface area of the lake is 1982 Ha (4987 acres) and maximum depth of 32 m (105 ft)
5. Lake Washington is located close to Lake Sammamish and it is the largest lake in King County with a surface area of 8700 Ha (21,500 acres) and a maximum depth of 65 m (214 ft)

The total number of years of experimental data for each lake varies from 3 to 6 years. The completeness of the data in a month and number of months of measured data available in a year varies for each lake. However, the years that we selected have sufficient data to characterize the maximum temperature of the entire year. Since we are analyzing the model uncertainty for the case of maximum temperature prediction, sufficient data means the lake temperatures have to be measured for summer months. The experimental measurements of every lake are summarized for each year and then we computed the maximum temperature recorded for the year at each depth. The location, size, maximum depth and the time span of experimental data collected are shown in Table 7-2. In addition, the resulted 95% prediction intervals are given in Table 7-2. These intervals are calculated for each lake separately.

`

Table 7-2 Description of lakes used for model uncertainty analysis

	Lakes				
	OSU pond	Ice Lake	Otisco Lake	Lake Sammamish	Lake Washington
Location	36°8'15" N, 96°0'22" W	45°18'55" N, 92°46'08" W	42°52'35" N, 76°17'49" W	47°36'19" N, 122°5'19" W	47°36'34" N, 122°15'33" W
State	Oklahoma	Minnesota	New York	Washington	Washington
Surface area ha (acres)	1.2 (3)	17 (41)	760 (1878)	1982 (4987)	8700 (21500)
Maximum depth m (ft)	4 (13)	16 (53)	20.1 (66)	32 (105)	65 (214)
Years of experimental data collected	2	6	3	4	4
Number of data points	13	79	49	97	188
Mean error °C	0.2	-0.9	-0.5	0.5	0.5
Upper limit of the 95% confidence interval °C	3.1	1.9	3.6	2.6	2.5

First, we have plotted the predicted maximum temperature profile along with the maximum temperatures calculated from the experimental measurements for all five lakes. Figure 7-15 shows an example of such annual maximum temperature comparison plot of Lake Washington for the year 2011. Figure 7-16 shows the difference between the experimental and predicted maximum temperatures at each depth

The experimental peak temperatures correspond well the peak temperature predicted by the model, but uncertainties remain. The epilimnion and hypolimnion regions contributed lesser uncertainties (less than 1 °C) indicating that temperatures closer to surface until epilimnion depth and the temperatures at the bottom region (hypolimnion) can be predicted by the model very

`

accurately. However, there are relatively larger differences can be seen in the depth range of 10 m – 20 m. This is the region of high temperature gradient (more than 0.5°C/m) called thermocline. Most of the errors in the thermocline region is potentially due to the effect of epilimnion deepening due to varying wind conditions. Since the variation of the epilimnion and hypolimnion temperatures over a day is very less, the difference between the measured and predicted daily temperature of these regions are less and will be within the difference associated with the time of measurements made in a day. Therefore, these temperatures can very well represent the annual maximum temperatures irrespective of the daily time step model.

The depth of the epilimnion starts to vary in early summer and tends to deepen during late summer. Its depth is more sensitive to the subtle influences of wind acting on the surface of a lake. This causes the epilimnion depth to change continuously within a day and over a year. The location of thermocline is a delicate balance between wind mixing and surface heating. The deeper epilimnion in a lake is due to the combined effect of high air temperatures and wind speed that possibly occur during summer. It is important to understand that even a small variation in epilimnion depth would vary the thermocline temperatures to significant amount because of sharp temperature gradient in that region.

The lake model is the vertical mixing model that takes the average daily wind speed to calculate the epilimnion depth. So, we can say that the model represents the daily average epilimnion depth and so the thermocline temperatures. But in reality, significant change in epilimnion depth can occur within a day depend on the variation of wind speed and affects the thermocline temperatures. Thus, it is reasonable to expect that significant difference in the thermocline regions, which caused the wide prediction interval on a statistical basis.

This is clearly seen in Figure 7-17 which shows annual maximum temperatures predicted by model at every 5 m of the lake and experimental annual maximum temperatures at

`

corresponding depths. Such deviations cannot be recognized in a statistical way by establishing relationships because of the fact that the temperatures down the depth of the water column are not linear.

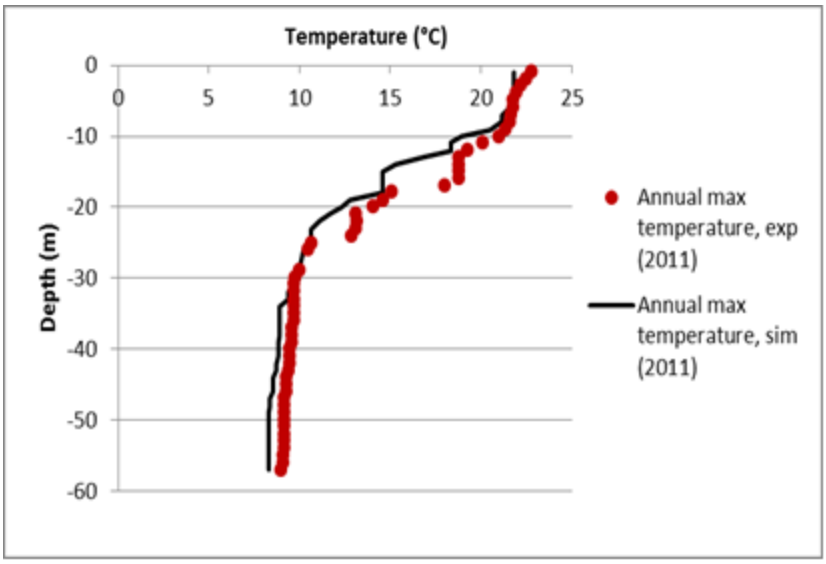

Figure 7-15 Comparison of annual maximum temperature profile predicted by model with the experimental measurements for Lake Washington and for the year 2011

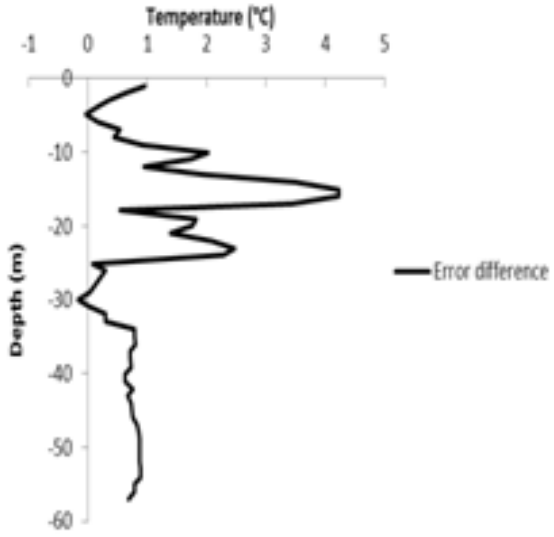

Figure 7-16 Difference between model and the experimental measurements for Lake Washington and for the year 2011

`

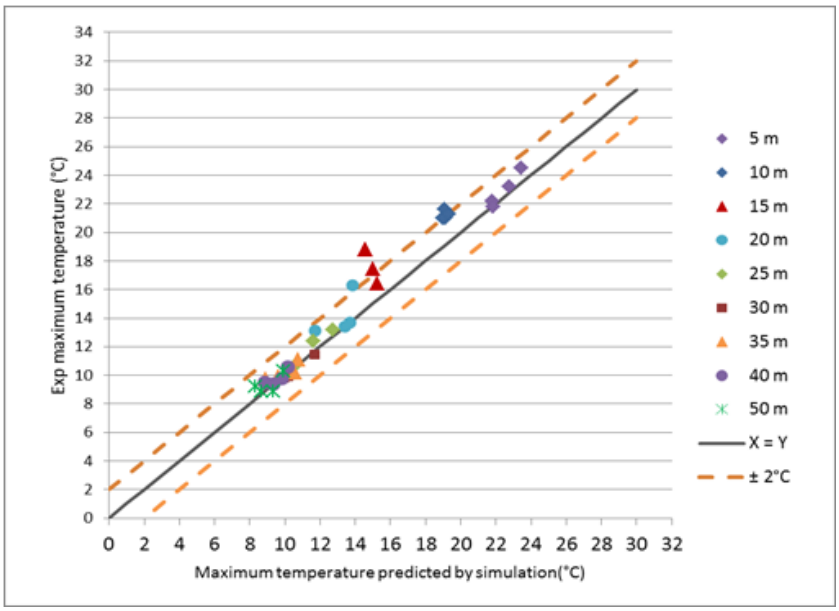

Figure 7-17 Comparison between measured and simulated annual maximum temperatures for Lake Washington for the year 2011

7.5.2. Prediction of Lake Water Design Temperatures

The lake model discussed in the previous section was developed in FORTRAN 90 and it is used to predict design temperatures at desired depths of the lake according to the lake bathymetry and EPW weather data input. In order to automate the lake simulation for every site across United States, the Microsoft Excel VBA program has been developed to create and run the script file. The script file runs the lake model for each location and stores the predicted design annual maximum and minimum temperatures at desired depths in a database.

The physical features of the lakes are characterized by their size and shape and have different surface area, maximum depth and bathymetric profiles. It is practically impossible to cover the bathymetrical diversity of lakes with a single geometrical shape. However, since we are presently primarily interested in testing the model driven procedure, it was decided to test the approach with few lake descriptions.

`

We selected three representative lake sizes with specific bathymetric profiles to predict the design temperatures using typical meteorological weather data. The lake sizes are selected in such a way it represents small, medium and large in sizes. The lakes are placed in 926 locations in the continental US for which we have Energy Plus typical meteorological weather data. The major advantages of using TMY weather files are the availability and accessibility. TMY weather files are available for overwhelming number of locations around the world and also they can be easily accessed for design engineers. In addition, it is expensive to acquire actual weather data for all possible locations. Thus, using TMY weather data in the lake model it is possible to generate design temperatures for a different lake sizes by placing at various places. The combination of lake descriptions we selected and SWHE depths at which the design temperatures are generated is shown in Table 7-3

Table 7-3 Lake descriptions and SWHE depths where the design temperatures are generated

Lake name based on size	**Lake Size Ha(acres)**	**Maximum depth m (ft)**	**SWHE depths m (ft)**
3 acres pond	1.2 (3)	3.8 (12)	1.5 (5), 2.5 (8), 3.5 (11.5)
41 acres lake	17 (41)	16 (52)	5 (16), 10 (33), 15 (49)
1878 acres lake	760 (1878)	20 (66)	5 (16), 10 (33), 15 (49), 18 (59)

Before adding the model uncertainty to the predicted results, the procedure was tested for 41 acre lake. Figure 7-18 shows the annual maximum temperatures predicted by the lake model for 3 acre pond at 1.5 m (5 ft) depth. The isotherm shows the annual maximum temperatures of 926 locations across United States generated using TMY weather data.

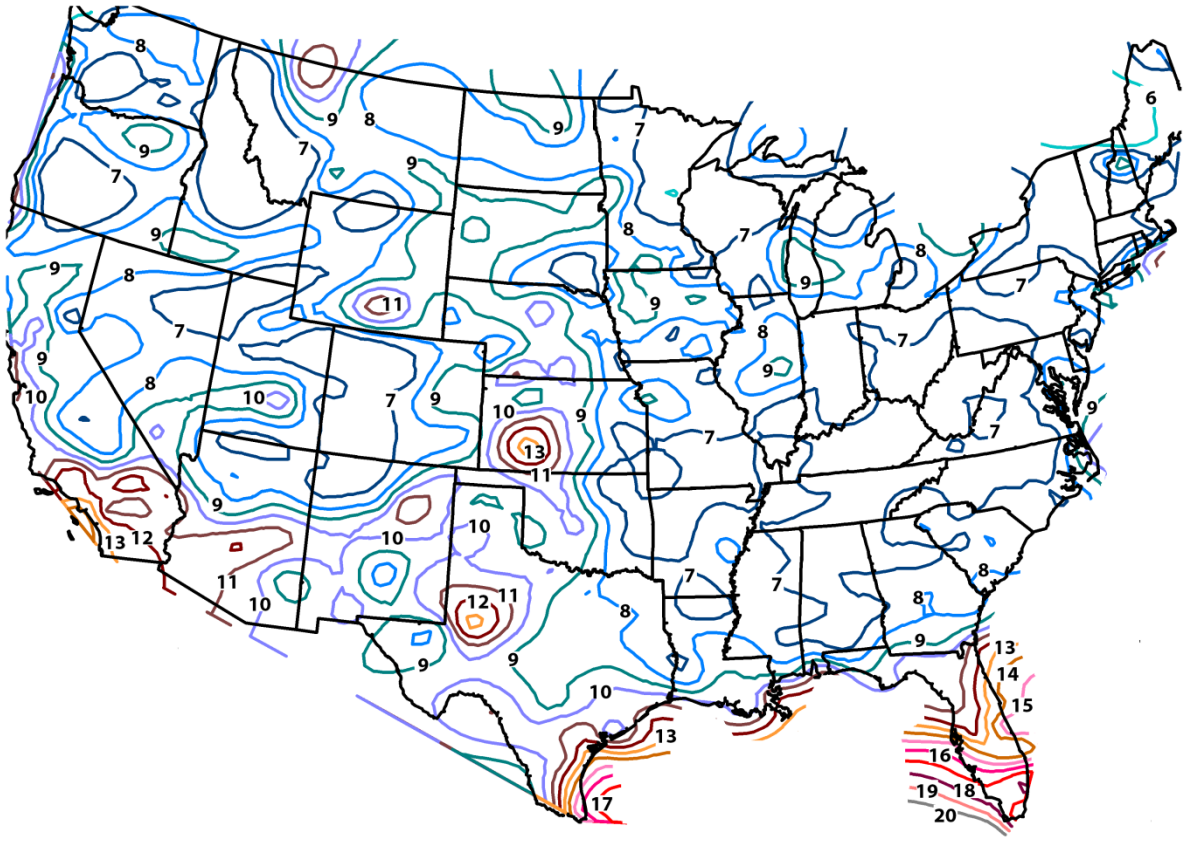

Figure 7-18 Annual maximum temperatures (°C) for a 41 acres pond at depth of 10 m (33 ft) generated using TMY weather data (without adding any uncertainty)

A notable thing in Figure 7-18 is the 'hotspot' in southwest Kansas, which shows that there is significant temperature difference between the nearby sites. To be specific the two stations Dodge City (37°45′35″N 100°1′6″W) and Garden City (37°58′31″N 100°51′51″W) located in the south west Kansas showed the temperatures of 12.2 °C and 14 °C at 10 m depth of 41 acres lake. The two stations, which are 49 miles apart showed the difference of about 1.8 °C.

Comparing the weather data of two cities, we found that in Dodge City the daily average wind speed of 8.6 m/s on October 7 causes the surface-mixed layer to extend until to the depth of 10 m. This leads to the primary conclusion that the temperature difference is related to the

`

coincidence between high surface temperatures, wind speed, time of year, and epilimnion depth. It turns out that the peak temperatures at the depths of a lake where the epilimnion could possibly deepen are controlled by subtle influences of weather. Hence, an important question arises that how well the temperatures predicted by typical meteorological year represent actual peaks that may occur during extreme climate conditions.

At this point of investigation, a significant thing we found is that the choice of generating design temperature, based on typical meteorological data is not a completely correct procedure, because it is characterized in such a way it does not include local climate extremes. This urged us to check the maximum temperatures prediction using actual weather data of many years. TMY weather data is derived from many years, such as 30 years of actual weather data by combining most representative observations of the month and does not represent the worst-case scenarios of a location. This raises a possibility that the lake temperature in extreme climate conditions at certain depths may go above or beyond the TMY predicted limits.

During summer conditions, temperature profiles are governed by the balance between naturally-stratifying effects of temperature decreasing with depth and the naturally de-stratifying effects of wind acting on the surface. This means that lake temperature profiles can change relatively rapidly when exposed to high winds for a sustained period. Furthermore, temperature profiles are seldom linear with depth. Rather, the thermocline or transition zone can readily shift up or down as wind speeds vary. Typical meteorological years are assembled in such a way as to not use the same months at adjacent weather sites. This has the effect of creating hot spots in the lake temperature data when one of the typical meteorological years contains very windy days not present at nearby sites.

To illustrate this with an example, we placed the 3 acre lake in Phoenix, Arizona and simulated it using several years of actual weather data and TMY weather data. Figure 7-19 shows

`

the variation of maximum temperatures predicted by the model using actual weather data and TMY weather data. It can be seen that from Figure 7-19 the maximum of maximum temperatures predicted using actual weather data is 12.2 °C resulted in 1975 that seems to the hottest year in the 30-years. On the other hand, the maximum temperature predicted using TMY is 8.5 °C that makes a difference of around 3.7 °C. Maximum of maximum refers to the highest value in the 30-year actual weather data simulations i.e. the maximum temperature for the warmest year in the 30-year in the data set. These results provide further evidence that the impact of year-to-year weather variations may be significant for predicting design temperatures.

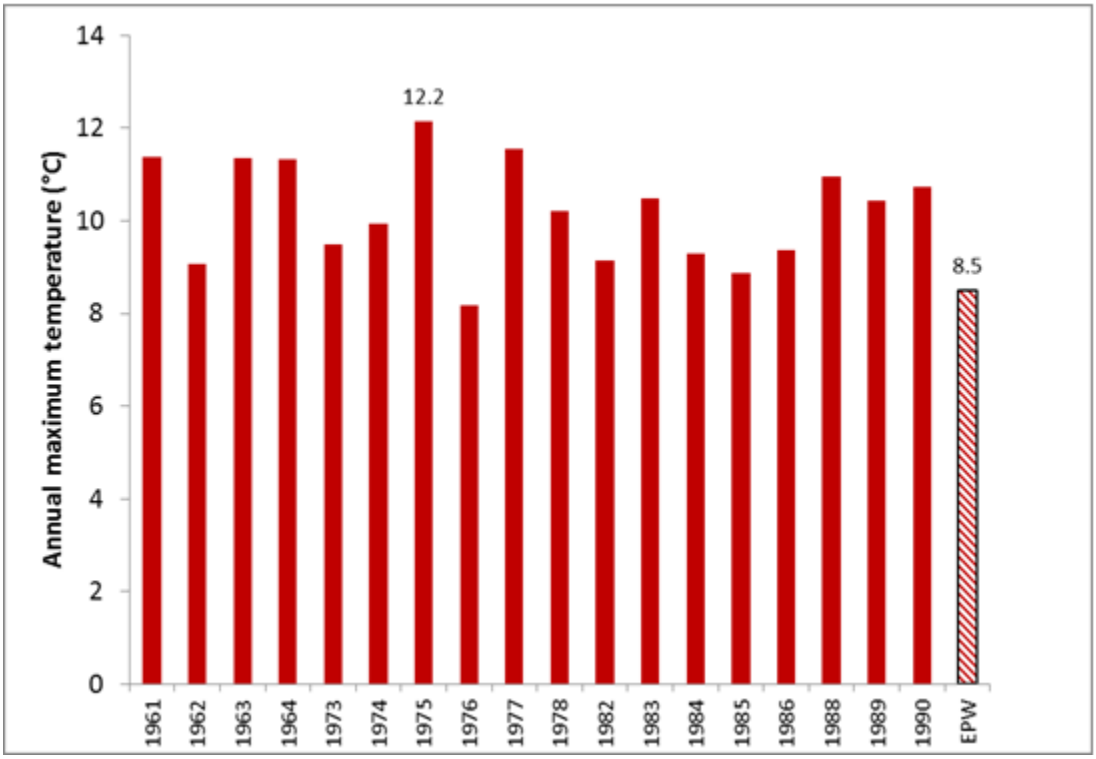

Figure 7-19 Annual maximum temperatures for a 3 acres pond at depth of 1.5 m (5 ft) generated using actual weather data and EPW weather data of Phoenix, Arizona

`

7.5.3. Uncertainty Analysis in Using TMY Weather Data

Generally, the maximum lake temperature occurs during late summer and minimum lake temperature occurs during late winter. But then again, the lake annual maximum and minimum temperatures at each depth and the time of occurrence may be expected to change every year because of significant climatic changes from year-to-year and its implications on lake temperature. The consequence of any warm extremes in the climate may be dramatic in lakes that causes more heating and thus affects the stratification. Furthermore, with the combined forces of persistent winds, can shift the epilimnion depth and the maximum temperatures would increase beyond the limit predicted by typical meteorological year weather data. Therefore, an uncertainty analyses is necessary to obtain the estimates of design temperatures exceedence from an EPW simulated temperatures i.e. to analyze how well the EPW generated design temperatures can represent actual year peak temperatures.

As a first step, we therefore collected the historical weather data needed to find the uncertainties in design temperatures predicted using EPW are obtained from Solar and Meteorological Surface Observational Network (SAMSON) dataset that we discussed before in this paper. All the weather files have been converted to a format required by the lake model with the key parameters such as air temperature, solar radiation, wind speed, relative humidity and cloud cover. In order to neglect the erroneous results, which may occur due to missing weather data, we eliminated years that would require filling of data, even for a single day. On that basis, each SAMSON station weather file has minimum of 4 years weather data to maximum of 30 years weather data.

The statistical analysis was performed through the calculation of prediction intervals that gives us the quantitative estimates of uncertainty associated with the TMY predicted design temperatures. For all 208 locations and for the 3 lakes shown in Table 7-3 we simulated the lake/location combination for a single typical year and for multiple years using real SAMSON

`

data. The script files are used to run the series of SAMSON actual weather data for 208 different locations in United States that extracted the design temperatures for each station-year.

7.5.3.1. Uncertainty in the prediction of maximum temperatures

Two types of statistical analysis were done for the case of maximum temperatures considering the two different comparisons

- First, we computed the difference between the maximum temperature at each depth/lake/location for each year and the maximum temperature for each combination based on the TMY file.
- Secondly, we computed the difference between the maximum temperature at each depth/lake/location for all years and the maximum temperature for each combination based on the TMY file.

Both analyses have the strength to explain the difference between the temperatures predicted using TMY and actual weather data. For example, if it shows close match for the first type of comparison it tells us the TMY generated design temperatures are reliable in those locations. If the second type of comparison shows the close match then the location is likely had no extreme weather conditions recorded in the span of years for which its actual weather data is analyzed. Clearly, the two types of statistical analyses can then tell us the average expected difference between a maximum temperature generated with a single TMY file and that generated with multiple years of actual weather data.

The histograms shown in Figure 7-20 and Figure 7-21are the results of two types of comparison for 3 acres pond at the depth of 1.5 m depth. This is the region of epilimnion where the temperatures respond to vary with air temperatures and wind speed. The skewness of the histograms as shown this figure is typical for every depth we analyzed. Figure 7-20 shows the comparison between TMY generated design temperature and the temperatures generated with

each station year weather data. The frequency of errors nearly follows a normal distribution. The uncertainties within ±1°C may have mild climates that are close to typical weather conditions. A negative or positive variation indicates that, in a particular actual year, the predicted maximum temperature using actual weather data for that year is, less than or greater than that using TMY weather data. The difference within ±1 °C between the annual maximum temperature of particular year and TMY explains that the recorded meteorological data of these years are relatively mild. We may argue that there for other few stations, which had the extreme climate conditions have uncertainties beyond ±1°C. Figure 7-21 shows the comparison of annual maximum temperatures predicted using TMY and the maximum of maximum temperatures predicted using actual weather data for the corresponding location. This clearly explains the range or the peak i.e. the maximum temperature can increase beyond the TMY predicted limit.

Some of the maximum deviation occurred in stations located in Texas and California that showed the difference of around 3°C. Since these places are relatively, warm and record of likely warm climate extremes caused the temperature increase in the shallow lake. Therefore, in order to assess the generality of TMY design temperature prediction from the standpoint of geographical distribution we computed prediction intervals at every depths of each lake listed in Table 7-3

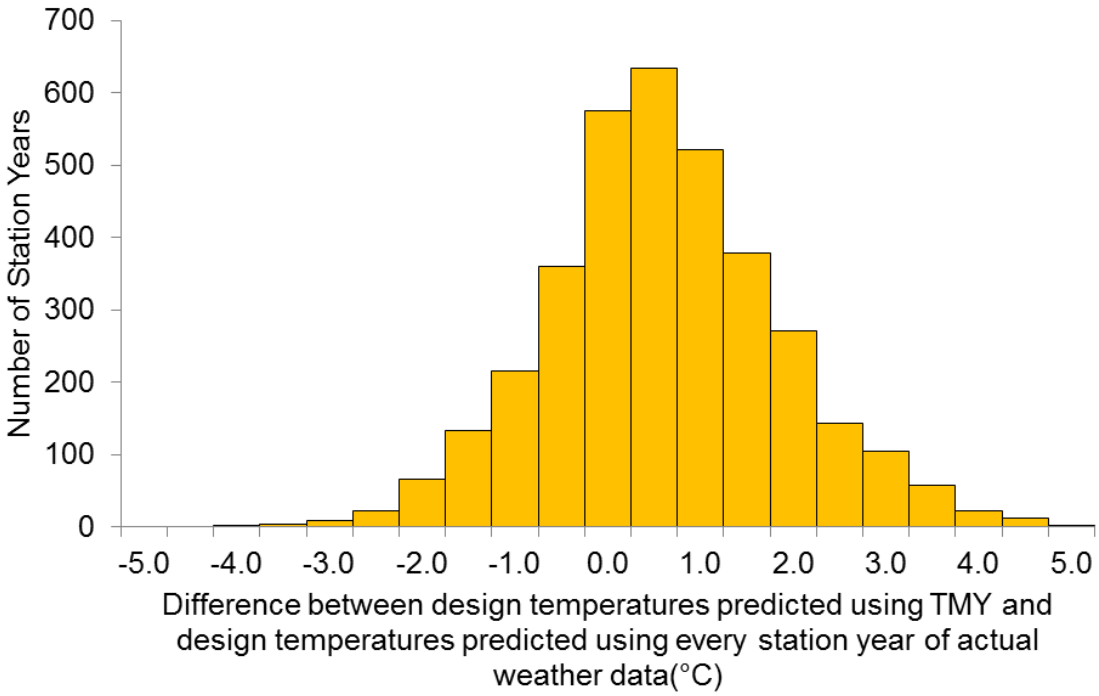

Figure 7-20 Histograms correspond to statistical analyses - 1 for OSU research pond at 1.5 m depth

`

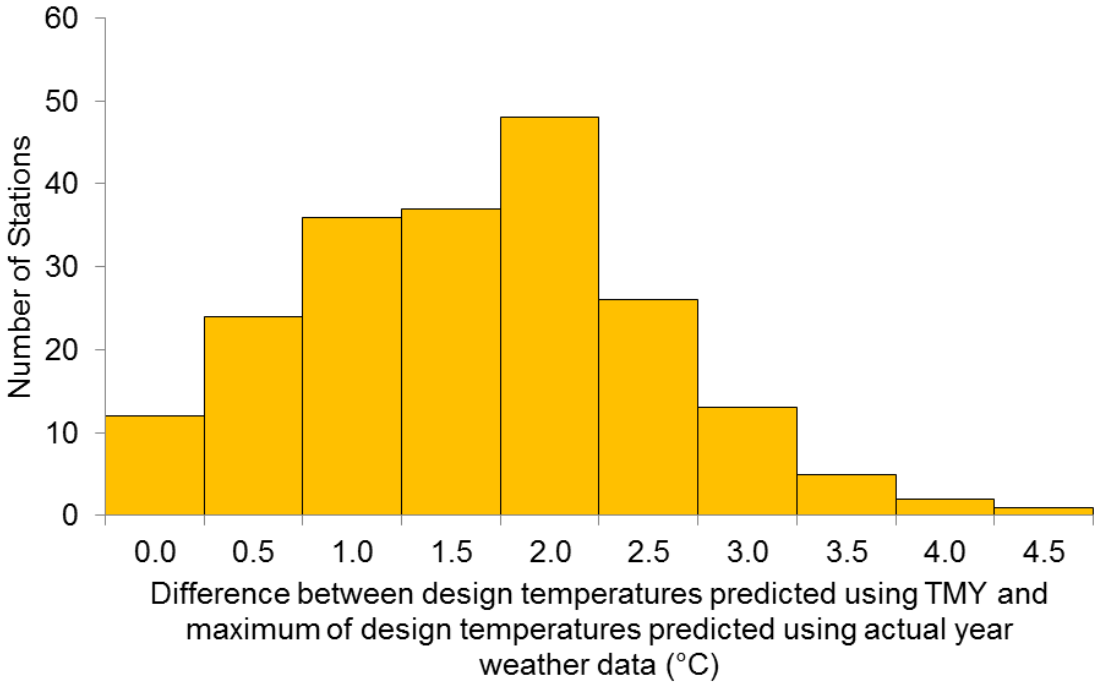

Figure 7-21 Histograms correspond to statistical analyses - 2 for OSU research pond at 1.5 m depth

Based on a standard statistical analysis, we calculated the mean difference and the variance corresponding to a certain prediction interval. For this calculation, we selected 95% confidence interval, then with the variance associated to the 95% confidence, we can find for a given lake and depth the temperature difference above the TMY predicted maximum that corresponds to

a) 95% confidence that the temperature will not be exceeded in any year.

b) 95% confidence that the temperature will not be exceeded in the number of years

The prediction intervals for the case of maximum temperatures resulted for all lake depths are listed in Table 4. For tabulating design temperatures, the statistical analysis (b) will give us the best estimate of a design temperature since this variance includes the peak occurred.

`

We propose applying these numbers, which have been determined for 208 SAMSON locations to all 1042 TMY locations as a best estimate of the amount by which the TMY-only under predicts the maximum temperature or over predicts the minimum temperature.

Table 7-4 95% confidence interval for maximum design temperatures

Lake name	**SWHE depths (m)**	**Mean Error (MAX. of SAMSON - TMY) (°C)**	**95% Confidence Interval (MAX. of SAMSON - TMY) (°C)**	
			Lower Limit (°C)	**Upper Limit (°C)**
3 acres pond	1.5	1.3	-0.5	**3.2**
	3.5	1.4	-0.7	**3.4**
41 acres lake	5.0	1.3	-1.8	**3.1**
	10.0	2.0	-0.1	**4.1**
	15.0	1.9	-0.8	**4.6**
1878 acres lake	5.0	1.3	-1.7	**3.0**
	10.0	1.3	-0.6	**3.3**
	15.0	1.6	-0.7	**4.0**
	18.0	1.7	-0.8	**4.1**

`

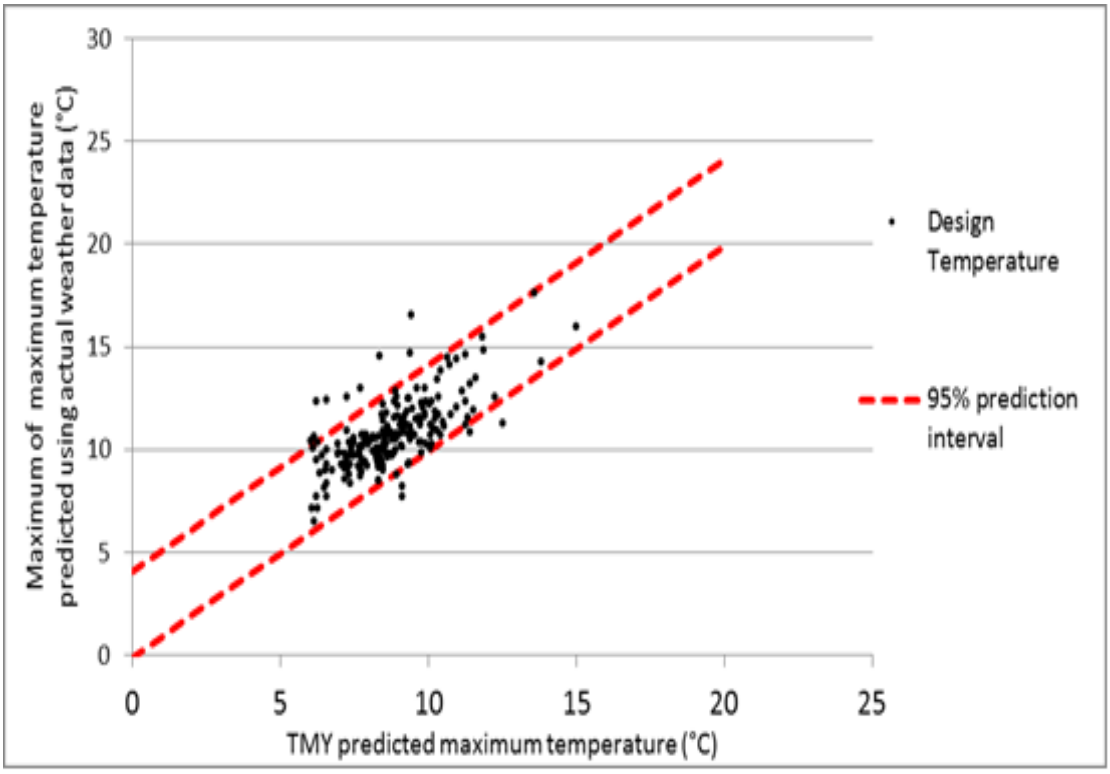

Figure 7-22 Scatter plot showing the comparison of maximum temperatures predicted by TMY and actual weather data of 41-acre lake at 10 m depth

Figure 7-22 shows the comparison of TMY predicted maximum temperature and the one predicted using actual weather data. Note that the uncertainties resulted due using a TMY weather file are not linear with the maximum temperature prediction. The prediction intervals at each depth of the lakes remain almost constant except at the depth of 15 m for 41 acres lake, which involves the largest uncertainty in the statistical analysis.

The clustered points are the locations where the difference between the TMY predicted and actual weather data predicted maximum temperatures are almost same. Indeed, the 'high extreme summers' are found in the distinctive years of actual weather data for every location, which produced large differences between TMY and actual weather data, consequently, wide prediction intervals. The large differences (scattered points) are resulted from the warm locations

`

such as Texas, Louisiana, Florida and California. The uncertainty due to using TMY and model uncertainty are added in quadrature to produce a total uncertainty estimate, which is used as error allowance in the design temperature database. Figure 7-23 shows the relative contribution of TMY and model uncertainties to the total uncertainty

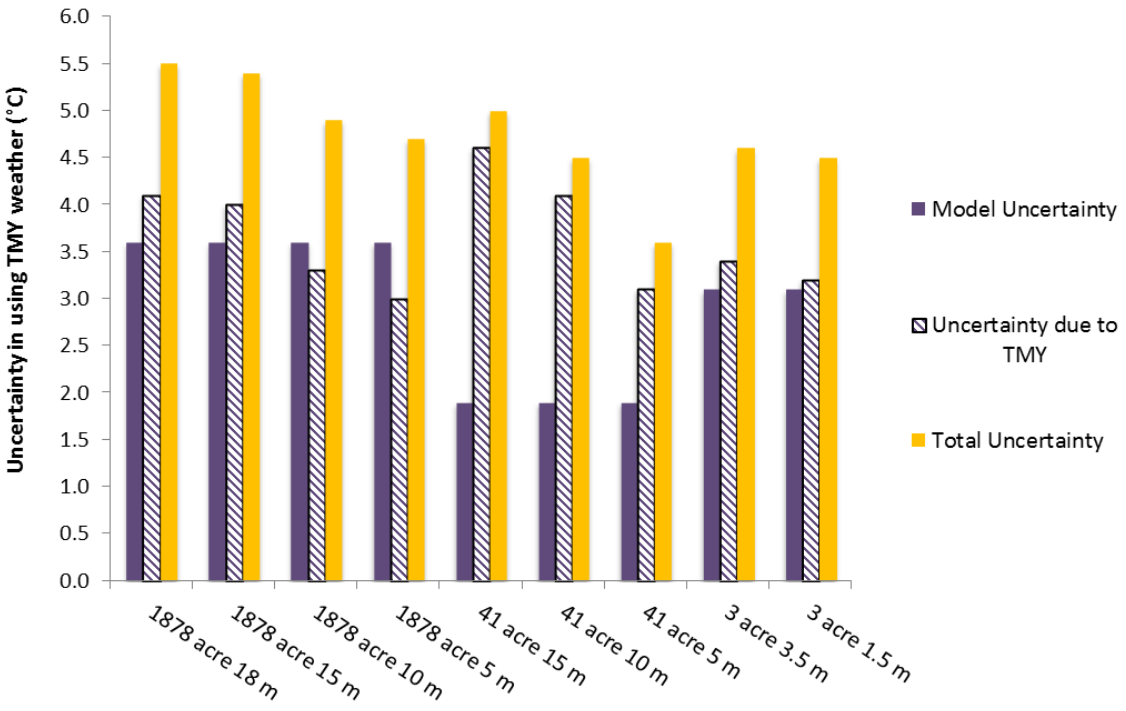

Figure 7-23 Maximum temperature uncertainties resulted from the statistical analysis of 95% prediction intervals

7.5.3.2. Uncertainty in the prediction of minimum temperatures

If the air temperature above the lake is sufficiently cool, it will freeze the lake water and forms ice on the surface of the lake. The water temperature under the ice stays very cold near 0 °C. Therefore, the statistical analysis for minimum temperature differs from the analysis of maximum temperatures.

`

The statistical analysis for the case of minimum temperatures considers the comparison of minimum temperature at each depth/lake/location for all years and the minimum temperature for each combination based on the TMY file. Here a fresh attempt is made to address the uncertainty in predicting minimum design temperatures. Calculating uncertainties is not as straightforward as the maximum temperatures. This is because we have to account for lake freezing in the minimum temperature analysis. To proceed further, we divided this comparison of minimum temperatures into two cases based on how close is the minimum temperature to freezing. There are two types of analysis performed in the case of minimum temperatures, one for the temperatures predicted by the actual weather data, which are close to freezing and another for the relatively high temperatures which would be in places like Texas, California and Florida

Case 1: Minimum temperatures close to freezing

We introduce a dimensionless number called *f*. It is calculated for each comparison of 'minimum of minimum actual temperatures' and a corresponding 'TMY predicted minimum temperature'

$$f = \frac{T_{TMY,\min} - T_{all,\min}}{T_{TMY,\min} - 0} \tag{73}$$

Where $T_{TMY,min}$ is the lowest temperature of all years of minimum temperatures predicted using actual weather data for a depth/lake/location, $T_{all,min}$ is the minimum temperatures for a corresponding combination based on the TMY file

The dimensionless number *f* is the ratio of temperature difference between TMY and actual minimum temperature to the difference between TMY minimum temperature and freezing temperature (0 °C) for a given depth/lake/location. The fraction tells us how close the minimum temperature predicted by TMY is to freezing point of water and its value ranges between 0 and 1.

`

If a certain combination of depth/lake/location resulted in a value of *f* close to one, then it seems likely that the winter air temperatures in that location was cold enough to reduce the lake temperatures close to water freezing temperature of 0 °C i.e. the temperature at that depth/lake/location will likely go near-freezing temperatures.

If f is close to zero, then, it implies that the minimum temperature was close to the TMY prediction, which would be far away from freezing conditions. In other words, we expect that the temperature at that depth/lake/location is unlikely to go near-freezing temperatures. When *f* is close to one, the temperature at that depth/lake/location will likely go near-freezing temperatures whereas if it is close to zero, then, we expect that the temperature will not likely go near-freezing temperatures.

For instance, we compared the actual minimum temperature and EPW predicted minimum temperature of all 208 SAMSON locations and calculated *f* values for a 3 acre pond at 1.5 m depth (Figure 7-24) and 41 acre lake at 10 m depth (Figure 7-25). It can be seen from Figure 7-24 the values of more tend to 1 and in Figure 7-25 more values of *f* is around 0.5. It explains us that for most of the locations, the temperatures at 1.5 m depth of 3 acre shallow pond are either close to freezing point or at freezing point. At 10 m depth of a 41 acre lake, the minimum temperatures for most of the locations are half way close to freezing temperature.

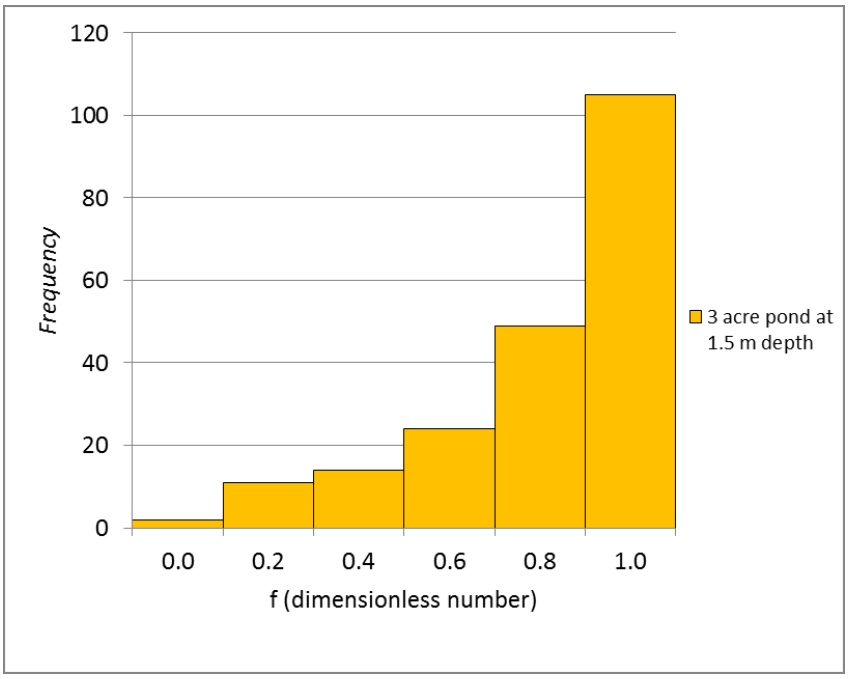

Figure 7-24 Value of *f* calculated for the minimum temperatures of a 3-acre pond at 1.5 m depth

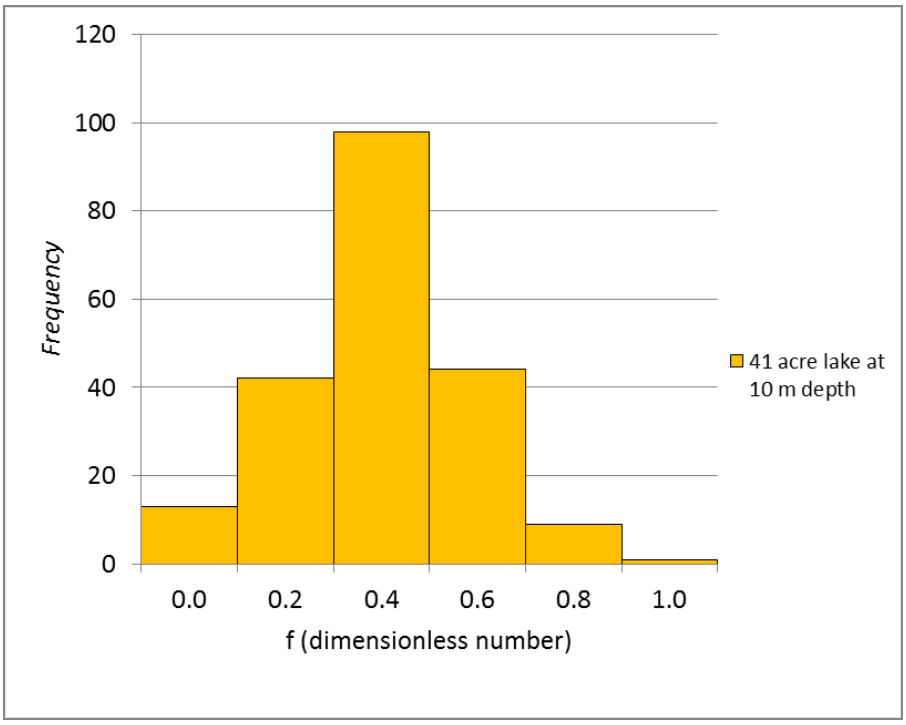

Figure 7-25 Value of *f* calculated for the minimum temperatures of a 41-acre lake at 10 m depth

`

Finally, the 95% percentile of *f* is calculated for each depth and this was deducted as the uncertainty allowance of the minimum temperatures predicted by TMY. By doing this, we could expect reasonable minimum temperatures rather than below zero and unrealistic freezing temperatures.

Case 2: Minimum temperatures far from freezing

The second part of minimum temperature analysis is for the temperatures, which are far away from freezing, and occurs in 'hot' places in southern region of United States. In this case, we identified the 'maximum difference' i.e. the largest possible error between TMY and actual weather data predicted minimum temperature. We deducted this 'maximum difference' from the TMY predicted minimum temperatures

7.6. Results and discussion

This section brings together the estimated overall uncertainty and predicted design temperatures. The isotherm plots are developed by adding the temperatures predicted using TMY and the uncertainty allowances.

7.6.1. Maximum temperature isotherms

Figure 7-26, Figure 7-27 and Figure 7-28 shows annual maximum temperature isotherms for 3 acre lake at depth of 3.5 m (11.5 ft), 41 acres lake at depth of 10 m (33 ft) and 1878 acres lake at depth of 18 m (59 ft) respectively.

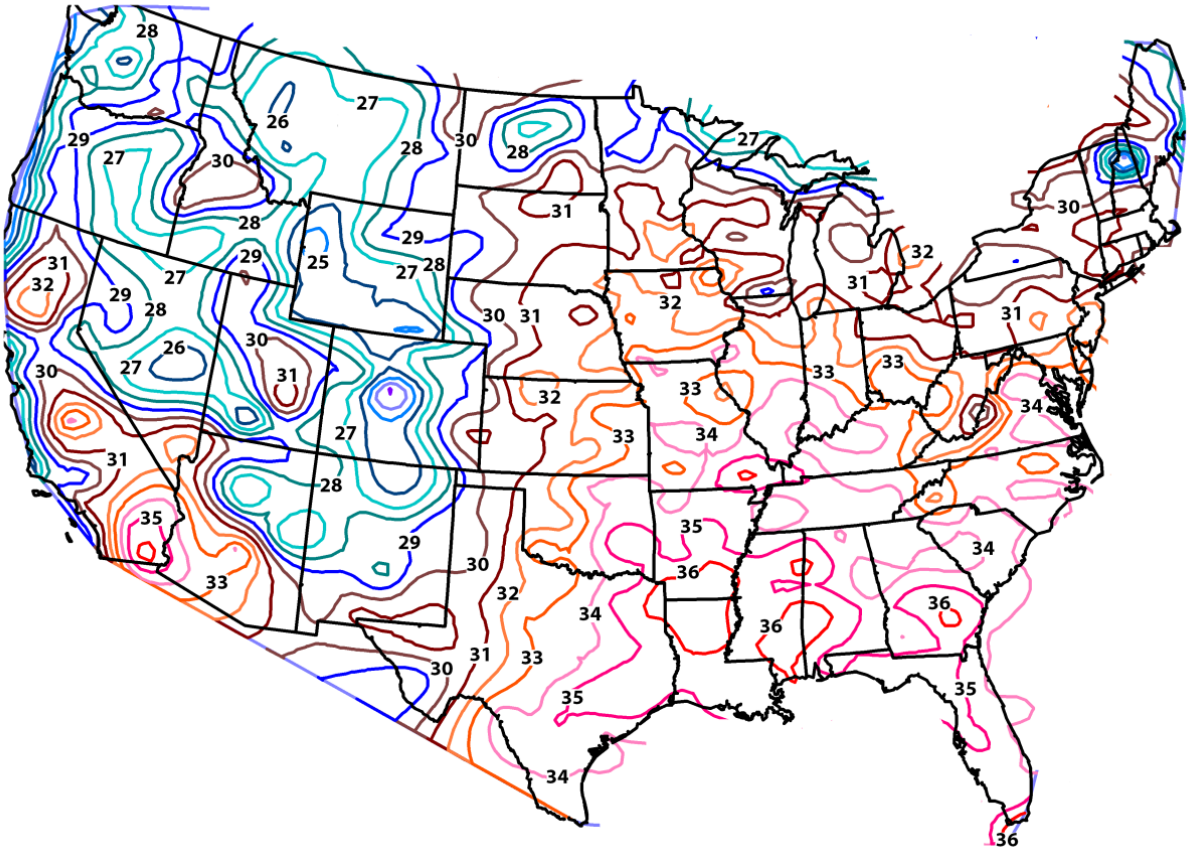

Figure 7-26 Annual maximum temperatures (°C) for 3 acre lake at depth of 3.5 m (11.5 ft)

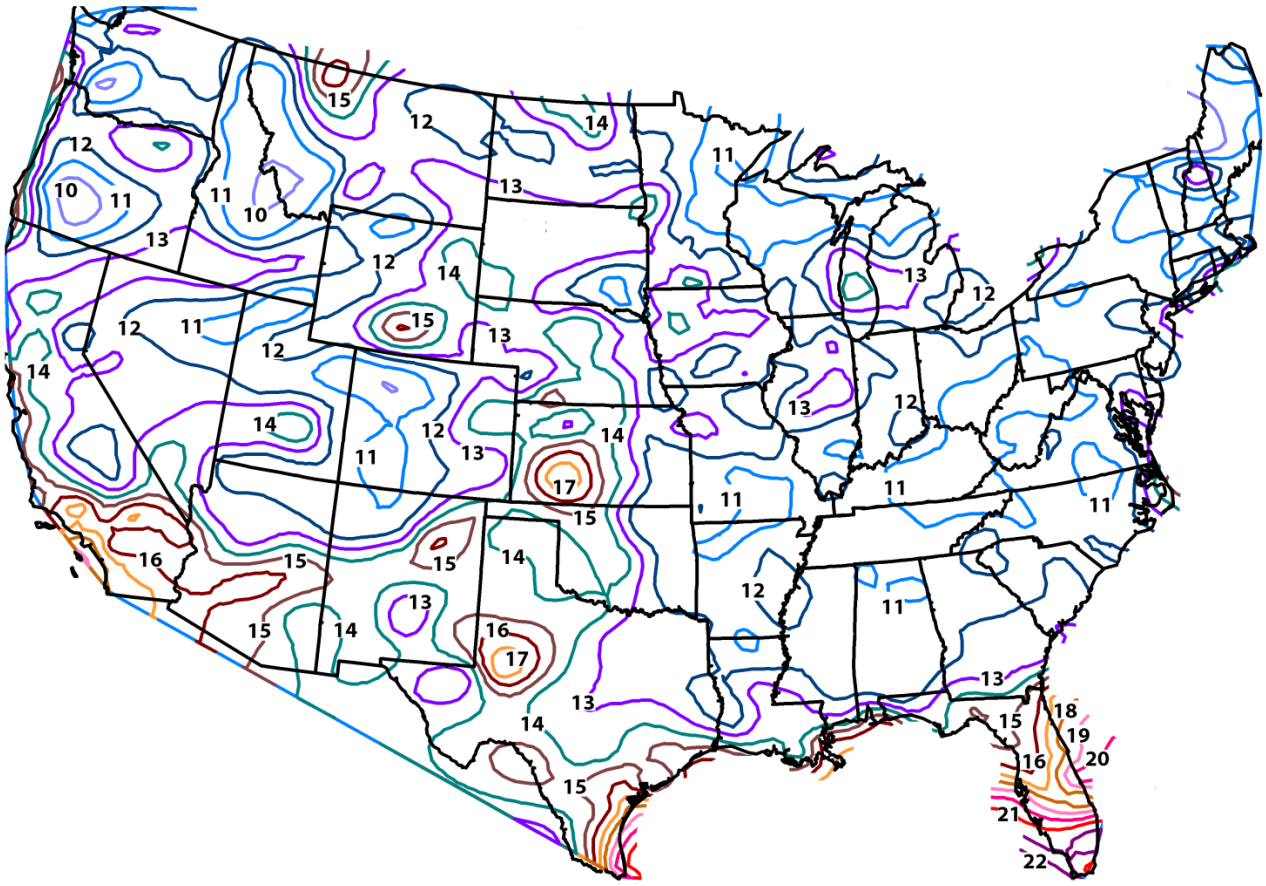

Figure 7-27 Annual maximum temperatures (°C) for 41 acres lake at depth of 10 m (33 ft)

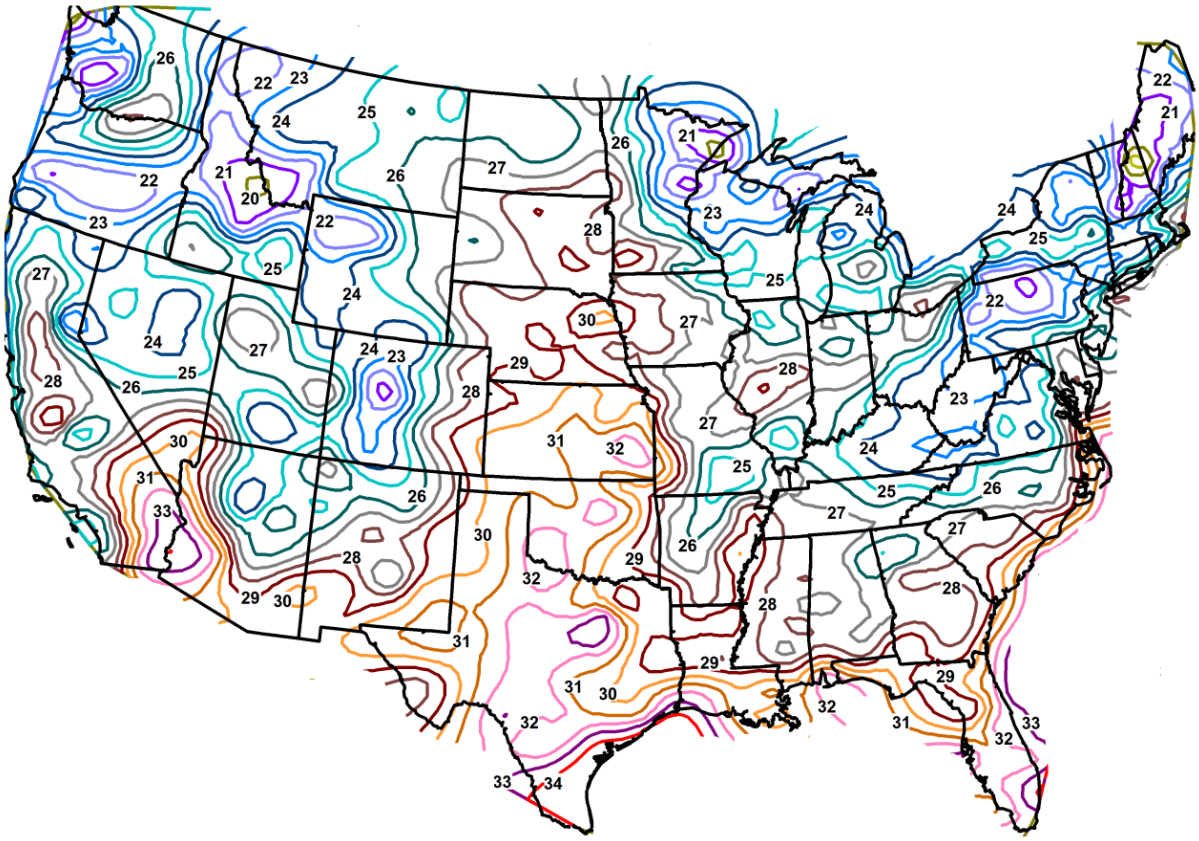

Figure 7-28 Annual maximum temperatures (°C) for 1878 acres lake at depth of 18 m (59 ft)

As we see before in this chapter, hot spots still exist (Figure 7-27) at 10 m depth of 41 acre lake at the same location of Dodge City, Kansas and it can be attributed to the fact that very high wind speed drives the epilimnion deeper and increases the temperature. Furthermore, to substantiate this idea we searched for experimental evidence, which can reflect the similar phenomenon in measured data. Unfortunately, we do not have data for the hypothetical lake in Dodge City. Nor is this example a perfect match to what we found in the Dodge City lake; the peak wind speed is much lower than what we had in the Dodge City data. However, it does illustrate some of the issues involved with a daily simulation as well as the effect of an abrupt increase in wind speed, so we present it here.

`

Figure 7-29 shows the hourly and daily average wind speeds for the location of Lake Sammamish from 6th through 8th of October 2008, which can be interpreted, as the lake was subjected to calm condition, then windy and then calm again.

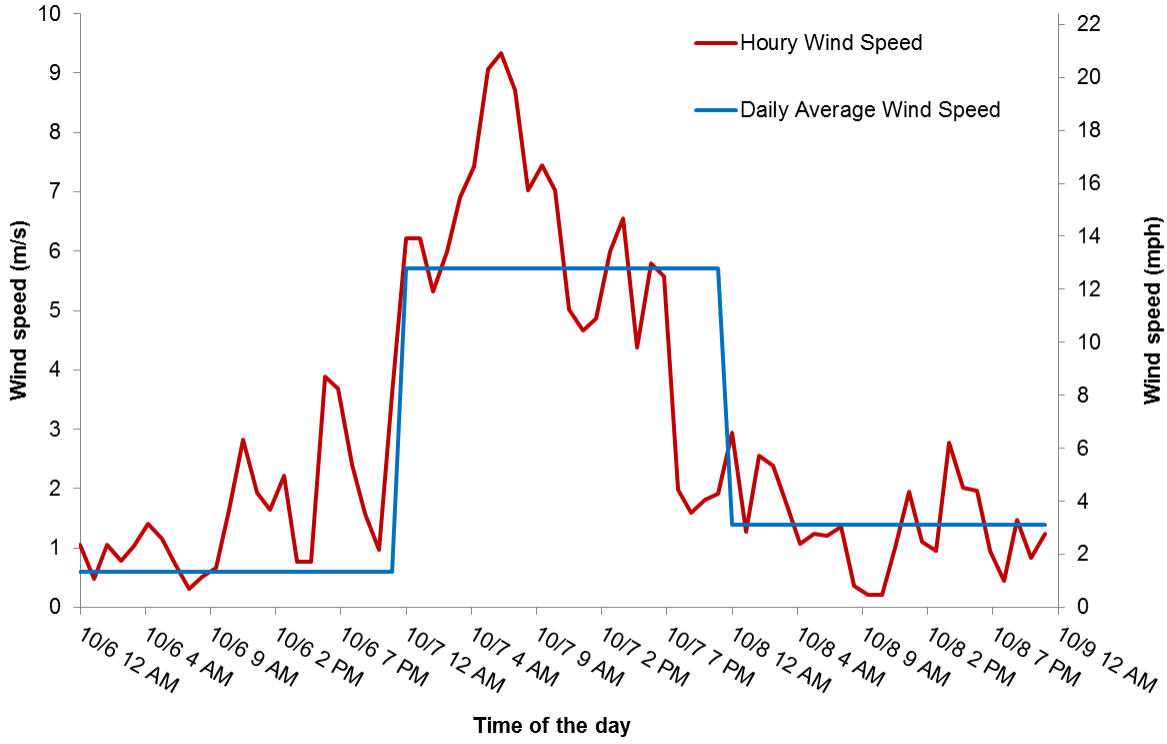

Figure 7-29 Hourly and daily average wind speed for Lake Sammamish, Oct. 6th – 8th, 2008

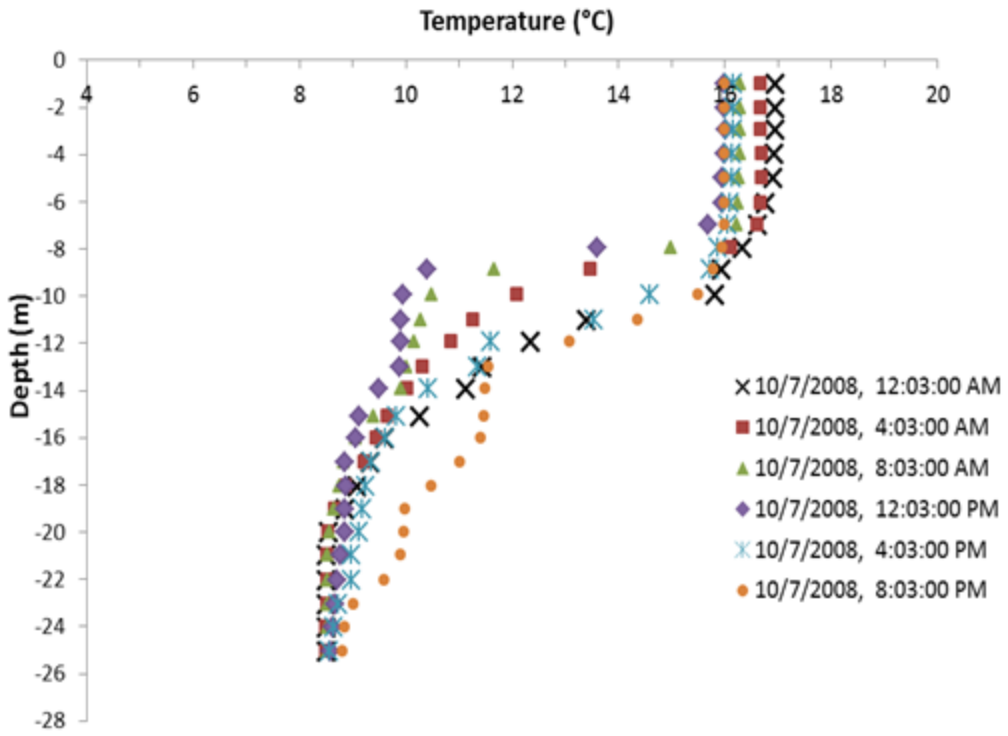

Figure 7-30 Temperature profiles for Lake Sammamish, October 7

The entire variation of experimental temperatures over a day on October 7 along with the simulated temperature profile is put in perspective in Figure 7-30. As we discussed before the hourly temperature variation in epilimnion and hypolimnion are less over a day. The temperature changes in the epilimnion region, between 1 – 10 m depth, are within 1 °C**.** At lower depths around 20 m depth, we can see some variations in the hypolimnion temperatures about 1-2 °C over a day. Nevertheless, the temperatures in the thermocline region at the depth of approximately 6 °C, the temperature cools by about 6 °C during first half of the day, and then warms by about 6 °C during the second half of the day. The proximate cause of this is the epilimnion becoming shallow and increasing in depth. Apparently, weaker winds produced a shallow epilimnion during early hours of a day; conversely, stronger winds during later hours

`

caused the epilimnion deepening. It is also noticeable in Figure 7-30 that on the same day, the 'warm front' propagates to the depth of about 23 m at the end of the day around 8 PM.

So, we can conclude from this experimental evidence that, at least, a windy day can affect temperatures down to a significant depth. The hotspots seen in Figure 7-27 for a 41-acre lake at 10 m depth is also for the same reason. We also have seen a similar effect in Lake Sammamish even though it is 5000 acre with a maximum depth of 32 m on a day when the average wind speed is less than half what it was on the day in question in Dodge City, Kansas.

A further potential observation that is subjected to discussion is the notable difference between the maximum temperatures of 41-acre lake at 10 m depth (Figure 7-27) and the maximum temperatures of 1878-acre lake at 18 m depth (Figure 7-28). Particularly, it is necessary to address the question whether the temperature of a 41-acre lake at 10 m depth would be that low of 11°C to 13°C in the southeast warm climatic zones such as Arkansas, Mississippi, Alabama and Georgia. Although the two lakes are subjected to same climatic conditions, the maximum temperatures are different in the hypolimnion regions of the lakes. This may be attributed to the morphological[1] differences between the two lakes. Since the two lakes have different area-to-depth ratio and so the bathymetry, the physical response of the lakes to meteorological conditions are different.

The 41-acre lake is highly deep for its size. These types of lakes do not have enough mixing and do not turnover completely. Thus, there is always cold water remaining in the hypolimnion region. These types of lakes that have large relative depths are known as '*meromictic*' lakes in the field of limnology (Hakala 2004; WOW 2013). On the other hand,

---

[1] Morphology refers to the geometric characteristics of the lake – shape, depth, lake bottom roughness. When quantified, this is sometimes referred to as lake morphometry. Håkanson, L. (1981). *A manual of lake morphometry*. New York, Springer-Verlag.

`

1878-acre lake is much larger lake and considerably deep for its size mixes completely. The limnological terminology to distinguish these types of lakes is '*holomictic*' (Hakala 2004; WOW 2013)

Generally, these types of lakes completely mix from top to bottom so that the hypolimnion region has warm water for respective period in a year. Furthermore, there are no such types of lakes comparable to 41-acre lake in the southern region of United States, which leaves us with no option to validate the results. Nevertheless, we verified the predicted temperatures with experimental measurements of Bull Shoals lake located in the city of Branson Missouri obtained from Galloway and Green (2003).

The surface area and maximum depth of the lake is 45000 acres and 64 m. Despite this lake is large and deep when compared to 41-acre lake, it turns out to be that this lake is relatively deep for its area. The experimental measurements of the lake shows that from August 1994 to December 1994, the temperatures ranges between 8°C - 9°C at the depth of approximately 55 m. This may not be the best verification of our results. However, the lakes for which the depth is relatively higher, we can argue that there could be relatively cold water in the hypolimnion region that is not subjected to any type of mixing in the lake.

7.6.2. Minimum temperature isotherms

Figure 7-32, Figure 7-34, Figure 7-37 shows the annual minimum temperatures of 3 acres pond at depth of 3.5 m (11.5 ft), 41 acres lake at depth of 10 m (33 ft) and 1878 acres lake at depth of 18 m (59 ft) respectively. Some places show lake temperatures below freezing. In other words, the worst case analysis is that the lake will freeze. Again, it is difficult or impossible to identify a lake for which the TMY predicted close to the minimum. The lower limit of the confidence interval, which was calculated in the previous section, is simply added without regard to whether or not the lake went from not freezing to freezing. So, in some locations perhaps the

`

lake that is shown as freezing to a certain depth will not freeze that deep. But it would be expected to be very close to freezing

An Excel database of design temperatures design temperatures for each lake at each depth predicted by the lake model is also been developed through this approach and this will have no difficulty for a design engineer in finding the appropriate design temperatures.

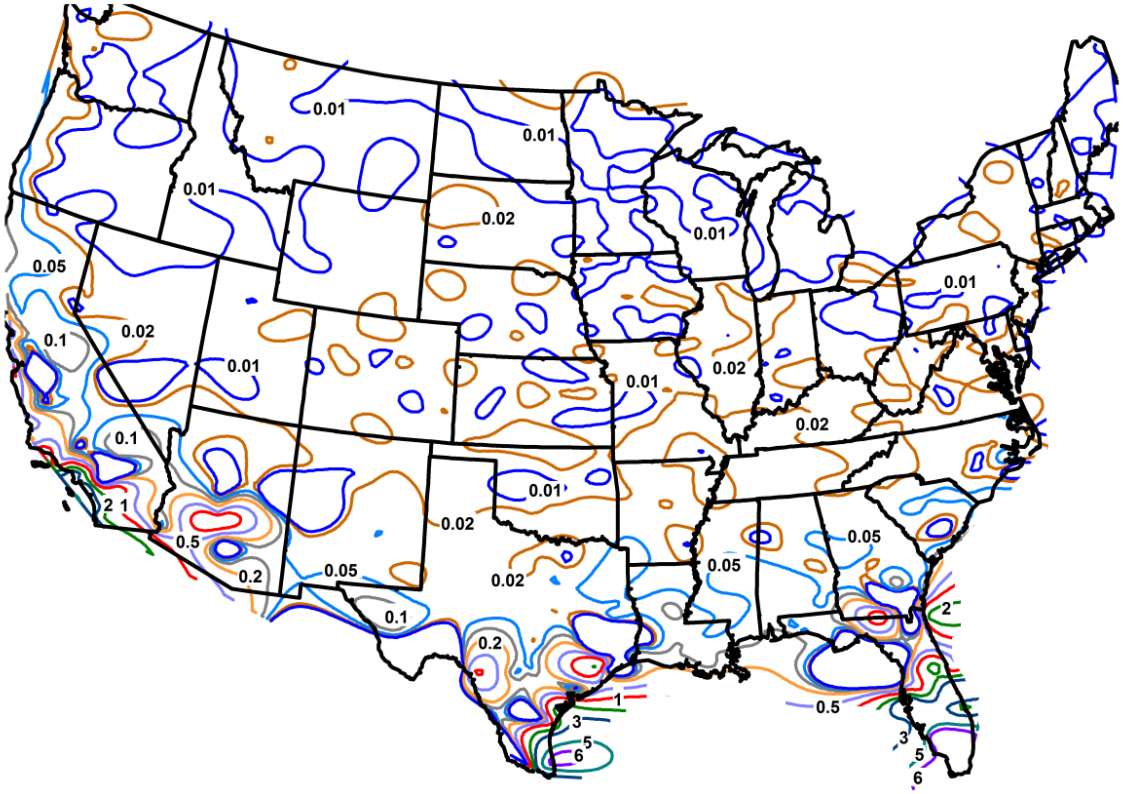

Figure 7-31 Minimum design temperatures (°C) for 3 acre pond at depth of 1.5 m (5 ft)

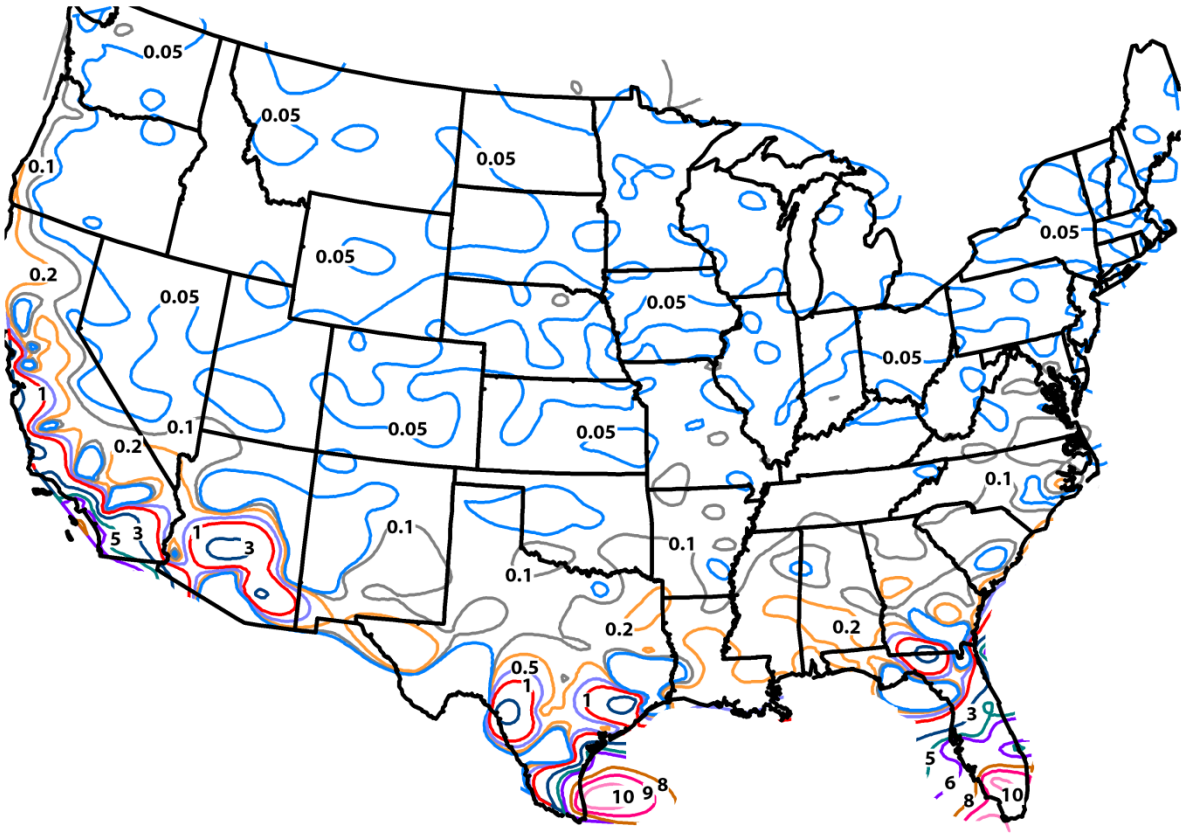

Figure 7-32 Minimum design temperatures (°C) for 3 acres pond at depth of 3.5 m (11.5 ft)

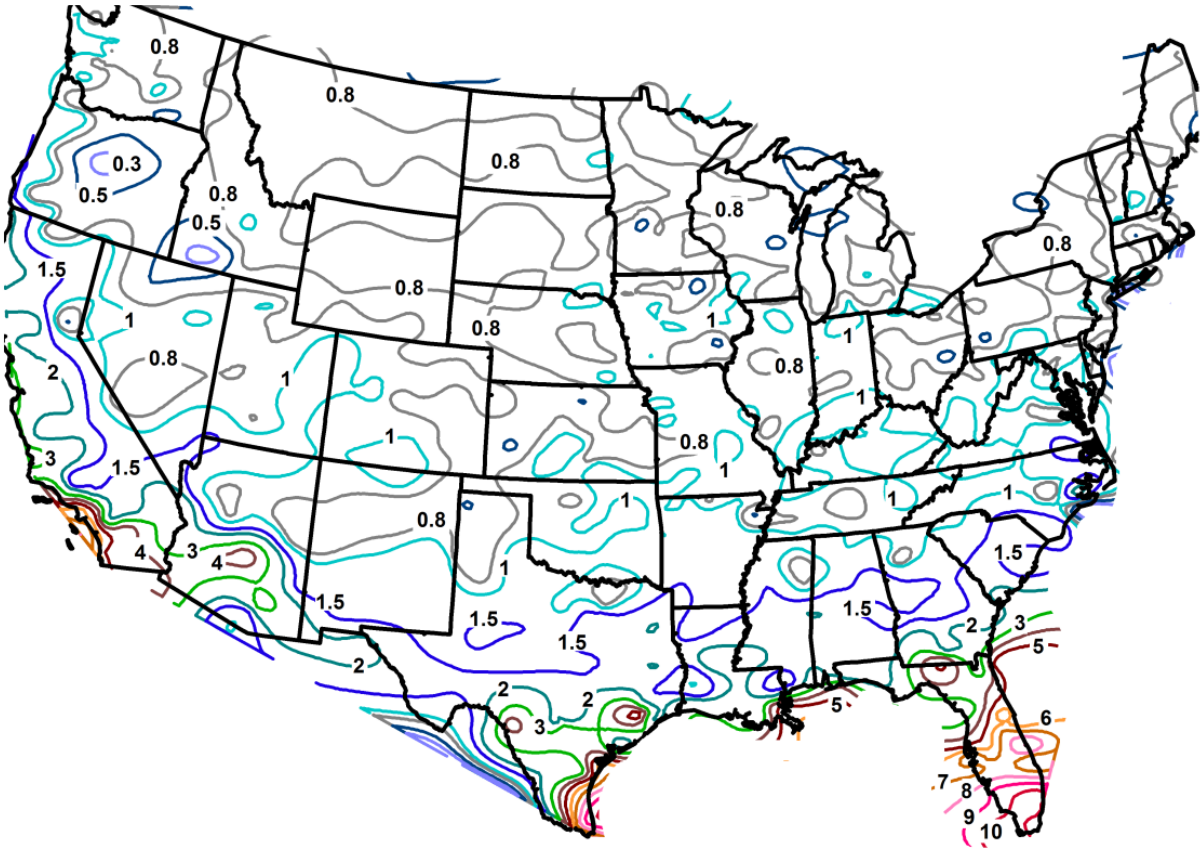

Figure 7-33 Minimum design temperatures (°C) for 41 acre lake at depth of 5 m (16 ft)

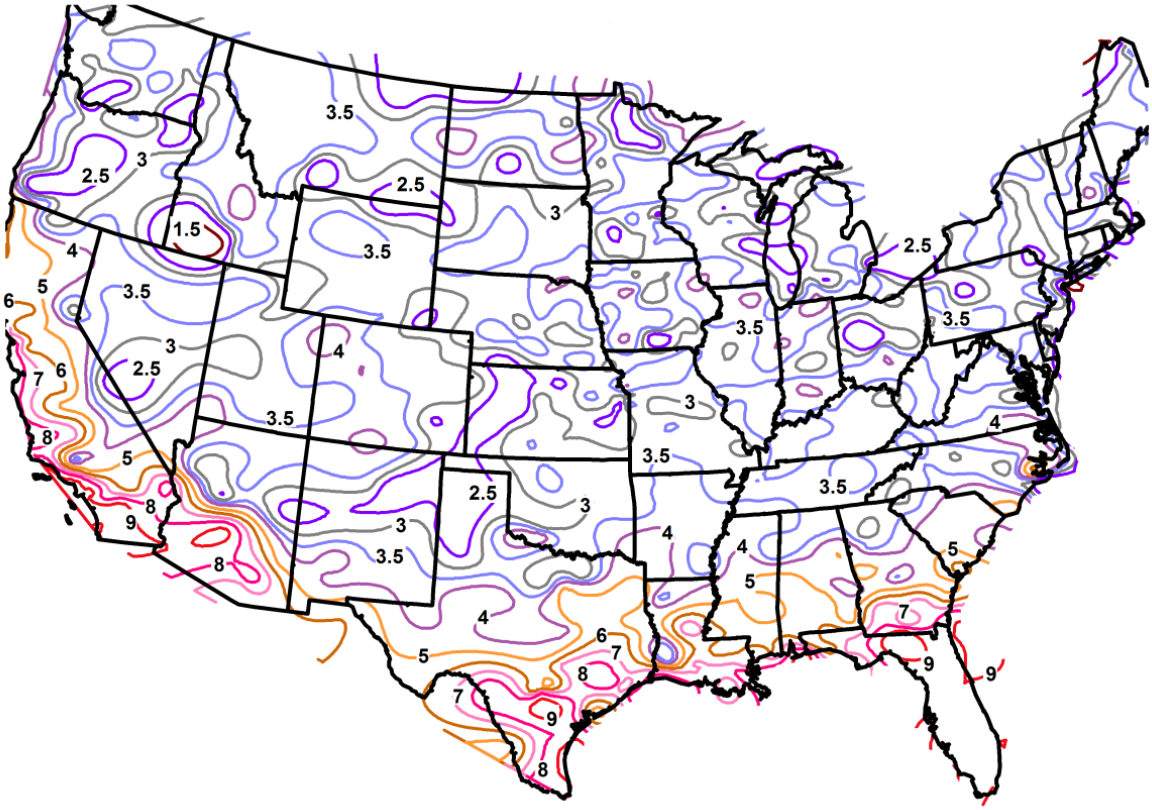

Figure 7-34 Minimum design temperatures (°C) for 41 acres lake at depth of 10 m (33 ft)

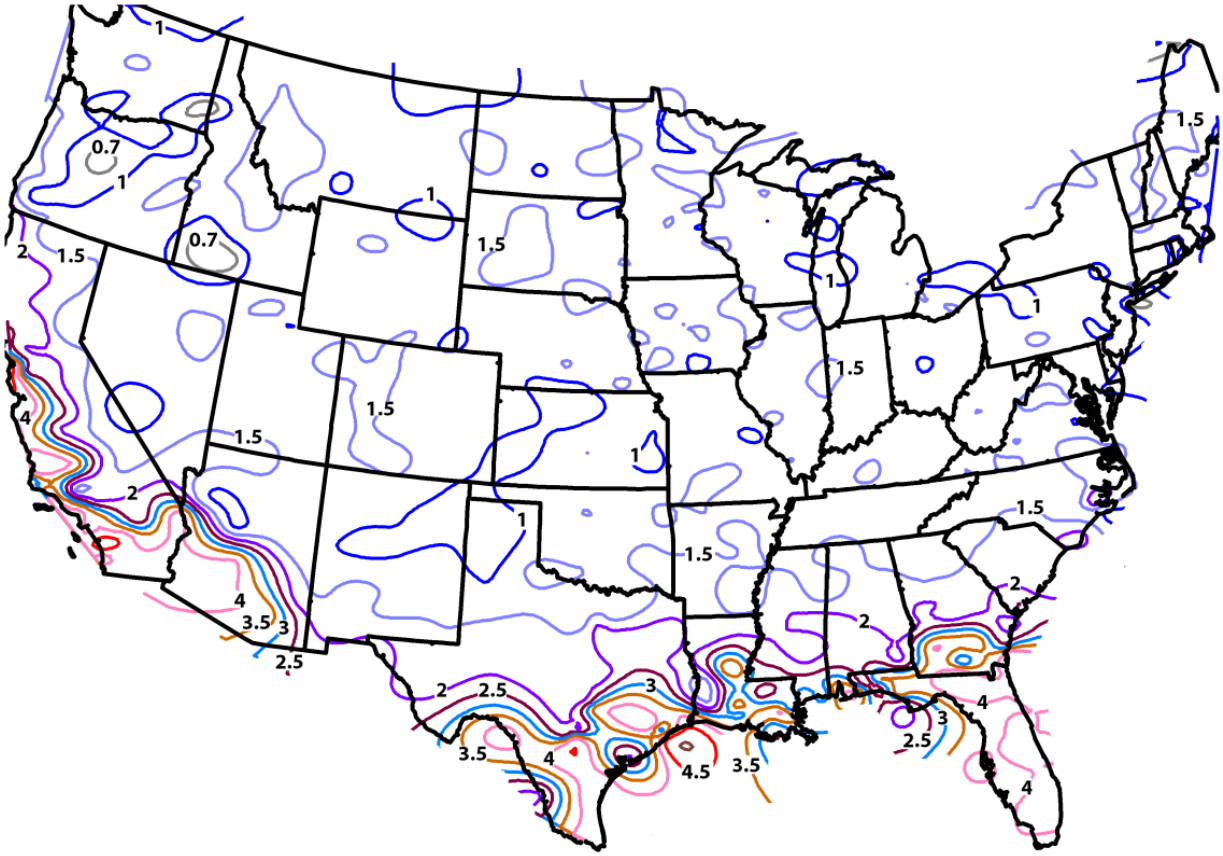

Figure 7-35 Minimum design temperatures (°C) for 41 acre lake at depth of 15 m (49 ft)

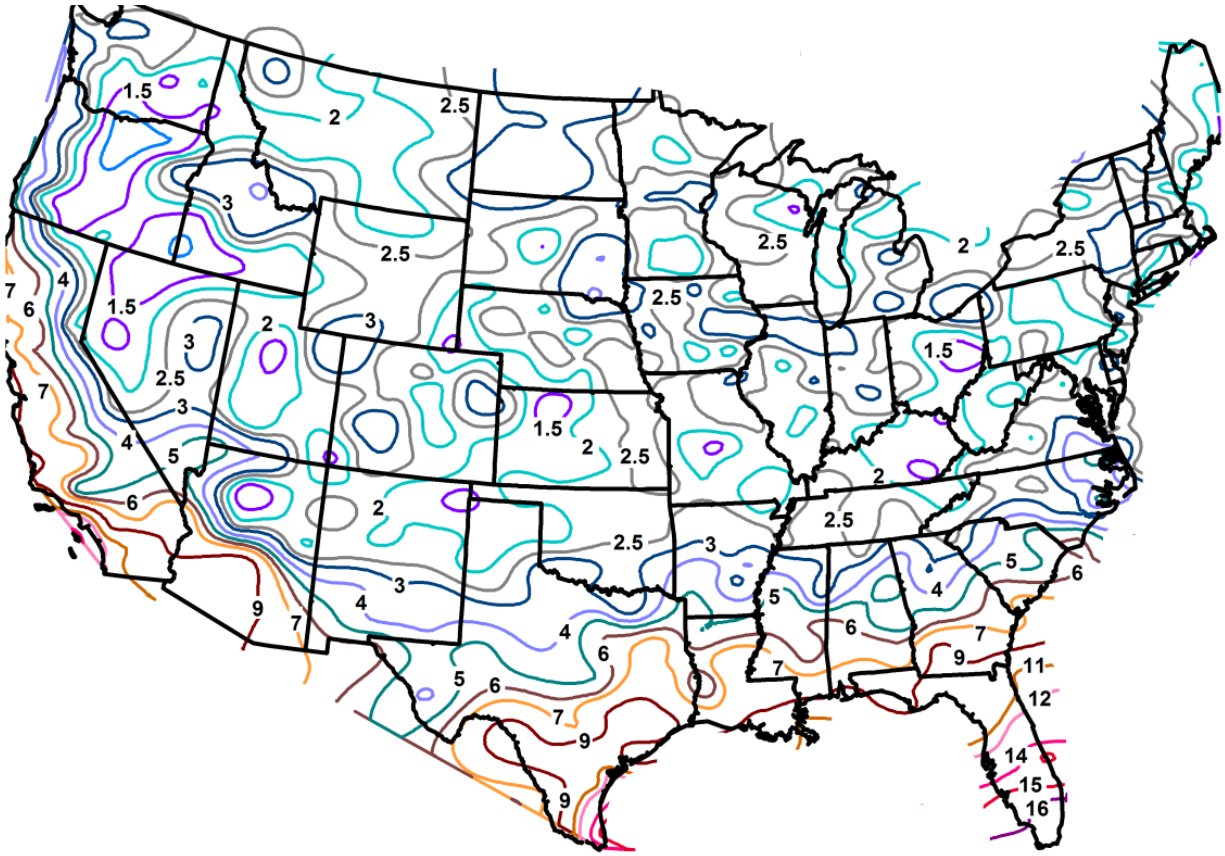

Figure 7-36 Minimum design temperatures (°C) for 1878 acre lake at depth of 5 m (16 ft)

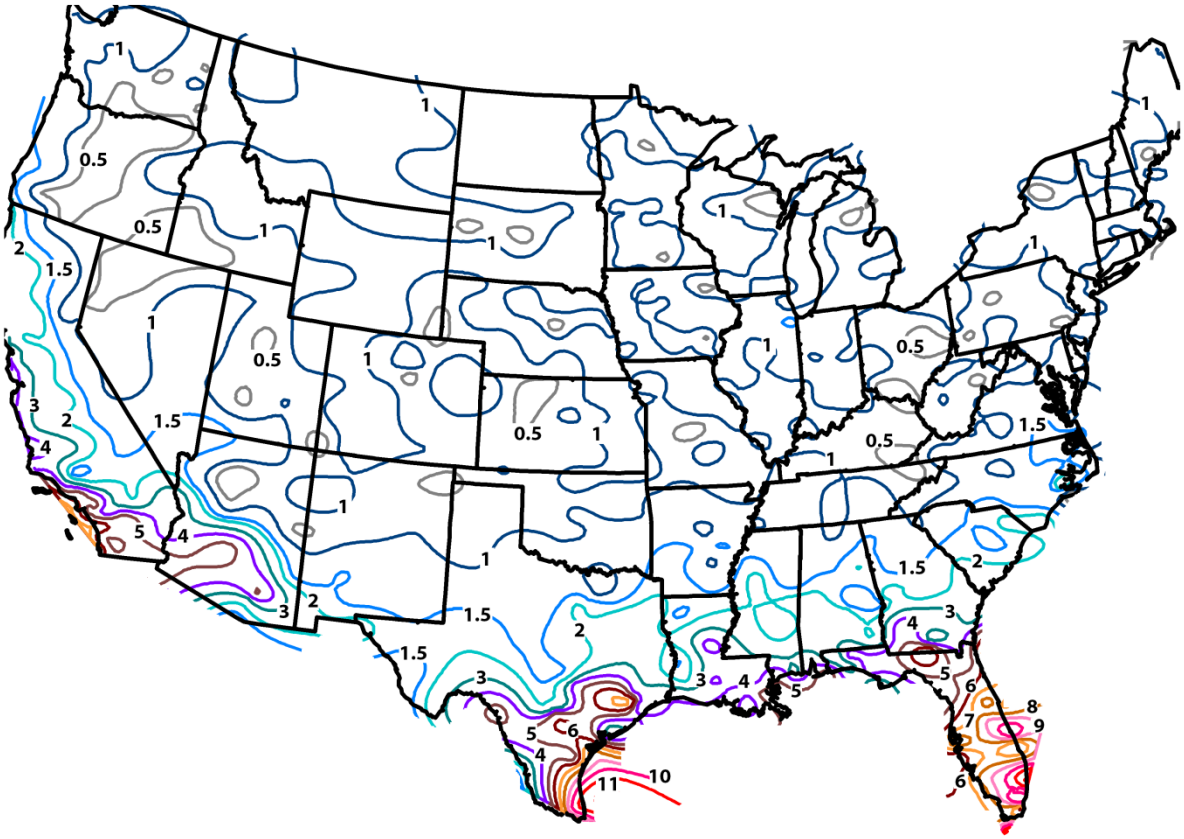

Figure 7-37 Annual minimum temperatures (°C) for 1878 acres lake at depth of 18 m (59 ft)

The 41-acre and 1878-acre lakes are large enough so they do not have near-freezing temperatures, unlike small shallow ponds.

7.7. Conclusions

Overall, the SHWP systems can offer effective heating and cooling to the buildings, yet, as noted earlier, the required design data and procedures remains limited. Three different approaches were investigated to estimate design temperatures. The water-temperature-data-driven approach is unsatisfactory because the data are very sparse from either a geographical standpoint or temporal standpoint. The satellite-data approach is unsatisfactory for a number of reasons, including the fact that even developing a database of temperatures at the surface of a water body

`

would require enormous effort and seems to be expensive. And even then, success would be uncertain. Finally, an approach involving lake simulation combined with lake descriptions and typical meteorological data is chosen as a satisfactory approach and generated design temperatures for specific lake sizes and depths.

The lake simulation model is used to derive minimum and maximum lake temperatures as a function of depth. The uncertainties associated with the model and due to using TMY are calculated for each lake separately. The total uncertainty is added to the model predicted design temperatures and isotherms maps are developed.

The advantages of using this approach is its geographic distribution across United States by utilizing TMY-type (EnergyPlus) weather files. As well as, the design temperatures can be predicted at any desired depths where a heat exchanger can be possibly placed. Although, the concept is appealing, the TMY uncertainty analysis so far produced wide prediction interval. The uncertainties stemming from using TMY weather data are greater than model uncertainty. From the investigation of uncertainties in prediction of design temperatures of three different lake types, we can say that the uncertainties associated with the model varies from 2 °C to 3.5 °C whereas the uncertainties in using TMY weather file ranges from 3 °C to 4.6 °C. This high range of uncertainties due to using TMY weather data can be rectified using a number of years of actual weather data. However, there are some constraints in acquiring complete actual weather data sets for locations in either the continental United States or worldwide. Actual weather data has significant numbers of gaps that require expertise and time to fill. Neither the expertise nor the time were available for this project.

From the model perspective, the analysis illustrates one of the limitations of using daily time steps – there is a limit to the accuracy that is inherent in using a daily time step. Furthermore, the applicability of this approach is limited by certain factors as summarized below

`

- It relies on simulations that have limited validations, because data sets that could be used to determine minimum and maximum temperature as a function of depth are available for only a few lakes.
- It relies on a typical meteorological year, yet minimum and maximum lake temperatures are not likely to occur during typical years.
- Lakes come in a wide variety of surface area, depths, and bathymetric profiles. Yet, we can reasonably tabulate temperatures for only a few varieties of lakes
- The lake simulations are for stagnant lakes – lakes where inflows have a negligible effect on the temperatures.
- Maximum lake temperatures are unlikely to occur at the same time as peak cooling loads. Using maximum lake temperatures in conjunction with peak cooling loads may result in oversizing of the surface water heat exchanger

The electric demand of SWHP systems is usually less than air source heat pump systems because of stable lake temperatures. However, for systems in colder climates placed in shallow ponds near-freezing pond temperatures may cause ice formation on the surface of heat exchanger and decrease the efficiency of the system. Once the SWHE is completely ice-covered, the heat pump entering fluid temperatures may cause the heat pump to shut down. Therefore, some type of backup heating is recommended for such systems.

`

8.

CONCLUSIONS AND RECOMMENDATIONS FOR FUTURE WORK

Surface water heat pump systems are efficient building heating/cooling systems, which have received considerable attention recently. These systems are advantageous compared to air source heat pump systems yet there are no design or energy analysis tools to assist design engineers.

This thesis developed lake model and SWHE model that can be used as part of design and energy analysis tool for SWHP systems. The robust lake model along with SWHE model have been developed as a stand-alone FORTRAN tool and also implemented in EnergyPlus environment with some necessary changes. In practice, the numerical lake model that matches exactly with the real world scenario is not possible. The lake model is built on certain underlying assumptions to decrease the complexity in the inputs and to decrease the computational time.

The model is specifically designed to provide daily lake temperatures along the depth to analyze the interaction between lake and heat exchanger. The model predicted lake temperatures are compared with historical experimental measurements collected from different sources. The predicted lake temperature matches closely with the experimental data except at the depths in the thermocline region. Relatively high error in this region is due to inaccuracy in the prediction of epilimnion depth. Typical errors outside the thermocline region are on the order of 1.5 °C. In the thermocline region errors are typically 3 °C. From the experimental data collected from Lake

`

Sammamish in Seattle Washington, it is observed that the epilimnion depth is more sensitive to wind speed. This suggests that the enhancement of the lake model to work at hourly time steps model may improve the accuracy of the prediction of epilimnion depth and thus the accuracy of the thermocline temperatures.

The lake temperatures are not very sensitive to Secchi depth input. Therefore, the lake model was developed in such a way it takes in the annual average Secchi depth that in turn is used in the calculation of solar radiation penetration to the water layers below the surface. Since epilimnion depth increases with increase in transparency of a lake, it would be useful to incorporate the algae dynamics in the lake model in order to predict the epilimnion depth and thermocline temperatures more accurately.

The lake model is developed for stagnant lakes – lakes where inflows have a negligible effect on the water temperatures. However, for some lakes, which are connected to a river, the lake temperatures are likely to change due to inflows/outflows. Since water temperatures of river inflow and the lake temperatures are different, mixing is induced due to density differences. So, developing a lake model which can account for inflows/outflows would be one of the recommendations for future research. Also, the model assumes constant lake water level. The lake simulation could be modeled in more realistic way in future if it is modified to accommodate water level change.

The surface water heat exchanger model simulates heat transfer and exiting fluid temperatures for four SWHE configurations. The model includes a feature to account for freezing on the surface of the heat exchanger. The SWHE freezing model calculates heat transfer rate and buoyant force on the SWHEs. The model includes ice formation on SWHE coils (spiral-helical, flat spiral and slinky)) by dividing a heat exchanger coil into several segments but for flat plat heat exchanger, it is treated as a single component. The calculation of ice overlapping angle

`

between adjacent coil segments is developed only for spiral-helical coil. The reduction in outside heat transfer coefficient during the time of ice formation is handled in the model by including a penalty coefficient. An appropriate penalty coefficient is determined from the sensitivity analysis done to match the model predicted results with experimental data. During ice formation, exiting fluid temperatures of a spiral helical coil are validated with experimental measurements, which shows good agreement. However, when it comes to buoyancy, the SWHE model predicts the onset of freezing a few hours earlier than the actual experimental start of freezing.

A surface water heat pump simulation, consisting of lake model and surface water heat exchanger model was implemented in EnergyPlus. One of the key decisions in the implementation is how the time-step issue is handled between lake model and SWHE model. Though EnergyPlus is a variable time step model, the lake model has been implemented as a daily time step model. It takes in the daily weather data and performs the set of calculations to predict the lake temperatures. The lake simulation lags by one day in the building simulation. The lake model begins for each simulation day and then run the surface water heat exchanger model for the rest of the day. This is repeated for all the days of simulation. The lake temperature variation over a day is generally low except near the surface of a lake. Also, the actual change of lake temperatures from day to day is relatively small. Therefore, the energy consumption differences caused because of the lag in lake model by a day should be negligible.

In Chapter 6, the stand-alone configuration of the lake model combined with SWHE model is used in a case study to analyze the water temperature variation by heat rejection or extraction. In most cases, the variation of lake temperatures is negligible. However, when the system is extremely loaded (high heat rejection or extraction), the lake temperatures varies significantly. In these cases, thermal plumes originating from a heat exchanger depth carries the heat upwards or downwards in the lakes.

`

The effect of heat rejection or extraction that cause the lake temperature variation of 1°C and 2°C is analyzed in this chapter using three different simplified HX sub models. Since HX sub-model 3 is a type which splits-the-difference between two limiting case type models (HX sub-model 1 and HX sub-model 2), HX sub-model 3 is selected here as the best to give design recommendations. Time constraint precluded the development of a detailed and more thorough analysis of thermal plume model. A major limitation of this study is the results are based only on the simulations and there are no experimental data to validate the results. Based on the limited information, the results are presented for 4 different locations and 3 different lake types.

On looking at the results, we can say that the heat rejection rate is relatively sensitive to lake site particularly for 1°C and 2°C temperature variation. There is substantial difference depending on lake type and location and no definitive trend in the results related to either lake type or location. This makes it difficult to recommend a single heat rejection/extraction rate that suits for every case that has been analyzed. However, we could say from limited locations and lake types analyzed, a maximum 1°C temperature increase in lake temperature is caused by a low heat rejection rate of 7 tons/acre to high heat rejection rate of 46 tons/acre. Similarly, a range for heat rejection rate that caused maximum 2°C temperature rise is 14 tons/acre to 92 tons/acre.

The maximum allowable loading for specific lake/location is considered as the heat rejection rate at which the temperature stratification is completely destroyed for shallow ponds and partially destroyed for large lakes. At this point of maximum loading, the lake temperature will be increased significantly from undisturbed lake temperatures. In all the three lake types analyzed, significant temperature de-stratification (i.e. lake temperatures at heat exchanger depth is half way between undisturbed and completely destratified cases) occurs approximately at the loads between 38 tons/acre and 143 tons/acre

`

From the 3 lake sites analyzed for heat extraction rates, Seattle WA requires relatively high heat extraction rates to cause specific temperature variation in a lake compared to other two locations. The results also points out that the heat extraction rate that cause a lake temperature drop of 1°C or 2°C increases with lake size. Useful recommendation can be drawn from the results as a 'range of heat extraction rates'. In this way, a range from 2 MBtuh/acre to 464 MBtuh/acre caused the lake temperature to drop 1°C and range of 4 MBtuh/acre to1043 MBtuh/acre caused the lake temperature drop to 2°C.

Chapter 7 discussed the design data generation procedure using the lake model. Only, an approach involving lake simulation combined with lake descriptions and typical meteorological data seems to be feasible. The lake simulation model is used to derive minimum and maximum lake temperatures as a function of depth. The uncertainties associated with the model and due to using TMY are calculated for each lake separately. The total uncertainty is added to the model predicted design temperatures and isotherms maps are developed.

The advantages of using this approach is its geographic distribution across United States by utilizing TMY-type (EnergyPlus) weather files. As well as, the design temperatures can be predicted at any desired depths where a heat exchanger can be possibly placed. Although, the concept is appealing, the TMY uncertainty analysis so far produced wide prediction interval. The uncertainties stemming from using TMY weather data are greater than model uncertainty. From the investigation of uncertainties in prediction of design temperatures of three different lake types, we can say that the uncertainties associated with the model varies from 2 °C to 3.5 °C whereas the uncertainties in using TMY weather file ranges from 3 °C to 4.6 °C. This high range of uncertainties due to using TMY weather data can be rectified using a number of years of actual weather data. However, there are some constraints in acquiring complete actual weather data sets for locations in either the continental United States or worldwide. Actual weather data has

`

significant numbers of gaps that require expertise and time to fill. Neither the expertise nor the time were available for this project.

The electric demand of SWHP systems is usually less than air source heat pump systems because of stable lake temperatures. However, for systems in colder climates placed in shallow ponds near-freezing pond temperatures may cause ice formation on the surface of heat exchanger and decrease the efficiency of the system. Once the SWHE is completely ice-covered, the heat pump entering fluid temperatures may cause the heat pump to shut down. Therefore, some type of backup heating is recommended for such systems.

`

REFERENCES

AASG (2011). Association of American State Geologists. http://www.kgs.ukans.eduyAASG/AASG.html.

Adams, E., D. J. Cosler and K. R. Helfrich.(1990). Evaporation from heated water bodies: Predicting combined forced plus free convection. *Water Resources Research* 26(3): 425-435.

Ali, M. E.(2006). Natural Convection Heat Transfer from Vertical Helical Coils in Oil. *Heat Transfer Engineering* 27(3): 79-85.

Bashyam, K. C.2013.*Development of a lake simulation model and a design tool for surface water heat pump systems*. Masters thesis. Oklahoma State University, Oklahoma.

Bashyam, K. C., M. Selvakumar and J. D. Spitler.(2013b). Modeling of lakes for surface water heat pump systems – sub model sensitivity study.

Blumberg, A. F. and G. L. Mellor.(1987). A Description of a Three-Dimensional Coastal Ocean Circulation Model. *Coastal and Estuarine Sciences* 4: 1-16.

Chiasson, A. D., J. D. Spitler, S. J. Rees and M. D. Smith.(2000). A Model for Simulating the Performance of a Shallow Pond as a Supplemental Heat Rejector with Closed-Loop Ground-Source Heat Pump Systems. *ASHRAE Transcations* 106(2): 107-121.

Chiasson, D. A., D. J. Spitler, J. R. Simon and D. M. Smith.(2000). A Model for simulating the performance of a shallow pond as a supplemental heat rejecter with closed-loop Ground-Source Heat Pump Systems. *ASHRAE Transactions* 106(2): 107-121.

Churchill, S. W. and H. H. S. Chu.(1975). Correlating equations for laminar and turbulent free convection from a horizontal cylinder. *International Journal of Heat and Mass Transfer* 18(9): 1049-1053.

Crocker, G. B. and P. Wadhams.(1989). Modelling Antarctic Fast-Ice Growth. *Journal of Glaciology* 35(119): 3-8.

Dake, J. M. and D. R. F. Harleman.(1969). Thermal stratification in lakes: analytical and laboratory studies. *Water Resources Research* 5(2): 484-495.

Dake, J. M. K. and D. R. F. Harleman.(1969). Thermal stratification in lakes: Analytical and laboratory studies. *Water Resources Research* 5(2): 484-495.

Dargahi, B. and S. G. Setegn.(2011). Combined 3D hydrodynamic and watershed modelling of Lake Tana, Ethiopia. *Journal of Hydrology* 398(1–2): 44-64.

Davin, B. L., J. Nordling and K. Sandart.(1981). Heat pumps using heat from lakes and the sea. *International Journal of Ambient Energy* 2(1): 41-45.

DOE. (2012). EnergyPlus energy simulation software.

Edinger, J. E., D. W. Duttweiler and J.C.Geyer.(1968). The response of water temperatures to meteorological conditions. *Water Resources Research* 4(5): 1137-1143.

EIS (2012). Energy Information Services - Temperature profiles of surface water bodies. http://geokiss.com/surwatertemps.htm.

`

Ellis, C. R., H. G. Stefan and R. Gu.(1991). Water Temperature Dynamics and Heat Transfer Beneath the Ice Cover of a Lake. *Limnology and Oceanography* 36(2): 324-335.

EnergyPlus (2012). Weather data sources EnergyPlus energy simulation software. http://apps1.eere.energy.gov/buildings/energyplus/weatherdata_sources.cfm.

EnergyPlus. (2012a). *Getting Started with EnergyPlus*, U.S. Department of Energy.

EPA (2011). United States Environmental Protection Agency. http://www.epa.gov/storet/.

Fang , X. and H. G. Stefan.(1996). Long-term lake water temperature and ice cover simulations/measurements. *Cold Regions Science and Technology* 24: 289-304.

Feng, J., J. Gao and P. Woods.(2012). Study on the maximum installed capacity of surface water source heat pump systems. *Advance Materials Research* 368 - 373: 3853-3856.

Fisher, J. I. and J. F. Mustard.(2004). High spatial resolution sea surface climatology from landsat thermal infrared data. *Remote Sensing of Environment* 90(3): 293-307.

Florida Lakewatch (2013). Florida's volunteer water quality monitoring program. http://lakewatch.ifas.ufl.edu/.

Ford, D. E. and H. G. Stefan.(1980). Thermal predictions using integral energy model. *Journal of the Hydraulics division* 106(1): 39-55.

Galloway, J. M. and R. Green. (2003). Simulation of hydrodynamics, temperature and dissolved oxygen in Bull Shoals lake, Arkansas, 1994-1995, Water-Resources Investigations Report U.S. Geological Survey.

Gu, R. and H. G. Stefan.(1990). Year-round temperature simulation of cold climate lakes. *Cold Regions Science and Technology* 18(2): 147-160.

Gu, R. and H. G. Stefan.(1990). Year round temperature simulation of cold climate lakes. *Cold Regions Science and Technology* 18: 147-160.

Gu, R. and H. G. Stefan.(1995). Stratification dynamics in wastewater stabilization ponds. *Water Research* 29(8): 1909-1923.

Hakala, A.(2004). Meromixis as a part of lake evolution - observations and a revised classification of true meromictic lakes in Finland. *Boreal environment research* 9(1): 37-53.

Håkanson, L. (1981). *A manual of lake morphometry*. New York, Springer-Verlag.

Hamilton, D. P. and S. Schladow, G (1997). Prediction of water quality in lakes and reservoirs. Part I - Model description. *Ecological Modelling* 96: 91-110.

Hamrick, J. M. (1992). *A three-dimensional environmental fluid dynamics computer code: Theoretical and computational aspects*, Virginia Institute of Marine Science, College of William and Mary.

Hansen, G. M.2011.*Experimental tesign and analysis of spiral-helical surface water heat exchanger configurations*. Masters thesis. Oklahoma State University, Oklahoma.

Hansen, G. M.2011.*Experimental testing and analysis of spiral-helical surface water heat exchanger configurations*. Masters thesis. Oklahoma State University, Stillwater.

Hattemer, B. and S. P. Kavanaugh.(2005). Design temperature data for surface water heating and cooling systems. *ASHRAE Transactions* 111(1): 695-701.

`

Hayter, E. J., M. A. Bergs, R. Gu, S. C. McCutcheon, S. J. Smith and H. J. Whiteley. (1998). HSCTM-2D, a finite element model for depth-averaged hydrodynamics, sediment and contaminant transport. U. S. E. E. R. Laboratory. Athens, GA.

Hondzo, M. and H. Stefan.(1993). Regional water temperature characteristics of lakes subjected to climate change. *Climatic Change* 24(3): 187-211.

Hondzo, M. and H. G. Stefan.(1993). Lake water temperature simulation model. *Journal of Hydraulic Engineering* 119: 1251-1273.

Hondzo, M. and H. G. Stefan.(1993). Regional water temperature characteristics of lakes subjected to climate change. *Climatic Change* 24(3): 187-211.

Imberger, J. and P. F. Hamblin.(1982). Dynamics of lakes, reservoirs, and cooling ponds. *Annual Review of Fluid Mechanics* 14(1): 153-187.

Imberger, J., J. Patterson, B. Hebbert and I. Loh.(1978). Dynamics of Reservoir of Medium Size. *Journal of Hydraulics Division* 104(5): 725-743.

Jassby, A. and T. Powell.(1975). Vertical patterns of eddy diffusion during stratification in Castle Lake, California. *Limnology and Oceanography* 20(4): 530-543.

Jekel, T. B., J. W. Mitchell and S. A. Klein.(1993). Modeling of Ice-Storage Tanks. *ASHRAE Transcations* 99(1): 1016-1024.

Ji, Z. G., M. R. Morton and J. M. Hamrick.(2001). Wetting and drying simulation of estuarine processes. *Estuarine, Coastal and Shelf Science* 53(5): 683-700.

Johansson, H., A. A. Brolin and L. Håkanson.(2007). New approaches to the modelling of lake basin morphometry. *Environmental Modeling and Assessment* 12: 213-228.

Johansson, I.(1983). Comparison between soil, rock, ground water and lakes as heat source for heat pumps. *16th International Congress of Refrigeration* 5: 311-317.

Kavanaugh, S. P. and K. D. Rafferty. (1997). Ground-source heat pumps : design of geothermal systems for commercial and institutional buildings. Atlanta, American Society of Heating, Refrigerating and Air-Conditioning Engineers**:** 167 p.

King County (2012). King county lake monitoring buoys. Retrieved 9/28/2012, http://green.kingcounty.gov/lake-buoy/Data.aspx.

Lakebase (2011). GLEON Lakebase - The repository of limnological, political, economic, and social information about lakes of the world. http://lakebase.gleon.org/.

Launiainen, J. and B. Cheng.(1998). Modelling of ice thermodynamics in natural water bodies. *Cold Regions Science and Technology* 27(3): 153-178.

Lawson, R. and M. A. Anderson.(2007). Stratification and mixing in Lake Elsinore, California: An assessment of axial flow pumps for improving water quality in a shallow eutrophic lake. *Water Research* 41(19): 4457-4467.

Lehner, B. and P. Döll.(2004). Development and validation of a global database of lakes, reservoirs and wetlands. *Journal of Hydrology* 296(1–4): 1-22.

Lepparanta, M.(1991). A review of analytical models of sea-ice growth. *Atmosphere-Ocean* 31: 123-138.

McCormick, M. J. and D. Scavia.(1981). Calculation of vertical profiles of lake-averaged temperature and diffusivity in Lakes Ontario and Washington. *Water Resources Research* 17(2): 305-310.

MichiganDEQ (2011). Michigan department of environmental quality-Michigan's volunteer lakes monitoring program. http://www.michigan.gov/deq.

`

Mitchell, M. S. and D. J. Spitler.(2013). Open-loop direct surface water cooling and surface water heat pump systems- A review. *HVAC&R Research* In Press.

Molineaux, B., B. Lachal and O. Guisan.(1994). Thermal analysis of five outdoor swimming pools heated by unglazed solar collectors. *Solar Energy* 53(1): 21-26.

NCDC. (1993). Solar and Meteorological Surface Observation Network, 1961-1990, Asheville, North Carolina:National Climatic Data Center, U.S. Department of Commerce.

Neto, J. H. M. and M. Krarti.(1997). Deterministic model for an internal melt ice-on-coil thermal storage tank. *ASHRAE Transactions* 103(1): 113-124.

Omstedt, A.(1990). A coupled one-dimensional sea ice–ocean model applied to a semi-enclosed basin. *Tellus A* 42(5): 568-582.

Perovich, D. K. (1996). *The optical properties of sea ice / Donald K. Perovich ; prepared for Office of Naval Research*. [Hanover, N.H.] :, US Army Corps of Engineers, Cold Regions Research & Engineering Laboratory ; [Springfield, Va. : Available from National Technical Information Service.

Pezent, M. C. and S. P. Kavanaugh.(1990). Development and verification of a thermal model of lakes used with water source heat pumps. *ASHRAE Transactions* 96(1): 574-582.

Prabhanjan, D. G., T. J. Rennie and G. S. Vijaya Raghavan.(2004). Natural convection heat transfer from helical coiled tubes. *International Journal of Thermal Sciences* 43(4): 359-365.

Raphael, J. M.(1962). Prediction of temperature in rivers and reservoirs. *Journal of the Power Division, Procedings of the American Society of Civil Engineers* 88(P02): 157-181.

Riley, M. J. and H. G. Stefan.(1988). Minlake: A dynamic lake water quality simulation model. *Ecological Modelling* 43(3–4): 155-182.

Rogers, G. F. C. and Y. R. Mayhew.(1964). Heat transfer and pressure loss in helically coiled tubes with turbulent flow. *International Journal of Heat and Mass Transfer* 7(11): 1207-1216.

Rohden, C. v., K. Wunderle and J. Ilmberger.(2007). Parameterisation of the vertical transport in a small thermally stratified lake. *Aquatic Sciences - Research Across Boundaries* 69(1): 129-137.

Salimpour, M. R.(2009). Heat transfer coefficients of shell and coiled tube heat exchangers. *Experimental Thermal and Fluid Science* 33(2): 203-207.

Saloranta and Andersen. (2004). My lake (v.1.1): Technical model documentation and users guide. Oslo, Norway, Norweigian Institute for Water Research**:** 44.

Saloranta, T.(2000). Modeling the evolution of snow, snow ice and ice in the Baltic Sea. *Tellus* 52A: 93-108.

Saloranta, T. M.(2000). Modeling the evolution of snow, snow ice and ice in the Baltic Sea. *Tellus A* 52(1): 93-108.

Saloranta, T. M. and T. Andersen. (2004). Mylake (v.1.1): Technical model documentation and user's guide. NIVA-report 4838. Olso,Norway, Norwegian Institute for Water Research. **44**.

Saloranta, T. M. and T. Andersen.(2007). MyLake—A multi-year lake simulation model code suitable for uncertainty and sensitivity analysis simulations. *Ecological Modelling* 207(1): 45-60.

`

Schneider, K. and W. Mauser.(1996). Processing and accuracy of landsat thematic mapper data for lake surface temperature measurement. *International Journal of Remote Sensing* 17(11): 2027-2041.

Sengupta, S., E. Nwadike and S. S. Lee.(1981). Long term simulation of stratification in cooling lakes. *Applied Mathematical Modelling* 5(5): 313-320.

Silver, S. C., A. F. Milbitz, J. W. Jones, J. L. Peterson and B. D. Hunn.(1989). Component models for computer simulation of ice storage systems. *ASHRAE Transactions* 95(1): 1214-1226.

Srinivasan, J. and A. Guha.(1987). The effect of bottom reflectivity performance of a solar pond. *Solar Energy* 39(4): 361-367.

Stefan, H. G., J. J. Cardoni, F. R. Shiebe and C. M. Cooper.(1983). Model of light penetration in a turbid lake. *Water Resources Research* 19(1): 109-120.

Svensson, T. and L. O. Sorman.(1983). Pipe heat exchangers on lake bottoms. *Proceedings: Stockholm, June 6-8, 1983* 2: 679.

Swinbank, W. C.(1963). Long-wave radiation from clear skies. *Quarterly Journal of the Royal Meteorological Society* 89(381): 339-348.

Tucker, W. A. and A. W. Green.(1977). A time-dependent model of the lake-averaged, vertical temperature distribution of lakes. *Limnology and Oceanography* 22(4): 687-699.

TVA (2011). Tennessee valley authority-east Tennessee reservoir maps. http://www.tnfish.org/ReservoirLakeMapsTennessee_TWRA/TennesseeReservoirLakeMaps_TWRA.htm.

USACE (2011). United States Army Corps of Engineers. http://www.usace.army.mil/.

USGS. (2011). United States Geological Survey-Water Resources of the United States. http://ar.water.usgs.gov/data-bin/maumelle/ts.pl.

Watts, A. (2010). Designing a pond loop using Slim Jim geo lake plate.

Wilcox, S. and W. Marion (2008). Users manual for TMY3 data sets. http://www.doe2.com/download/weather/tmy3/users_manual_for_tmy3_data_sets.pdf.

Wloczyk, C., R. Richter, E. Borg and W. Neubert.(2006). Sea and lake surface temperature retrieval from landsat thermal data in northern Germany. *International Journal of Remote Sensing* 27(12): 2489-2502.

WOW (2011). Water on the Web-Monitoring Minnesota lakes on the internet and training water science technicians for the future - A national on-line curriculum using advanced technologies and real-time data, University of Minnesota-Duluth, Duluth. http://WaterOntheWeb.org.

WOW (2012). Water on the Web-Monitoring Minnesota lakes on the internet and training water science technicians for the future - A national on-line curriculum using advanced technologies and real-time data, University of Minnesota-Duluth, Duluth. Retrieved June 20, 2012, http://WaterOntheWeb.org.

WOW (2013). Lake Ecology. Retrieved April 5, 2013, http://www.waterontheweb.org/under/lakeecology/05_stratification.html#.

Yen, Y. C. (1981). Review of thermal properties of snow, ice and sea-ice. Hanover,NH,USA, US Army Cold Regions Research and Engineering Laboratory.

`

VITA

MANOJKUMAR SELVAKUMAR

Candidate for the Degree of

Master of Science

Thesis: APPLICATION OF LAKE AND SURFACE WATER HEAT EXCHANGER SIMULATIONS FOR ENERGY CALCULATIONS AND DETERMINATION OF DESIGN TEMPERATURES AND CONSTRAINTS

Major Field: Mechanical Engineering

Biographical:

Education:

Completed the requirements for the Master of Science in Mechanical Engineering at Oklahoma State University, Stillwater, Oklahoma in May, 2013.

Received Bachelor of Engineering in Mechanical Engineering at Anna University – Arunai Engineering College, Chennai, Tamil Nadu, India in 2009.

Experience:

Employed as a Research assistant in the School of Mechanical and Aerospace Engineering, Oklahoma State University, Stillwater, Oklahoma from July 2011 to May 2013.

Employed as a Teaching Assistant in the School of Mechanical and Aerospace Engineering, Oklahoma State University, Stillwater, Oklahoma from August 2010 to June 2011.

Professional Memberships:

American Society of Heating, Refrigerating, and Air Conditioning Engineers, Inc. (ASHRAE student member).